FC COATED MICRO/NANOPARTICLES FOR HUMORAL IMMUNE SYSTEM MODULATION

A Dissertation

Presented to

The Academic Faculty

by

Patricia Marie Pacheco

In Partial Fulfillment

of the Requirements for the Degree

Doctor of Philosophy in Bioengineering from the

Woodruff School of Mechanical Engineering

Georgia Institute of Technology

December 2014

FC COATED MICRO/NANOPARTICLES FOR HUMORAL IMMUNE SYSTEM MODULATION

Approved by:

Dr. Todd Sulchek, Advisor
Woodruff School of Mechanical Engineering
Georgia Institute of Technology

Dr. Andrés García
Woodruff School of Mechanical Engineering
Georgia Institute of Technology

Dr. Julie Babensee
School of Biomedical Engineering
Georgia Institute of Technology

Dr. David M. White
National Centers for Animal Health
U.S. Department of Agriculture

Dr. Julia Champion
School of Chemical and Biomolecular Engineering
Georgia Institute of Technology

Date Approved: November 10, 2104

To all of my friends and family who have helped me get to where I am today

ACKNOWLEDGEMENTS

There are many people who played a large part in me getting to where I am today. My family members have always been my biggest supporters and the ones I could fall back on when things got tough. My mother, Lynda Leon, is an amazing example of a strong, successful woman who seemed to make having it all seem so easy. My father, Israel Pacheco Jr., has always pushed me to be my best and instilled the values and work ethic that I will carry forward. Dave Leon has always been there to support me and make me stand up for what I believe in (and what team I root for). Trudi Pacheco makes things feel like home and is always there to lend an ear when you need to talk. My sister Natasha Pacheco has been the one I can always turn to about anything as well as the special issues that arise as a fellow PhD student. Nick Pacheco has shown me to never give up and can always make me laugh. The other same-day baby, Isabel Leon, is the reason why I do what I do. While she keeps me silly, I hope I can be a good role model for all that I know she can become. In general, all of my family has been an incredible source of support for me. This includes my grandparents, who have loved me unconditionally and making them proud makes my day. My many uncles, aunts, and cousins have also been a great support network for me and they always make sure I have a great time when we're all together. Overall my family has always been my greatest source of support and love and I will always be grateful for them.

I would never have pursued engineering if it wasn't for the support I first received in Mission, TX from my computer science teacher Luis Chaire. He took the time to teach me even when I was no longer his student and pushed me to be better. In general, all of my teachers, from elementary to high school, have always known that I could succeed but

never let me slack off. During my time as an undergraduate student at the University of Michigan, there were certain student advisors, such as Lyonel Milton, Stacie Edington, and Dr. Susan Montgomery, who kept me on the right path to graduation and graduate school. I also had great mentors and support from faculty members including Drs. Alan Wineman, Ellen Arruda, James Ashton-Miller, Sridhar Kota, and Michel Maharbiz who introduced me to the rigors of research and challenged me to always think critically. The Society of Hispanic Professional Engineers chapter at Michigan not only gave me the professional skills I needed to succeed, but they also provided an invaluable network of people I can always turn to. I also made incredible, life-long friends at Michigan including Brandie Chun, Layne Scherer, Adam Paul and Andrew Rinke who also kept me balanced.

When I came to Georgia Tech, I was drawn to the lab of Dr. Todd Sulchek by his enthusiasm and creativity. Along this journey, we've had to go into some very unchartered territory, but Dr. Sulchek has always challenged and supported me through this interesting project. Dr. Andrés García always kept me on my toes, but he also was incredibly supportive of my project as well as me as a BioE student. Dr. Julia Babensee was resource for all things immunology which was a new field for me, but she provided the guidance and support that made my project better. Dr. Julie Champion kept me grounded and pushed me to think deeper about how my project is part of the bigger picture. Dr. David White always reminded me about the fun and excitement of science as well as providing a valuable and different perspective of my project.

My lab members have also played an important role in my experience here at Georgia Tech. We were all the founding members of the Sulchek Lab and had to learn

how we wanted the lab to run. Kipp Schoenwald, Wenwei Xu, Billy Wang, Daniel Potter, Tom Bongiorno, Damien Noga, Jennifer Tang, Ahmad Haider, Bushra Tassaduq, and Betsy Campbell have helped me thinking critically about my project and provide a unique perspective. Tom has been especially helpful in keeping the lab running and I would not have been able to finish my project without his help. I have also had the privilege of working with some amazing undergraduates. They not only helped me with my project, but they made me a better teacher and reminded me how important it is to cultivate the next generation of engineers and scientists.

One of the great benefits of the Bioengineering program at Georgia Tech is the amazing community. This has enabled to make great connections and collaborate with a variety of labs. Dr. Suraj Sable from the CDC was an immense resource for our new endeavor and was always available to answer my many questions. Hazel Stevens and Kellie Templeman were always there for me when I had questions about any procedure or experiment. They were also the ones who showed me how best to run a lab. The faculty here at Georgia Tech has been very helpful, both academically and professionally, including Drs. Ravi Bellamkonda, Johnna Temenoff, Susan Thomas, Todd McDevitt, Mark Prausnitz, Bob Guldberg, and Krish Roy. When I first started working in the lab, I did not have the benefit of senior students within my own lab, but I luckily had the support of senior students from other labs at Georgia Tech. The list of names is too long to list, but seeing how their challenges and how they overcame them to graduate and become successful, was a constant motivation. I would also like to thank the IBB community at large for their support in all things research and non-research. This includes the IBB front office staff, with special thanks to Colly Mitchell and Meg

McDevitt, and building services including James Goddard, Allen Echols, and Steve Woodard. Chris Ruffin was such an advocate for the students of the BioE program and he was also a great calming presence to all of the stresses we encountered along the way. Laura Paige has been incredibly supportive and when I graduate it will be because she was looking out for me.

My peers at Georgia Tech have contributed to the memories I will truly take with me forever. My participation in the Bioengineering and Biosciences Unified Graduate Students, Bioengineering Graduate Association (formerly BGSAC), GT Salsa, and Latino Organization of Graduate Students kept me balanced while also helping me grow as leader. They also grounded me in the larger importance of having an impact on the community. I consider myself lucky to be part of such an amazing cohort, not only within the BioE community, but the greater bioscience and engineering community at large. This group not only helped me at times with my research, whether it was teaching me a technique or lending me a reagent, but they also were there for me in general. Together, we tried new restaurants, new activities, and new things in general, and have truly made my time here above all, fun. While I am sure to forget a few names, I would like to thank Kristin Loomis, Saujan Sivaram Mei Zhan, Ashley Allen, Alice Li, Tanu Thote, Inthu Somasuntharam, Akhil Srinavasan, Brian Wile, Riley Zeller-Townson, Eric Alonas, Marilyn Dysart, Nassir Mokarram, Timothy Kassis, Jen Lei, and Lauren Priddy. Kristin Loomis in particular was willing to not only live with me for 4 years, but she was the first person to give me real confidence in my new role as Bioengineer. My time within the salsa community, especially with Taran Lundgren, Nuno Filipe, Laura Nuta, and Fuquan Ferrell, proved to very important in that it added to my teaching skills as well as kept me balanced, no pun intended. Finally, I would like to thank Arthur Hernandez for being nothing but incredibly supportive as I finished my thesis. He not only kept me fed and watched our puppies, but also looked out for me and did everything he could to make

sure I was taken care of, including making me laugh and keeping me happy. I am indebted to all of the people I have mentioned here as well as the ones I'm sure I have forgotten. All of these people took some of their time and helped me get to where I am today. Thank you, thank you so much.

TABLE OF CONTENTS

LIST OF TABLES

LIST OF FIGURES

LIST OF SYMBOLS AND ABBREVIATIONS

Ab	Antibody
ANOVA	Analysis of variance
APC	Antigen presenting cell
BCG	Bacillus Calmette-Guerin
BSA	Bovine Serum Albumin
CD	Clusters of differentiation
cDNA	Complementary deoxyribonucleic acid
CFU	Colony forming units
CO2	Carbon dioxide
Dapi	4',6-diamidino-2-phenylindole
DMEM	Dulbecco's Modified Eagle's Medium
DMEM/F-12	Dulbecco's Modified Eagle's Medium: Nutrient Mixture F-12
EDTA	Ethylenediaminetetraacetic acid
EIA	Enzyme immunoassay
ELISA	Enzyme-linked immunosorbent assay
FAB	Antigen binding fragment
FBS	Fetal bovine serum
Fc	Crystalizable, or constant, fragment
FcR	Crystalizable, constant, fragment receptor
FDA	United States Food and Drug Administration
FITC	Fluorescein isothiocyanate
FM4-64X	Fixable analog of N-(3-triethylammoniumpropyl) -4-(6-(4-(diethylamino) phenyl)hexatrienyl)pyridinium dibromide
G	Gravity
IC	Immune complex
IFN	Interferon
IGF1	Insulin-like growth factor 1
IgG	Immunoglobulin G
IgM	Immunoglobulin M
IL	Interleukin
iNOS	Inducible nitric oxide synthase
IPA	Isoproyl alcohol
LAMP-1	Lysosomal-associated membrane protein 1
LPS	Lipopolysaccharide
M-CSF	Macrophage colony stimulating factor
MFI	Mean fluorescent intensity
MHC	Major histocompatibility complex
mRNA	Messenger ribonucleic acid
Mφ	Macrophage
nm	nanometer
P/S	penicillin/streptomycin
PAMP	Pathogen associated molecular patterns
PBS	Phosphate buffered saline
PDGF	Platelet-derived growth factor

PE	Phycoerythrin
PerCP-Cy 5.5	Peridinin chlorophyll-Cyanine 5.5
PFA	Paraformaldehyde
PLGA	poly (D,L-lactic-co-glycolic acid)
qRT-PCR	Qualitative real time-polymerase chain reaction
RNA	Ribonucleic acid
S	Human serum
SD	Significantly different
TCC	Terminal complement complex
TGF	Transforming growth factor
Th1	Type 1 Helper T-cell
Th2	Type 2 Helper T-cell
TLR	Toll-like receptor
TNF	Tumor necrosis factor
TxRd	Texas Red
µm	micrometer

SUMMARY

The body's humoral immune response plays a larger role in the body's defenses beyond screening for invading pathogens. Modulation of this response is also vital for tissue regeneration, drug delivery, and vaccine development. The immune system operates within a complicated feedback loop and as such, altering the strength of the immune response can be approached from an engineering perspective. While a strong initial input can direct the response to either a pro- or anti-inflammatory bias, extreme responses can be deleterious, as in the case of allergic reactions or sepsis. Therefore, the objective of this thesis was to develop a novel biomaterials platform that can be used to alter the immune response in a tunable manner.

Antibodies are not only produced as a product of the adaptive immune response but are also powerful immunomodulators of the innate immune response through the activity of their Fc regions. Therefore, the overall hypothesis of this work was that coating microparticles with Fc ligands in variable surface densities would modify the input signal so that the immune response can be directed. Microparticle size was also investigated as a system variable to decouple the effects of physical versus metabolic signaling. The goal of this thesis was to analyze the effects of Fc coated particles on two major components of the humoral immune responses: macrophages and the complement system. The biophysical response of macrophage phagocytosis was evaluated; both Fc density and microparticle size had significant impacts on macrophage phagocytosis. Smaller microparticles (0.5 μm and 1 μm) coated with a high Fc density resulted in the greatest average number of particles per cell. However the larger microparticles (3 μm and 4.5 μm) resulted in fewer particles internalized but the greatest internalized volume

of particles per cell. These results provide a particle delivery "toolbox" for future applications involving phagocytosis by macrophages. The downstream effects of Fc particles on macrophage phenotype and phenotype plasticity were also analyzed. Results showed that gene expression varied in an Fc-density dependent manner, and that the addition of Fc coated particles can invert the response of LPS and IL-4 treated macrophages. When developed, these results are likely to have broader implications in the tissue regeneration and biomaterials fields.

The effects of the Fc coated particles were also tested in the context of the complement system, an often overlooked cascade of protein activation that results in cell opsonization and lysis. Cleaved components of the complement system are also powerful chemokines as they act as chemoattractants and may play an important role in vaccine adjuvants. The smaller particles of 0.5 μm and 1 μm resulted in the greatest levels of complement system activation. Fc density played a significant role in complement system activation, both through the classical and alternative pathway. It was observed that modifying density led to a binary response for smaller particles and a tunable response for larger particles. These results were tested in vitro by using Fc particles as a new form of antibiotic to direct complement-mediated bacterial cytotoxicity. Finally, Fc coated microparticles were then tested as an adjuvant in an attempt to better understand and improve the tuberculosis vaccine. These findings are significant to both the biomaterials and the larger immunology fields: it was observed that Fc microparticles can be used to tunably activate a wide range of immune processes, and could be used both to answer fundamental questions in immunology as well as to be used in important therapeutic applications.

CHAPTER 1 INTRODUCTION

The immune response represents a complicated and multi-facetted challenge, as it is a complex system operating within a series of layered feedback loops. Functionalized microparticles offer an opportunity to tune the outputs of these systems through simple adjustment of system variables, such as particle size, material properties, and surface coating. It has long been understood that the Fc region of an antibody is an important opsonin and immune activator. Fully understanding the effect of microparticle size and Fc density on the humoral immune response will answer fundamental questions in immunology. This will also allow future researchers to apply these results to a broad range of immunological disorders and biomaterials applications.

1.1 Motivation

The immune system plays a large role in a variety of pathological disorders, would healing, tissue regeneration, and infectious diseases. In many of these cases, modulating or controlling the immune response is an important facet of treatment. [1-9] However, when trying to control the immune system, it must be kept in mind that directing the response to a strong pro- or anti-inflammatory bias can be detrimental. In the case of autoimmune disorders, completely diminishing the immune response leaves the patient open to secondary infections. Over-stimulating the immune response can lead to tissue damage or anaphylaxis. For example, it has been shown that complement system components deposited on red blood cells can help mask incompatible antigens to prevent rejection in blood transfusions, but too much complement system activation will lead to red blood cell lysis. [10] Complement system activation has also been shown to increase the efficacy of vaccines as an alternative to traditional adjuvants, however this work is still in early research stages. [11-13] These are just a few examples that highlight the importance of having a platform capable of modulating the immune response.

There is also a significant need to better understand and control macrophage responses, to fully take advantage of their broad capabilities and phenotypic capacities. [1, 14-17] For example, research has shown that delivering anti-inflammatory activated macrophages to the site of spinal cord injury can lead to increased nerve regeneration while pro-inflammatory macrophages are detrimental. [18] A simple reagent that could be used to inhibit the inflammatory phenotype would therefore be of tremendous value to tissue regeneration efforts. As another example, *Mycobacterium tuberculosis* targets and reproduces within alveolar macrophages. Over 2 billion people have been infected with *M. tuberculosis* in recorded history, and there are over 8 million new cases each year resulting in 1.5 million deaths. *M. tuberculosis* can be treated with a stringent course of antibiotics, but there are a high number of cases of multi-drug resistant tuberculosis due to limited availability of drugs to complete a full course of treatment or poor compliance with the treatment protocol. This is especially true in cases in which patients also have another immuno-compromising infection such as HIV. [19-21] Therefore, a new approach to antibiotics for *M. tuberculosis* would be beneficial for these cases. Complement system proteins can be directly antimicrobial through the formation of the terminal complement complex (TCC) and have an additional function in the recruitment of other innate and adaptive immune factors and cells through the chemotactic and pro-inflammatory properties of their degradation products (C3a, C5a, etc.). The TCC cytotoxic action occurs through the formation of a nanoscale transmembrane channel leading to loss of integrity of the pathogen bilayer membrane and osmotic lysis. [22, 23] Finally, there is currently only one FDA approved vaccine, Bacillus Calmette-Guerin (BCG), which has an efficacy rate of 0-80%. If we can better understand and control macrophage response to the vaccine through novel adjuvants, we may be able to better improve the vaccine response and develop a improved way to treat the infection.

1.2 Specific Aims

The ability to control the body's immune response has long been an important goal in biomaterials research. [2, 24-27] Macrophages represent an important target for immunomodulation as they are capable of a broad range of phenotypes that have been shown to be activated upon exposure to external stimuli. [17, 28, 29] Specifically, macrophage phenotype can be altered and phagocytosis mediated through the binding of Fc surface receptors to the Fc domains of bound antibody to antigen-antibody immune complexes. [28-32] By functionalizing microparticles with variable densities and amounts of Fc to simulate these immune complexes, downstream effects on macrophage phenotype or phagocytosis efficiency can be modulated. [31] Fc coated microparticles can also be used to activate the complement system which can lead to a wide variety of applications including antibiotics, vaccine development, and viral clearance. [10-13, 33] Microparticles offer an ideal platform for immunoengineering as they enable us to alter a variety of physical and biochemical characteristics to tune a desired response. [26, 30, 34-37] While Fc receptor crosslinking in macrophages and complement system activation has been previously studied, it was not yet understood how Fc display on particles, and the combinatorial effects of Fc density and particle size, can affect these two systems. Therefore, this work focused on decoupling the effects of Fc density and microparticle size on macrophage phagocytosis and phenotype and on controlled complement system activation. Altering macrophage phenotype through Fc-mediated phagocytosis and activating the complement system can also have an impact on key adaptive immune components. This is why we applied Fc coated particle platform to better understand the tuberculosis vaccine, BCG.

The overall **objective** of this dissertation is to evaluate the effect of Fc particles on the humoral immune response. The overall **hypothesis** is that microparticles functionalized with a varied Fc density would provide a tunable platform for altering macrophage phenotype and humoral immunological effects.

1.2.1 Specific Aim 1: Characterize the effects of Fc functionalized microparticles on phagocytosis and macrophage phenotype.

The hypothesis is that a particle size and Fc density will affect macrophage response in a tunable manner. Functionalized microparticles with variable Fc densities were created. These particles were then delivered to macrophages and the amount of particle internalization was determined through flow cytometric and fluorescent microscopic analyses. Macrophage phenotype was characterized by evaluating gene expression of several cytokines using qRT-PCR. Cytokine secretion was then confirmed by testing for TNFα and IL-12 concentrations in conditioned media through ELISA.

1.2.2 Specific Aim 2: Modulate complement system activation for directed bacterial cytotoxicity.

The hypothesis is a high Fc density coating will lead to high levels of complement system activation and result in high levels of bacterial cytotoxicity. Microparticles of various sizes and Fc coating densities were delivered to human serum aliquots to determine complement system activation. After complement stimulation, microparticles were collected and incubated with primary antibodies specific for various complement components to characterize the specific complement pathways involved. Deposition of complement components on particles was confirmed using flow cytometry. A Monte Carlo simulation was used to validate a model that showed variations in Fc density could result in nonlinear activation of the complement system, which was observed experimentally. The experiment was repeated in C1 and Factor B deficient sera to determine which complement pathways were activated. Our Fc coated particles were observed to be cytotoxic by incubation with bacteria and analysis with a live/dead fluorescent staining by flow cytometry.

1.2.3 Specific Aim 3: Evaluate the *in vitro* effects of Fc functionalized microparticles on BCG-macrophage interaction.

The hypothesis is that Fc primed macrophages will lead to increased BCG phagocytosis and lysosome maturation. The interactions of macrophages treated with BCG and microparticles compared to BCG alone were quantified using flow cytometry and fluorescent and confocal microscopy. The amount of nitric oxide produced by macrophages was quantified as a result of BCG and/or Fc coated microparticles.

1.3 Innovation and Significance

The importance of innate immune components such as macrophages and the complement system is only paralleled by the complexity behind the intricate feedback systems controlling their activation. This fact makes these mechanisms both important foci of numerous research studies as well as difficult subjects of study. While the FcR and its corresponding activation pathways have previously been studied, applying this knowledge still holds great potential in the fields of biomaterials and vaccine development. Functionalizing microparticles with varied densities of Fc ligand provides a tunable method for modulating biophysical processes of macrophage phagocytosis, macrophage gene expression and phenotype, as well as complement system activation. This also represents the first time, to our knowledge, that the complement system has purposefully been activated through the use of a protein-functionalized biomaterial and applied as an antibiotic. These studies have identified Fc microparticles as a possible platform for a variety of clinical applications and could therefore aid in the translatability of this study. As *M. tuberculosis* primarily infects macrophages, the ability to deliver particles to macrophages and better engage macrophages with the BCG vaccine could greatly improve the efficacy of the vaccine and also offer a secondary option for infection treatment. This body of work is innovative through its application of a platform

technology to the problem of a rationally designed, initiated, and propagated “tunable” immune response.

CHAPTER 2 LITERATURE REVIEW

2.1 Macrophage Response

Macrophages are a key component of the immune system and perform a range of functions that span the innate and adaptive immune response. [17, 29, 38, 39] These cells reside in many different tissue spaces including the brain, lung, and lymphoid tissues. [40, 41] Recent studies have shown that some populations of tissue resident macrophages, such as microglia within the brain and Langerhans cells within the skin, are generated during prenatal development in the yolk sac. [29, 42, 43] For most macrophages, however, monocytes derived from myeloid progenitor cells generated within the bone marrow circulate through the body before entering the tissues as macrophages. [29] Macrophages respond to their surroundings due to stimuli to their numerous surface receptors. These surface receptors recognize a broad variety of inputs such as cytokines from nearby cells, pathogen associated molecular patterns displayed by pathogens, and apoptotic cells. Inputs from cytokines and crosslinking of surface receptors leads to phagocytosis and internalization of the original input (ie receptor or particulate) and further downstream internal signaling. [38, 39] While this role is the reason macrophages are typically thought of as first responders of the innate immune response, macrophages also play a key role in the adaptive immune system. Macrophages are capable of processing and presenting phagocytosed antigens to T and B cells as well as secreting cytokines that encourage recruitment of other immune cells. [38, 44, 45] Despite the protective effect macrophages can have, these cells also play a role in the promotion of many disease states, including atherosclerosis [46, 47], tumor microenvironments [3, 48], and tuberculosis [19, 49-51].

2.1.1 Macrophage Phenotype

Traditionally macrophages were thought to have only two distinct phenotypes: inflammatory (M1) and anti-inflammatory (M2). Macrophage phenotype has since become a more complex field of study, due to the large variety of phenotypes that have been described and the resulting impacts of those different phenotypes on wound healing and tissue regeneration. [15, 17, 27-29] Recent reviews have defined four distinct phenotypes with many more possible. These distinct phenotypes are categorized by cytokine output as well as up-regulation of specific surface receptors as highlighted in the table below (Table 1).

Table 1: Classification of Macrophage Phenotype.Summary of the various factors that can affect macrophage phenotype and the surface markers used to classify to macrophage phenotype. [15-17, 27, 28, 52]

Macrophage Phenotype	Input	Upregulated Cytokines	Surface Markers	Function
M1	IFNγ, LPS-TLR4 signaling, TNFα	IL-1, IL-6, IL-12, IL-15, IL-23, and TNFα	CD16, CD32, CD86, MHC II	Inflammatory, phagocytosis, acidification of phagosome and release of reactive oxygen species
M2a	IL-4, IL-13	TGFβ, IL-10, IL-1Ra, fibronectin 1, IGF1, PDGF	YM1, YM2, CD163, CD206	Immunity against parasites, growth stimulation, tissue repair
M2b	Immune Complexes, IL-1β or LPS	IL-10, TNFα, IL-1β, IL-6	CD80, CD86, MHC II, CD163	Pro- and anti-inflammatory function, B cell class switch, recruitment of regulatory T cells
M2c	IL-10, TGFβ, Glucocorticoids	IL-10, TGFβ	CD163, CD204, CD206	Debris scavenging, pro-healing, immunosuppresion

Factors that can directly affect macrophage differentiation include the types of particulates and pathogens that are phagocytosed, as well as signaling cytokines released by initial responders. [15, 17, 27-29, 52] While previous studies have shown that stimulating macrophages *in vitro* with IL-4 and IL-13 results in alternatively activated

macrophages [16, 52], one group of researchers showed that the outcome can be confounded depending on the presence and timing of a "danger" signal such as LPS. When macrophages were pretreated with IL-4 and then stimulated with LPS, there was a significant increase in TNFα and IL-12, indicating a skew towards a pro-inflammatory response. However, when macrophages were treated with LPS and IL-4 simultaneously, there was a sharp decrease in TNFα and IL-12 production.[40, 53] These results highlight the sensitivity of macrophages to the multiple stimuli that could be encountered *in vivo*.

2.1.2 Role of Fc Receptors

The Fc gamma receptor (FcγR) on macrophages recognizes the crystallizable fragment of IgG antibody molecules [39]. There are also additional Fc receptors on macrophages capable of recognizing other classes of antibodies. Antibodies are produced by B cells in response to encounters with presented antigen. B cells will originally produce IgM and IgD before antigen presentation which will lead to class switching. As a result of this, the B cells will now produce IgG, IgA, or IgE. [8, 9] Fc binding by macrophages initiates a number of signaling pathways [54] that lead to actin-myosin driven phagocytosis [55, 56]. FcR-mediated phagocytosis of opsonized particles proceeds through both biomolecular and biophysical pathways that result in engulfment of the opsonized particle within a phagosome. The ligation of Fc receptors has also been shown to decrease production of IL-12 and increase the production of IL-10 [57]. Ligation of FcRs has also been shown to drive T-cells into a Type 2 Helper T cell (TH2) phenotype [58], which leads to clonal expansion of B-cells and affinity maturation of produced antibody [59] and clearance of extracellular bacteria and parasites [60]. The Fc portions of immune complexes are also known activators for various components of the complement system, which then also aid in the recruitment of macrophages [61]. Another study on the effects of FcRs in relation to *Mycobacterium bovis* and *Leogionella*

pneumophilia suggested that engaging the FcγR triggers downstream cell signaling that results in increased levels of lysosome maturation. [62]

2.2 Complement System

The complement system represents another key, yet sometimes overlooked, component of the innate immune response. The complement system comprises a group of proteins that can become activated through one of three pathways: the classical, alternative, or lectin pathways (Figure 1). [22, 23, 63, 64] Both the classical and lectin pathways use C4 and C2 components, but recognize different binding sites. The classical pathway is typically activated through binding and formation of C1 proteins on the Fc regions of IgM or IgG molecules that have deposited on a cell or material surface. The lectin pathway was only recently discovered in 1990 and was found to activate through pattern recognition of mannose lectin regions on foreign pathogens. Finally, the alternative pathway becomes activated when the C3 component undergoes hydrolysis and cleaves into its active components, which periodically binds and unbinds to surfaces, and does not receive an inhibitory signal. Once one of these pathways is triggered, the complement proteins are catalytically activated in a cascade-type manner. The result of this activated cascade is the deposition of proteins (C5b-9) on the surface of the pathogen and the formation of the membrane attack complex, also known as a terminal complement complex (TCC), on the surface of the pathogen. The TCC forms a transmembrane channel resulting in the lysis of the pathogen. [22, 23]

These deposited complement component proteins also interact with other immune cells such as macrophages to aid in the clearance of the targeted pathogen. [23, 33, 63, 64] Recent studies have also shown that complement activation also plays a key role in the body's response to tumors [23, 65, 66] and improves the effectiveness of vaccines by acting as an adjuvant [12, 13].

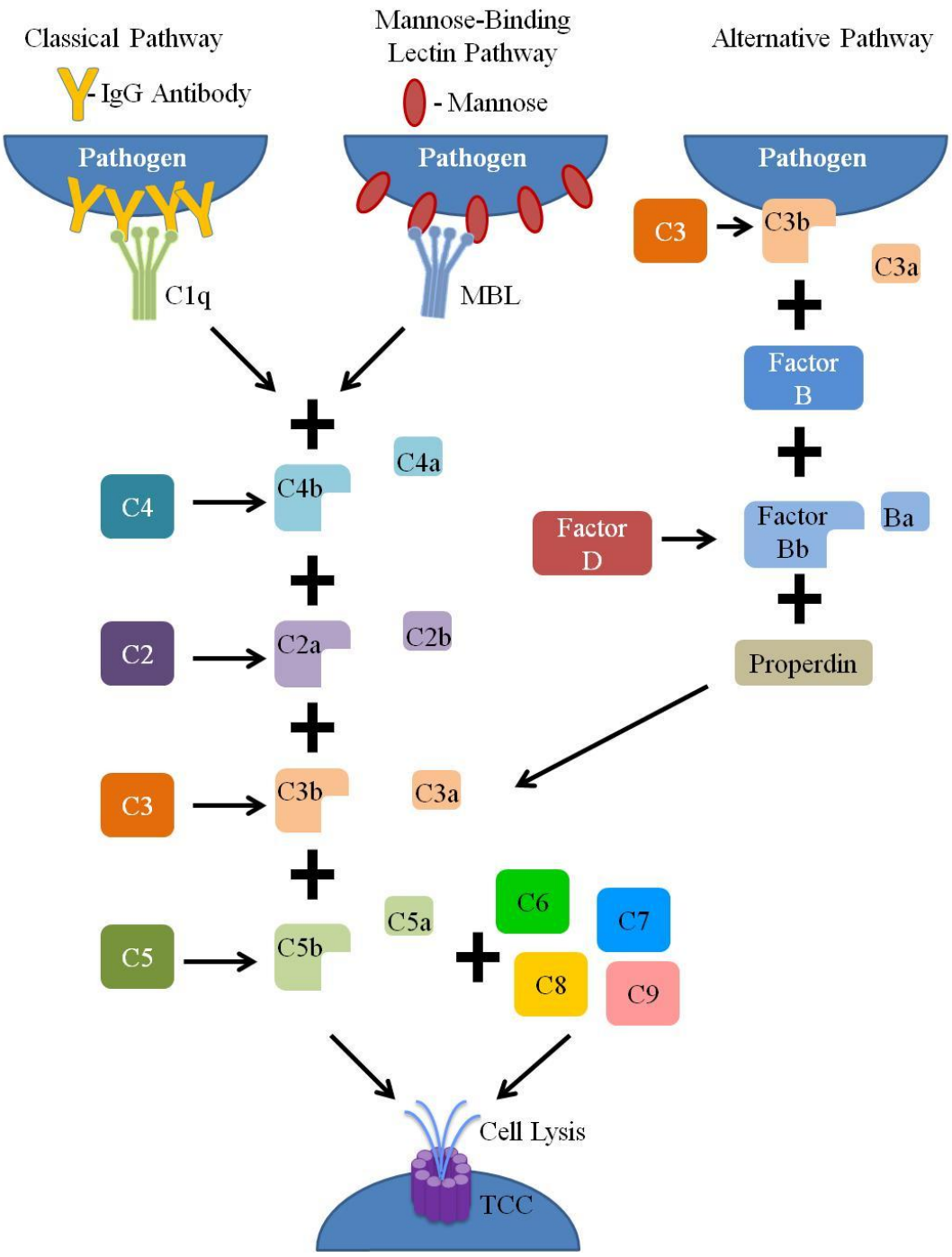

Figure 1: Overview of complement system activation pathways. The schematic illustrates the three different pathways of complement system activation which penultimately results in the formation of the terminal complement complex and subsequent cell lysis.

2.3 Microparticles for Immunomodulation

Biomaterials is an ever expanding field of applying biology and engineering design to create novel solutions to tissue regeneration, wound healing, drug delivery, imaging, and a wide variety of other biomedical goals. [41, 45] Particle based platforms can utilize multiple physical and chemical properties to generate a desired response. [26, 30, 37, 67, 68] Applications utilizing immunomodulation include both activating the immune response, for example in the case of adjuvants, or suppressing the activation of immune cells, for example to combat autoimmune disease. [69, 70] Microparticles have successfully been coated with antibodies that bind to cell specific receptors, such as anti-DEC-205 for dendritic cells [71] and anti-CD3 for T-cells [72], in order to increase cell activation and particle uptake. The size of the particle has also been shown to be a key factor in a variety of immune processes such as phagocytosis [26, 30, 73, 74] and lymphatic uptake [13].

Current biomaterials related research has focused on evaluating macrophage phenotype in response to biomaterial implantation with the goal of reducing the inflammatory state [2, 27, 75]. Previous studies have shown that administering particles, specifically poly(D,L-lactic-co-glycolic acid) (PLGA) particles, can enhance maturation of dendritic cells. [76] This would suggest that particles can be used to drive a specific cell phenotype. One recent study demonstrated plating macrophages onto different micropatterned surfaces could alter the macrophage phenotype, indicating that purely physical factors such as particle size may affect macrophage differentiation. [77] The driving factors affecting macrophage phenotype only highlight the complicated feedback system controlling cell signaling and the opportunities for a platform that can induce a specific phenotypic response.

A study on the effect of liposome surface charge showed that positively and negatively charge surfaces activated the classical and alternative pathway, respectively while neutral liposomes did not activate any of the complement pathways. [78] Others

have shown that different particle materials are capable of activating the complement system in various degrees. [13, 79, 80] One group specifically showed that polyhdroxylanted nanoparticles were able to successfully activate the complement system by binding to the C3b component. However polymethoxylated nanoparticles were not successful in complement system activation. The resulting complement system activation also increased vaccine efficacy by having an adjuvant effect. [13] The complement system also becomes activated by bulk surfaces. In one study, bulk polystyrene was used as model biomaterial and the ensuing complement system activation was determined to derive from the interaction of proteins that had adsorbed from plasma. [81]

2.4 Bacillus Calmette Guerin

Mycobacterium tuberculosis, the agent that causes tuberculosis (TB), is the most devastating bacterial pathogen of humans. It is responsible for nearly 1.5 million deaths and 8 million new infections each year worldwide. Currently, there is one approved vaccine for human use against tuberculosis: the Bacillus Calmette-Guerin (BCG) vaccine, an attenuated strain of *Mycobacterium bovis*. While this vaccine is effective when administered to infants, the efficacy of the vaccine is greatly diminished in adulthood. In fact, reports on the efficacy of the vaccine vary from 0-80%. [19-21, 49] This wide range in efficacy highlights a need for vaccine and/or adjuvant alternatives; several have been tried including modified BCG, modified *M. tuberculosis*, subunit vaccines, naked DNA and viral-vectored vaccines, and double stranded RNA capsids. [21] BCG itself is an attenuated strain of *M. bovis*. [49, 82] The body of work studying this issue indicates that the lack of immunological response is due to the ability of *M. tuberculosis* to reduce the amount of MHC II presentation on antigen presenting cells, such as macrophages, and that adjuvants that non-specifically activate APC's or promote cross priming of immune cells through both MHC I and II presentation may lead to a more effective immune response. [21, 83] Additionally, the BCG strain may have lost too much antigenicity due

to a high passage history, so some have focused on increasing the presentation of antigen.[49] In support of this hypothesis, one study showed that tissue resident macrophages and dendritic cells did not interact strongly with BCG after intradermal vaccination [82]. Therefore, increasing the interaction between these resident immune cells and the vaccine would likely improve vaccine efficacy.

CHAPTER 3 FC OPSONIZED MICROPARTICLES AFFECT MACROPHAGE PHAGOCYTOSIS AND PHENOTYPE[1]

3.1 Introduction

Uptake of particulate debris, fluid, and foreign substances by macrophages is a key aspect of the innate immune system [38, 39]. Macrophages are important generalist, first responder cells in the body that serve both recognition and degradative functions. Through recognition, engulfment, and processing of either self or non-self substances, macrophages remove waste; initiate, coordinate, regulate, and/or participate in immune responses; and monitor the body for deviations from homeostasis [84].

Biomedical applications that directly utilize phagocytosis stand to be substantially improved through greater understanding of the internalization process [85-87]. Particle internalization can be initiated through multiple pathways including toll-like receptors, scavenger receptors, complement receptors, chemokine or interleukin receptors, and the Fc receptor (FcR), which recognizes the crystallizable fragment of IgG antibody molecules [39]. Fc binding by macrophages initiates a number of signaling functions [54] that lead to actin-myosin driven phagocytosis [55, 56]. FcR-mediated phagocytosis of opsonized particles proceeds through both biomolecular and biophysical pathways that result in engulfment of the opsonized particle within a phagosome. After lysosome fusion to form a phagolysosome, oxidative, proteolytic, acidic, and other degradative processes decompose the engulfed substance [38, 39, 56]. The role of macrophages within the total immune response is broad, involving recruitment of many different cell types and

[1] Adapted and Modified from Pacheco, Patricia, David White, and Todd Sulchek. "Effects of microparticle size and Fc density on macrophage phagocytosis." PloS one 8.4 (2013): e60989.

interaction with cellular and molecular components to resolve the perceived "danger signal" [88]. For example, the Fc portions of immune complexes are also known activators for various components of the complement system, which then positively feeds-back to aid in the recruitment of additional macrophages [61]. Macrophages also assist in the progression from innate to adaptive immune responses. The ligation of Fc receptors decreases production of IL-12 [57], a cytokine key for the development of Type 1 helper T cell (Th1) phenotype [58, 89] while also driving T-cells into the Type 2 helper T cell (Th2) phenotype [58]. Th2 cell development subsequently leads to clonal expansion of B-cells and affinity maturation of produced antibody [59], aiding in the clearance of extracellular bacteria, viruses, and parasites [60].

Macrophages perform two important tasks through phagocytosis: sequestration and degradation of self particles (e.g. dead cells and debris), and elimination of foreign, non-self matter. In principle, both tasks proceed through a combination of physical cues, such as particle size, shape, and deformability [68], as well as biological cues such as recognition of pathogen-associated molecular patterns (PAMPs) or opsonized particles [39]. Therefore, it is likely that both physical and biological mechanisms are significant to regulating phagocytosis in macrophages. Understanding the biophysical and biological cues which trigger macrophage phagocytosis is important to improved utilization of phagocytosis in therapeutic microparticle delivery to macrophages.

Micro- and nanoparticles are commonly used and studied in the field of biomaterials, and specifically the study of phagocytosis, for applications such as drug delivery, vaccine delivery and development, and cancer therapies [67, 69, 90, 91]. Microparticles have long been used to study phagocytosis [30, 68, 92-94] in part due to their chemical and physical uniformity as well as their application in clinical settings. Multiple modeling studies on phagocytosis of particles, including computational models of 4-100 nm particles [95-97] and 3-11 μm particles [74, 98-100], which include consideration of the effects of cell cytoskeleton and ligand density on phagocytosis.

Experimental validation of these approaches which combine the effect of particle size and receptor density has been more limited. Previous experimental studies of Fc-mediated phagocytosis using microparticles [56, 93] did not examine the importance of the density of Fc ligands in conjunction with the size of the particle. Increasing the density of Fc on opsonized sheep erythrocytes caused macrophages to increase production of IL-10 and decrease production of IL-12 [32]. However in this study the effect of size and shape of the erythrocyte on phagocytosis was not explicitly examined or decoupled from Fc density. Other studies have shown that the shape of the particle can have a strong effect on phagocytosis [68]. In another study, the Fc density was varied on a spherical particle to understand the effects on cell signaling and commitment of the macrophage to phagocytosis. This study utilized 5.6 μm polystyrene particles with two different Fc densities and found that a high Fc density led to complete closure of the phagosome around the microparticle while a low Fc density resulted in binding of the particle to the macrophage but not internalization [93]. Numerous studies on phagocytosis have shown that particle size greatly affects the average number of microparticles internalized by the macrophage [30, 68, 90], but these did not address the impact of Fc density on internalization. Modeling and experimental approaches found that smaller particles are uptaken through both passive and active zipper mechanisms [74]. This study also found that actin polymerization is important for more regular phagocytic cups as it stabilizes receptor-ligand binding and suggests that active phagocytosis enables faster engulfment of the particle.

To evaluate the hypothesis that both Fc density and particle size significantly impact internalization by macrophages and macrophage phenotype, we investigated the effects of Fc ligand surface density on phagocytosis for a variety of particle sizes. As macrophages may utilize different physical and biochemical mechanisms for clearing foreign objects of a wide range of sizes (submicron to greater than 5 μm), we explicitly decoupled the effects of the physical signal resulting from particle size and the biological

signal resulting from variation in Fc density. By decoupling the biological and physical signals, we can better optimize particle-mediated delivery of therapeutic payloads to macrophages.

3.2 Materials and Methods

3.2.1 Microparticle Opsonization

Carboxylated yellow-green fluorescent polystyrene microparticles were purchased from Polysciences. To examine the effects of a broad range of sizes on internalization efficiency, we used 0.5 μm, 1 μm, 2 μm, 3 μm, and 4.5 μm particles. A schematic showing the Fc opsonization process is shown in Figure 1. For phenotype studies, nonfluorescent polystyrene microparticles, 0.5 μm and 1 μm, were purchased from Bangs Laboratories. The microparticles were incubated in a 1-2 mg/mL bovine serum albumin (BSA) (Sigma Aldrich) solution to adsorb a layer of antigen onto the particle surface. The concentration of BSA was chosen to be 10 times the saturating concentration for the amount of beads, as determined from manufacturer's specifications using the equation below (Equation 1).

$$S = (6 / \rho D)(C) \qquad \text{Equation 1}$$

Where S is the amount of protein required to saturate the particle surface, ρ is the density of the particle, D is the diameter of the particle, and C is the capacity of the particle for a specific protein. For BSA, the value of C was set as 3 mg/m^2 in accordance with the manufacturer's specifications. The concentration of BSA was increased in direct proportion to the total microparticle surface area to remove the density of the antigen as an experimental variable. To create particles with different densities of exposed Fc domains (i.e. different valencies), sheep (Abcam) or rabbit (Life Technologies) polyclonal anti-BSA IgG antibody was added in decreasing antibody mass to BSA mass

ratios thereby producing a range of exposed Fc densities, or Fc density ratio. We identified a 1:1 ratio of added antibody to antigen that represents a condition of maximum Fc coverage. Dilutions of 1:2, 1:5, 1:10, and 1:50 ratio of added antibody to antigen were tested. For later experiments a molar ratio was followed with 2 moles of antibody to 1 mole of BSA, or a 2:1 ratio, identified as correlated to a maximum Fc coverage. The 2:1 molar ratio was found to be within 10% of added antibody of the 1:1 weight ratio. No added IgG, or a 0:1 ratio, indicates microparticles coated only with BSA antigen. A table of the amount of BSA antigen and opsonizing antibody added to each particle size is shown in Supplemental Figure 2. Microparticles were incubated with protein at room temperature for at least 2 hours in phosphate buffered saline (PBS) at a pH ~7.2 for all protein-binding steps. After each binding step, the microparticles were washed three times by centrifugation and PBS exchange. We observed only slight particle clustering in the case of 0.5 μm particles and negligible clustering for particles of other sizes. To verify the availability of Fc domains and to quantify the amount of Fc presented on each microparticle, a 10 μL aliquot from each Fc density condition was incubated with a TexasRed fluorescently labeled rabbit anti-sheep IgG secondary antibody or DyLight 650 labeled donkey anti-rabbit (Abcam). This process was repeated to create duplicate or triplicate particle groups.

3.2.2 Cell Culture

RAW 264.7 murine macrophages were used in the internalization assay. These cells were a gift from the lab of Niren Murthy and were originally purchased from ATCC (Manassas, VA). The cells were cultured in complete media composed of DMEM (Sigma Aldrich, St. Louis, MO) supplemented with 10% fetal bovine serum (FBS) (Atlanta Biologicals, Atlanta, GA) and 0.1% penicillin/streptomycin (P/S), and were grown in a humidified incubator at 37°C with 5% CO_2. For the internalization assay, cells were plated in a standard 6-well tissue culture plate at a density of approximately $3x10^5$ cells

per well. The cells were incubated in complete media for 24-48 hours until fully adherent. Supernatants were aspirated and the plates were washed twice with PBS. After the final aspiration, 0.5 mL of fresh DMEM followed by the microparticles, were added to each well.

L929 murine fibroblast cells were cultured as a source for M-CSF for bone marrow derived macrophage differentiation. These cells were purchased from ATCC and then grown in DMEM supplemented with 10%FBS and 1% P/S within a humidified incubator at 37°C and 5% CO2. The cells were initially plated at 470,000 cells were plated per 75cm^2 tissue culture treated flask. After one week, the cells were replated and the conditioned media was collected and passed through a 0.8 μm filter. The L929 conditioned media was then aliquoted and stored at -20°C.

Bone marrow derived macrophages were generated using previously published methods. [101, 102] The femurs and tibias from 5-8 week old female C57Bl/6 mice (IACUC A13005) were isolated and cleaned. The ends of each bone were clipped to expose the marrow. The basal media of DMEM/F-12 was used to fill a 10 mL syringe and was then passed through a 25G needle inserted into the bone marrow. This allowed us to flush out the bone marrow into a sterile petri dish. The bone marrow solution was then passed through an 18G needle multiple times to break up any clumps. We then transferred the solution through a 70 μm cell strainer into a 50 mL conical tube. The cell solution was then pelleted through centrifugation at 300G for 10 minutes. Following media decantation, the cells were resuspended in red blood cell lysis buffer at approximately 2.5 mL per animal. The cell solution was centrifuged at 300G for 5 minutes and then washed with DMEM/F-12 twice. After the final wash, the differentiation media was then added and cell concentration determined using a hemocytometer. The differentiation media was composed of DMEM/F-12, 10% FBS, 1% penicillin/streptomycin, and then supplemented with 20% L929 conditioned media. The collected bone marrow cells were plated in 10 cm non-tissue culture treated plastic petri

dishes at a concentration of 500,000 cells/mL in 10 mL. Cells were grown in a humidified incubator at 37°C and 5% CO2. On day 3, 5 mL of fresh differentiation media was added. On day 7, the dishes were washed with PBS to remove non-adherent cells, and fresh differentiation media was added. The cells were then removed by gently scraping as cell detachment solutions that were either enzymatic, such as trypsin and trypsin-EDTA solutions, or non-enzymatic, such as CellStripper (Corning), were found to be ineffectual and detrimental to cell health. The cells from all dishes were then collected in 50 mL conical tubes and centrifuged at 300 G for 10 minutes. The media was decanted and fresh differentiation media was added again. Cells were counted using a hemocytometer and the volume was adjusted to a concentration of 5E6 cells/mL. Approximately 1E6 cells were plated per well on a 6-well plate in differentiation media and allowed to incubate overnight prior to experiment. Successful macrophage differentiation was determined by adding fluorescently labeled antibodies for macrophage specific cell surface markers, including PE labeled F4/80 and PerCP-Cy 5.5 labeled CDllb antibodies. Macrophages were first incubated with anti-CD16/32 to block Fc receptors and a PerCP-Cy 5.5 anti-rat IgG2b K was used as an isotype control. This staining procedure showed that our differentiation technique yielded an over 80% macrophage purity sample.

3.2.3 Internalization Assay

Approximately 20-25 microparticles per cell were added to each well of plated macrophage cells for each condition tested. The cells and microparticles were gently mixed and then allowed to interact in a humidified incubator at 37°C with 5% CO_2 for approximately 1 ½ hours. A duplicate set of plated samples were incubated at 4°C to determine the rate of microparticle adhesion. After the incubation period, the well contents were aspirated and washed with PBS twice to remove particles that did not interact with the adherent cells. 1 mL of PBS was added after the final washing was

complete. The well was then scraped using a standard cell scraper and the entire contents were transferred to a microcentrifuge tube for analysis using flow cytometry. The internalization assay is illustrated in Figure S1 and was repeated 4 times for each Fc density and size condition.

3.2.4 Flow Cytometry

All samples were analyzed using a flow cytometer (Accuri C6) immediately after microparticle-cell incubation, collection, and mixing. To measure the amount of TexasRed-labeled secondary antibody per microparticle, the 630 ± 30 nm bandpass filter (suitable to detect TexasRed) was used in conjunction with the 533 ± 30 nm bandpass filter to detect the yellow-green fluorescence of the microparticle core. As the TexasRed emission spectrum overlaps part of the yellow-green fluorescence of the particles, results were compensated by subtracting the overlapping signal of the secondary antibody from that of the particle using the compensation tool in the CFlowPlus software (BD, Franklin Lakes, NJ). Due to high levels of overlapping fluorescence from the particle and secondary antibody, non-fluorescent microparticles and a FITC-labeled secondary antibody were used to estimate the density of exposed Fc on non-fluorescent particles. Flow cytometry was also used to estimate the particle concentration for each condition. To determine the number of microparticles phagocytosed for each Fc density condition and particle size, the populations were analyzed using forward scatter and microparticle core fluorescence. Events were gated on forward scatter to separate the larger cells from the smaller microparticles. Three populations were delineated: macrophage cells alone, microparticles alone, and microparticles collocated with cells. The number of microparticles per cell was then determined by measuring the mean fluorescent intensity (MFI) of the dual-signal population and dividing it by the average MFI of one particle within the dually-positive population, in accordance with previous methods [103].

ANOVA followed by Tukey-Kramer HSD post analysis was performed to determine significance using JMP software (SAS, Cary, NC).

3.2.5 Microscopy

In preparation for fluorescence microscopy and confocal microscopy, cells were plated onto sterile coverslips within a 6-well plate before the internalization assay. Each well was then washed with PBS 3 times and 0.5 mL of PBS added to each well after the final washing. The cells were stained in a 5 μg/mL solution of a lipid specific cell membrane stain, FM4-64X (Invitrogen, Carlsbad, CA) for 1 minute. After the incubation period, the cells were fixed with a 4% paraformaldehyde solution for 10 minutes and then rinsed 3-5 times with PBS. The cells were then treated with 4',6-diamidino-2-phenylindole (DAPI) to stain nuclear DNA. After a short incubation period, the coverslips were then removed from the well and transferred to a standard microscope slide. The stained cells were visualized with a Nikon Ti epi-fluorescence microscope and Zeiss LSM 510 VIS confocal microscope. Images were processed with the Nikon Elements and Zen Lite 2011 software.

3.2.6 Macrophage Phenotype Conditions and Cytokine Production

Approximately 20 microparticles per cell were added to each well of plated bone marrow derived macrophage cells for each condition tested. The 0.5 μm and 1 μm particles sizes and 2:1, 1:1, 1:5, and 0:1 (BSA only) antibody to antigen molar ratio were tested to determine their effect on macrophage cytokine production and predict macrophage phenotype. LPS (Sigma), at a final concentration of 1μg/mL, was used as a positive control for a M1, classically activated macrophage, and IL-4 (Antigenix), at a final concentration of 10ng/mL, was used a control for a M2, alternatively activated macrophage. The bone marrow derived macrophages and microparticles or chemical stimulus were gently mixed and then allowed to interact in a humidified incubator at 37°C with 5% CO_2 for approximately 4 hours. To determine if Fc coated particles are

capable of shifting the response of classically or alternatively activate macrophages, after an initial 4 hour incubation with LPS or IL-4, 0.5 μm and 1 μm particles with a 2:1 antibody to antigen Fc coating were added for an additional 4 hours. These phenotype incubation studies were repeated 3 times with duplicate wells for each condition. After the incubation period, the media from each well was collected and centrifuged at 1500 RPM for 10 minutes. The supernatant was then collected and frozen at -80°C for future cytokine secretion analysis. The wells were then washed with PBS twice to remove particles that did not interact with the adherent cells. Cell lysis buffer was added after the final washing and RNA collected using the RNeasy kit (Qiagen) in accordance with manufacturer's instructions. RNA purity and concentration was determined using a NanoDrop by measuring absorbance at 230 nm, 260 nm, and 280 nm. cDNA was then synthesized using the iScript Advanced cDNA Synthesis Kit for RT-qPCR (BioRad) to produce 500ng of cDNA for each condition. Qualitative real-time polymerase chain reaction was carried out using the Fluidigm 96.96 Gene Expression Profiling Chip using primers purchased through Fluidigm. The complete list of primers tested is listed in Table 2 and all primers were tested in triplicate on the chip. The threshold cycle (C_T) values were provided for each condition and cytokine or receptor as a result of the Fluidigm 96.96 Gene Expression Chip analysis. All values with a "Pass" rating were used to calculate the average C_T values for each condition and cytokine or receptor. These values were then used to calculate the fold change in mRNA expression for each cytokine or receptor and uploaded into the RT^2 Profiler PCR Array Data Analysis online tool (Qiagen) to calculate significance and cluster plots. To confirm that mRNA expression level corresponds to secreted protein amount, an ELISA (eBiosciences) was performed, according to manufacturer's instructions, to test for the following cytokines: TNFα, IL-1α, IL-10, and IL-12.

Table 2: Primers used for qRT-PCR Analysis

Gene Symbol	Reference Sequence ID
GAPDH	NM_008084.2
ActB	NM_007393.3
RPL13a	NM_009438.5
IL-18	NM_008360.1
IFN α	NM_010502.2
IFN β	NM_010510.1
IL-10	NM_010548.2
IL-12a	NM_001159424.1
IL-12b	NM_008352.2
TGF β	NM_011577.1
Nos-2	NM_010927.3
IL-6	NM_031168.1
IL-1α	NM_008361.3
IL-1β	NM_010554.4
IL-1ra	NM_001039701.3
TNFα	NM_013693.2
FcGr	NM_010186.5
IL-27b	NM_009438.5

3.3 Results

3.3.1 Fc Density Increases with Antibody to Antigen Ratio

The Fc density was estimated for each surface dilution and particle size using the MFI of the secondary antibody signal that was normalized to the maximum saturated value. The normalized MFI decreased as the Fc was diluted both for the larger particles (4 μm) and smaller particles (1 μm). (Figure 2 and Figure 3: Normalized mean fluorescent intensity to surface area and maximum Fc density.) These data indicate that Fc density was successfully manipulated for each particle size. Similar trends in Fc density were observed by flow cytometry for the fluorescent particles of all sizes used in the internalization assays (Figure A 1, A 2).

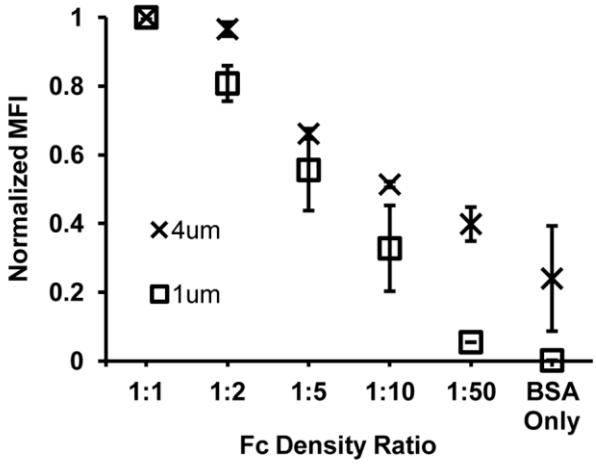

Figure 2: Normalized mean fluorescence intensity of microparticles labeled with fluorescently conjugated secondary antibodies. Decreasing normalized MFI corresponds to decreased Fc density for fluorescent particles. Due to possible non-specific absorption of the secondary antibody and difficulty in fully compensating for the high background fluorescence of the microparticle core, nonfluorescent microparticles were also opsonized and labeled thereby confirming our initial results.

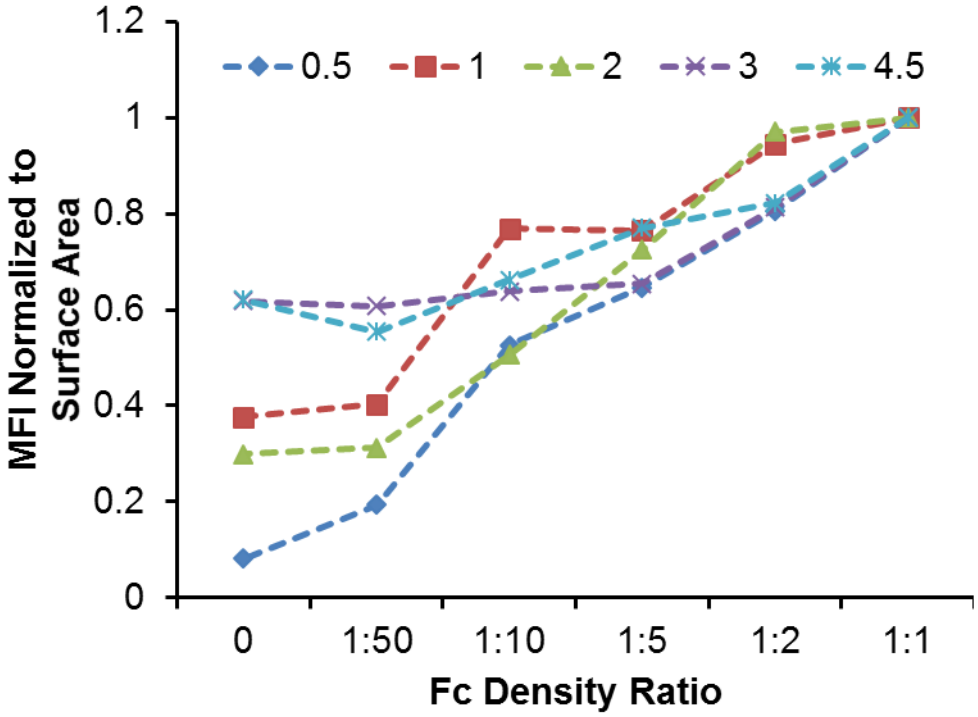

Figure 3: Normalized mean fluorescent intensity to surface area and maximum Fc density.
Confirms that as the Fc density increases, the normalized MFI increases as well. The MFI for each Fc condition and particle size was first normalized by the particle surface area and then normalized to the value for the highest Fc density of 1:1.

3.3.2 Effects of Fc Density on Microparticle Adhesion to Cell Surface

To determine the influence of Fc density and particle size on microparticle adhesion to macrophages, we performed the same internalization assay at 4°C, a temperature which inhibits internalization but not attachment [30, 94]. The average number of microparticles attached per cell was estimated from flow cytometric analysis for each Fc density and particle size condition (Figure 4). ANOVA was conducted to examine the independent effect of Fc density and particle size on cell attachment. Attachment of the 0.5 μm particles was significantly greater than that for the other four sizes. High Fc density also increased attachment of the 1 μm particles, but it did not enhance adhesion for the other particle sizes. Therefore, Fc does not play a strong role in particle attachment, with the exception of 1 μm particles at high density of Fc. However,

the lack of cellular activity at this temperature (active engulfment, receptor recruitment, etc.) may alter the adhesive properties at physiological conditions.

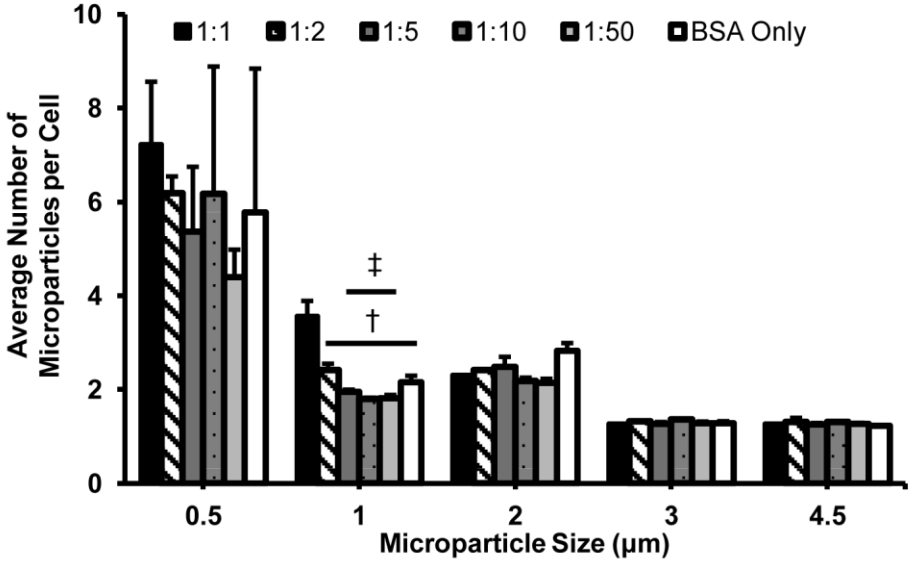

Figure 4: Average number of attached microparticles for each particle size and Fc density condition. As particle size increases, so does the degree of attachment. Overall, Fc density was not a significant variable for opsonized and BSA-only particles. †- Significantly different (SD) from 1:1, ‡- SD from 1:2, with $p < 0.05$, (N=2)

3.3.3 Effects of Fc Density on Microparticle Internalization

The average number of microparticles internalized per cell was measured with an internalization assay at 37 °C (Figure 5a). ANOVA of the average number of microparticles internalized per cell showed that both size and Fc density are significant variables at physiological temperatures. For smaller and medium-sized particles (0.5 μm, 1 μm, and 2 μm), the number of microparticles internalized per cell was significantly greater for the higher Fc density conditions of 1:1 and 1:2 than the lower Fc density conditions of 1:10 and 1:50. There was a significant decrease in the average number of microparticles internalized per cell for the 3 μm and 4.5 μm particles. Fc density was not a significant factor in the internalization of larger 3 μm and 4.5 μm particles. In addition, larger particles (3 μm and 4.5 μm) were generally internalized at lower numbers than small and medium-sized particles (0.5 μm, 1 μm, and 2 μm), for a given Fc condition.

However it should be noted that the medium-sized 2 μm particles showed an increase in internalization of BSA-only coated samples.

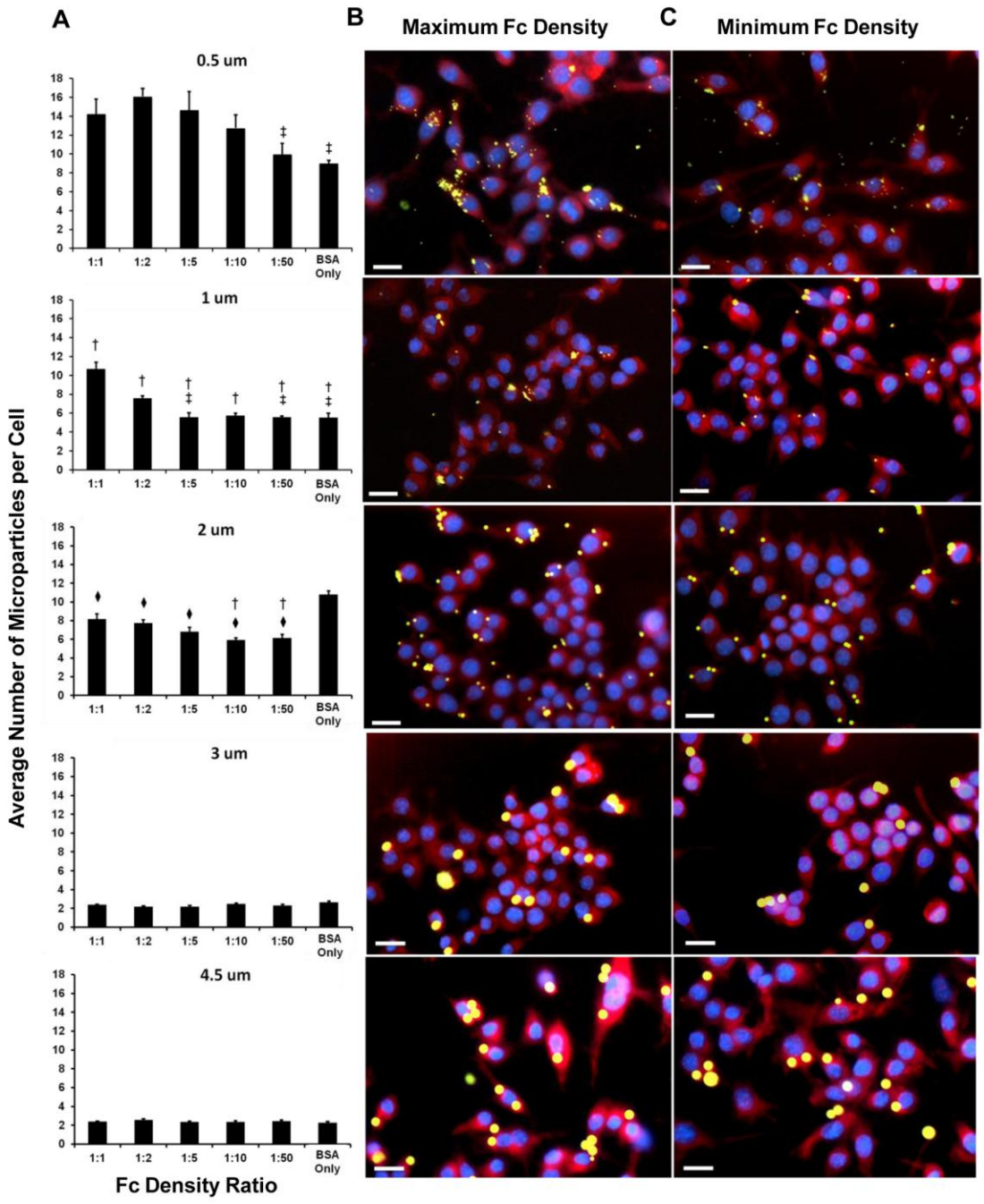

Figure 5: Average number of microparticles internalized per cell for each particle size and Fc density condition.

(A) Average number of microparticles per cell for each particle size for the various Fc density conditions. (†- Significantly different (SD) from 1:1, ‡- SD from 1:2, ♦- SD from BSA Only, with $p < 0.05$). These values were also illustrated through fluorescent microscopy by comparing images taken of RAW264.7 macrophages incubated with Fc functionalized particles. (B) Representative images for each size with the maximum Fc density ratio of 1:1. (C) Representative images for each size with the minimum Fc density ratio of 1:50. Scale bar represents 20 um. (N=4)

Representative images of the macrophages and microparticles after incubation are shown for the high Fc density ratio of 1:1 and the low Fc density ratio of 1:50 (Figure 5b, c). Inspection of these images illustrate the extent to which internalized microparticles are not distributed equally among macrophages, but instead tend to be phagocytosed by a subset of cells, especially for smaller particles functionalized with a high Fc density.

While the average number of phagocytosed microparticles per cell was significantly reduced for large particle sizes, the total volume of phagocytosed particles per cell increased with particle size. The total surface area of the internalized particles was also maximal for the 4.5 μm particles (Figure 6).

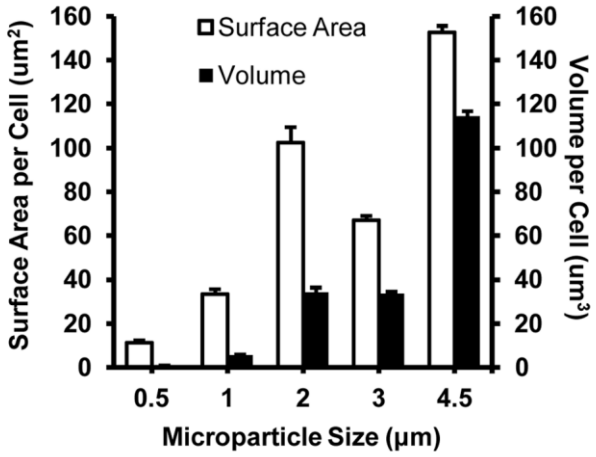

Figure 6: Average total volume and surface area of internalized microparticles.
Average calculated volume and surface area of microparticles internalized for the maximum Fc condition of 1:1 for each particle size. (N=4)

3.3.4 Combined Effects of Fc Density and Microparticle Size on Phagocytic Activity of Macrophages

The previous data show the decoupled effects of particle size and Fc density on the number of internalized microparticles. Since the number of macrophages plated was constant for each tested condition, we were able to compare the percentage of total macrophages that were phagocytic for each treatment using flow cytometry data. We considered a macrophage to be phagocytic if it contained at least one microparticle. The

percentage of phagocytic macrophages was found to be strongly dependent on both the particle size and the particle Fc density (Figure 7a). Interaction with the smaller particles (0.5 μm and 1 μm) at a low Fc density resulted in a greater percentage of phagocytic macrophages than with high Fc density. In contrast, the larger particles (3 μm and 4.5 μm) resulted in a slightly greater percentage of phagocytic macrophages for the high Fc density condition. For the 2 μm particle treated cells, the average percentage of phagocytic macrophages remained relatively constant regardless of Fc density, and was consistently higher compared to the other particle sizes.

Combining the results of macrophage phagocytic activity with the average number of particles internalized shows that for small particles (0.5 and 1 μm) a smaller percentage of the macrophages may be phagocytic, but they internalize a relatively large number of particles. The shift to a higher fluorescence signal for the high Fc density condition, observable for the 0.5 μm, 1 μm, and 2 μm particles, indicates that an increased average number of particles were internalized by phagocytic cells. In addition, there is an increase in the number of non-phagocytic cells seen in the 0.5 μm and 1 μm high Fc density histograms compared to the low Fc density, as indicated by an increased count of low fluorescence events. (Figure 7b) There was no observable shift in fluorescence dependent on Fc density for the larger particles of 3 μm and 4.5 μm. However this was expected as Fc density was a not a significant variable for the larger particles in our internalization studies. These data support the hypothesis that while the smallest particles (0.5 μm and 1 μm) functionalized with the highest Fc density are internalized in greater numbers, a smaller number of macrophages are involved in the internalization process.

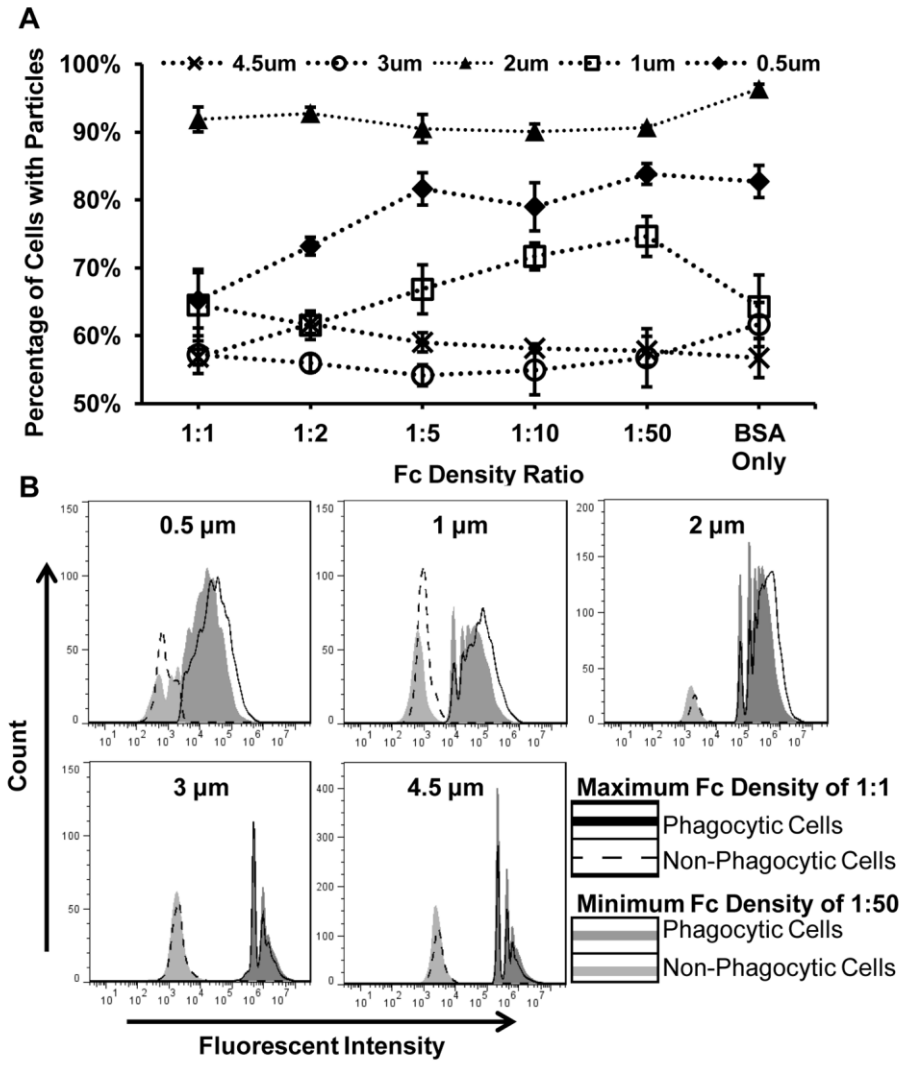

Figure 7: Effects of Fc density and particle size on the macrophage population.
(A) Percentage of phagocytic cells that each Fc density condition for each particle size with a dashed line to illustrate trends. (N=4) (B) Representative histograms of the FITC intensity for macrophages incubated with particles functionalized with the maximum Fc density of 1:1 and the minimum Fc density of 1:50. These histograms illustrate two groups: macrophages that have internalized at least one particle (phagocytic cells) and macrophages that did not internalize a particle (non-phagocytic cells).

3.3.5 Fc density and Microparticle Size Affect Macrophage Cytokine Expression

The results of the mRNA expression analysis suggest that both Fc density and microparticle size do affect expression. The fold change was calculated using two reference genes, GAPDH and RPL13a, as the third reference gene, Actβ, failed across the

chip. While the levels of GAPDH and RPL13a did change across different conditions, the expression did not significantly change when the fold change values were calculated using a single reference gene. A cluster plot showing the overall gene expression shows how the magnitude of expression shifts across all tested conditions (Figure 8). This shows the greatest changes occurring for the LPS and LPS + 1μm 2:1. The fold change graphs for each cytokine or receptor are grouped according to suggested functional phenotype: iNos, IL-12α, IL-12β, and Il-27β associated with M1 macrophages; IL-1α, IL-1β, and IL-6 associated with M1 and M2b macrophages; IL-10, IL-1ra, TNFα, TGFβ, and Fcγr associated with M2a and M2c macrophages; and IL-18, IFNα, and IFNβ associated in some cases with M1 macrophages. [1, 28, 52]

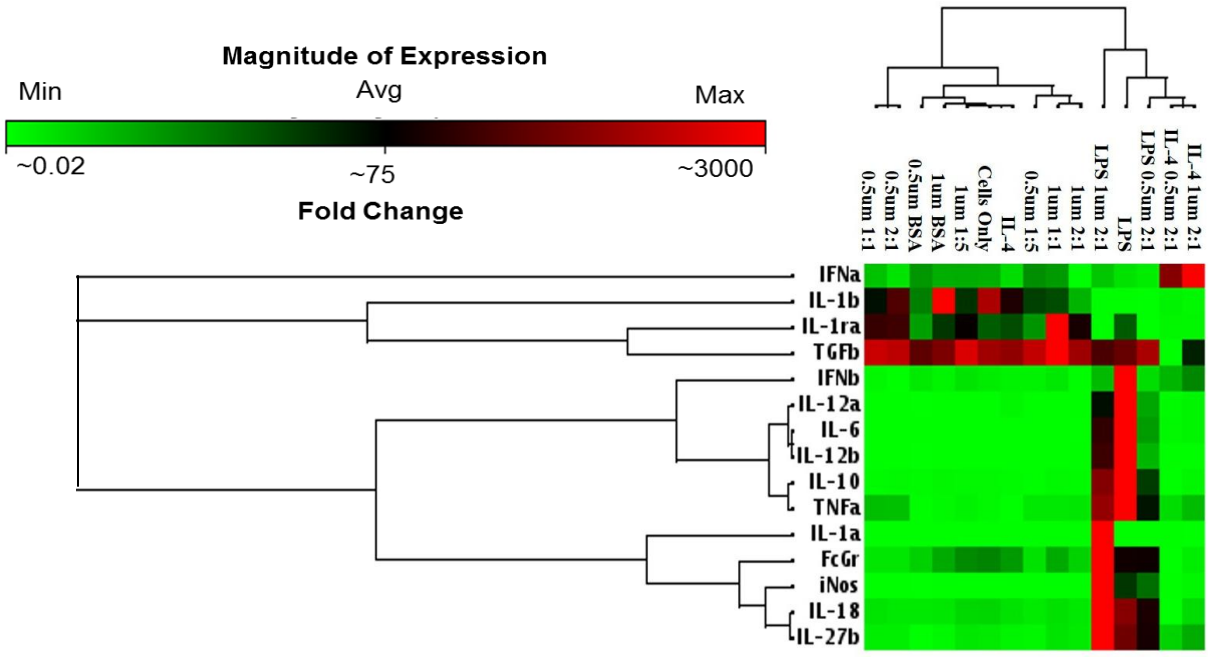

Figure 8: Cluster plot of magnitude of mRNA expression across all conditions

The cluster plot for 0.5 μm treated cells shows that the 2:1 and 1:1 functionalized particles elicited a similar response (Figure 9). It also suggests an inversion in gene expression from the untreated macrophage only group. ANOVA analysis showed the macrophages treated with 0.5 μm 1:1 Fc particles significantly different from the untreated macrophages, and macrophages treated with BSA only or 1:5 Fc particles. The

2;1 Fc condition was also significantly different from the BSA only coated condition. The fold change for each gene and condition compared to the untreated macrophage only group confirms this observation, but there is considerable variation across each condition. The high Fc density conditions of 2:1 and 1:1 resulted in increased expression of iNos, IL-12β, IL-1α, IL-1ra, and TNFα. Compared to the low Fc density 1:5 and BSA only conditions, the high Fc density treated groups resulted in lower expression levels of IFNα, IFNβ, and FcGr. We also see slight variations in IL-27β, IL-1β, IL-10, TGFβ, and IL-18. These small changes seem to be independent of Fc condition and an effect of the particle alone.

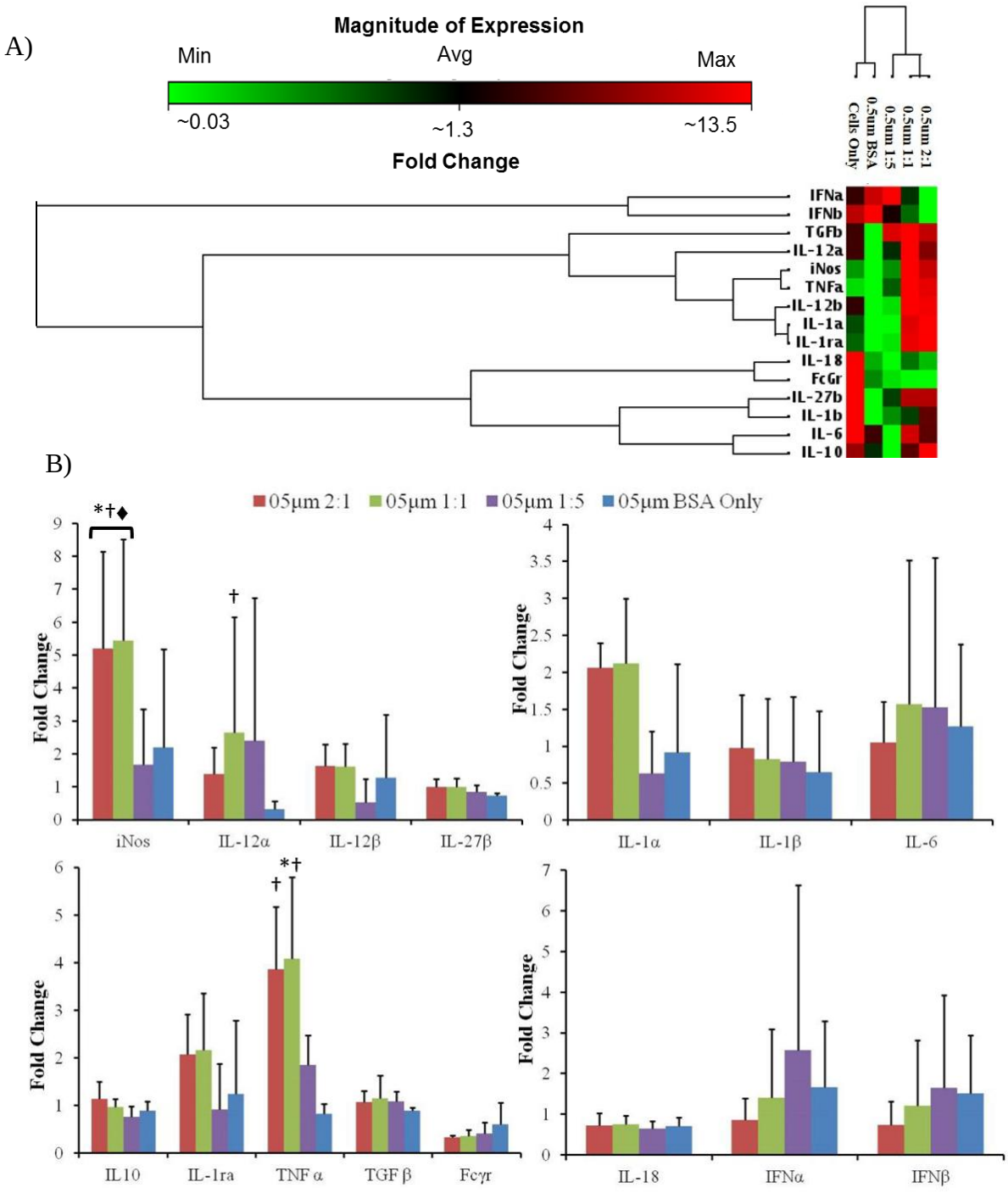

Figure 9: Effects of 0.5 µm particles and Fc density on cytokine and receptor mRNA expression.

(A) Cluster plot shows the shift in magnitude of gene expression and (B) Fold change graphs show expression levels compared to untreated macrophages. *, from Cells Only, †, from BSA Only, ♦, from 1:5, $p<0.05$, error bars represent standard deviation.

The 1 μm particle cluster plot suggests that the 1:1 had the greatest impact on gene expression (Figure 10). ANOVA analysis showed the macrophages treated with 1 μm 1:1 Fc particles significantly different from the untreated macrophages. The plot also shows that the highest Fc density condition of 2:1 resulted in minimal expression of most genes with the exception of TNFα. The fold change values show the same variability seen in the 0.5 μm treated groups. There are less difference between Fc density treatment and expression for a particular gene. The exception appears to be for iNos, IL-12β, and TNFα. Increasing the Fc density resulted in decreasing expression of IL-12α, IL-6, IL-10 and Fcγr compared to macrophages treated with BSA coated particles. Overall, the addition of 1 μm particles resulted in the increased expression of IL-1α and IL-1ra compared to untreated macrophages.

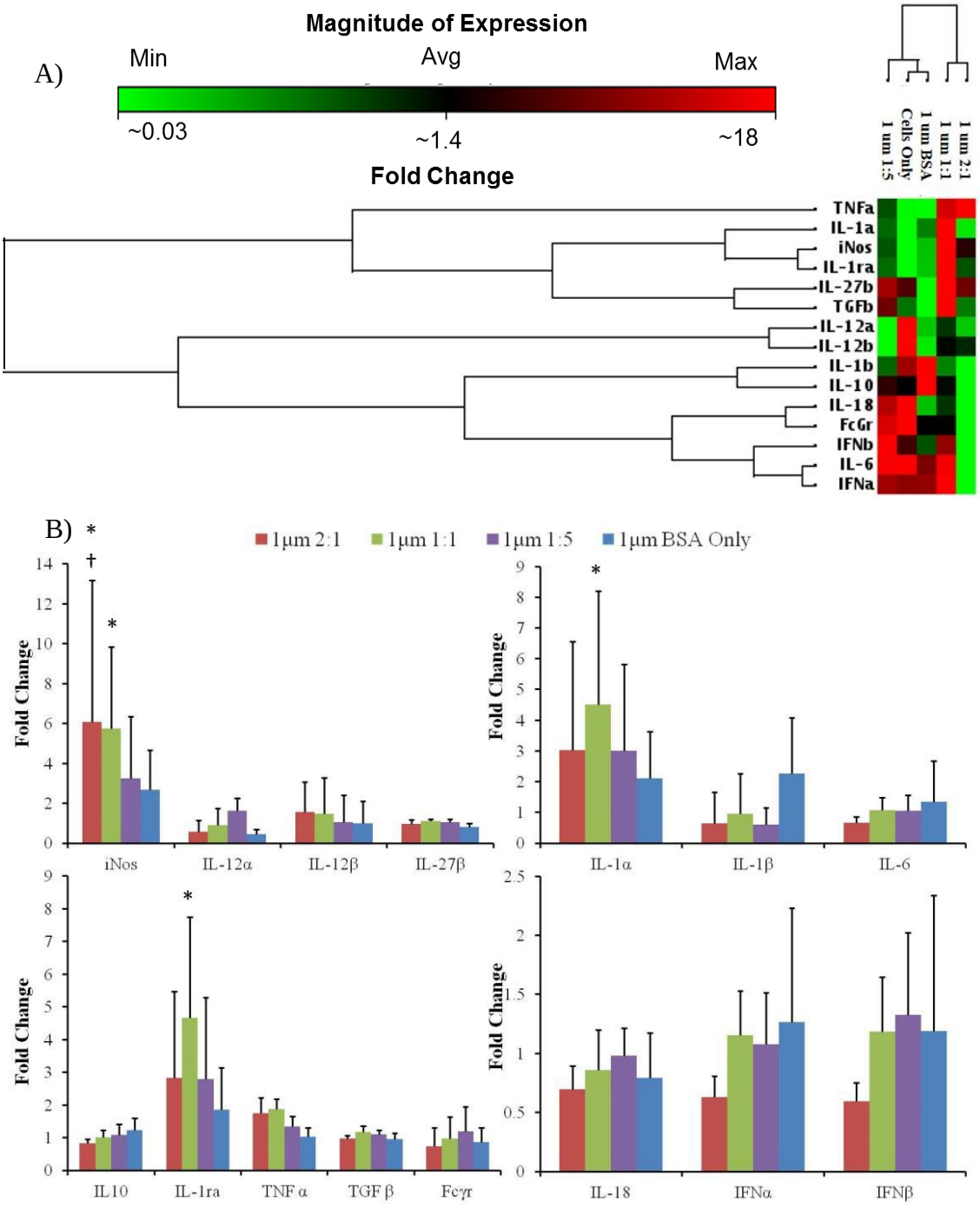

Figure 10: Effects of 1µm particles and Fc density on cytokine and mRNA expression levels.

(A) Cluster plot shows the shift in magnitude of gene expression and (B) Fold change graphs show expression levels compared to untreated macrophages. *, from Cells Only, †, from BSA Only, ♦, from 1:5, $p<0.05$, error bars represent standard deviation.

LPS was given to macrophages as a positive control to represent classically activated macrophages. The cluster plot for the LPS pretreated groups shows that adding high Fc density coated microparticles can invert the macrophage response, even though the LPS is still present (Figure 11). ANOVA analysis showed that the LPS only group and the LPS pretreated groups with 0.5 μm and 1 μm 2:1 Fc particles were significantly different from the untreated macrophages. The macrophages pretreated LPS and then 0.5 μm 2:1 Fc particles were also significantly different from macrophages treated with LPS alone. Specifically, a decrease in IL-12α, IL-12β, IFNβ, IL-1α, IL-6, IL-10, and TNFα as seen compared to the LPS only treated conditions. The addition of 0.5 μm Fc particles results in a stronger decrease in expression compared to the addition of the 1 μm Fc particles. There was an increase in expression of iNos after the addition of Fc coated particles. The expression for IL-27β, IL-18, IFNα, and TGFβ remained relatively unchanged across the different LPS and LPS with Fc particles conditions.

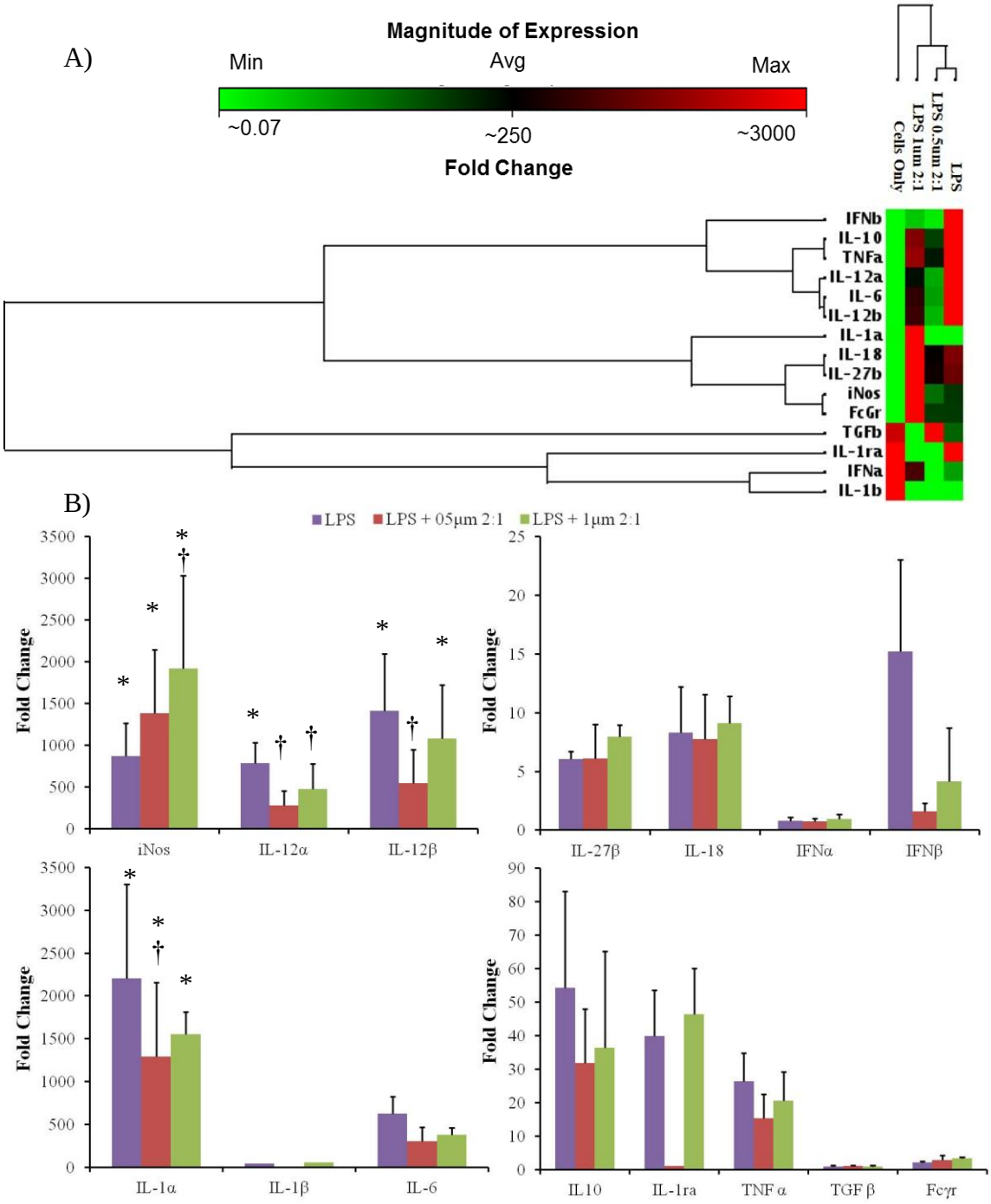

Figure 11: Effects of the addition of high Fc density particles after LPS treatment on cytokine and receptor mRNA expression.

(A) Cluster plot shows the shift in magnitude of gene expression and (B) Fold change graphs show expression levels compared to untreated macrophages. *, from Cells Only, †, from LPS Only, $p<0.05$, error bars represent standard deviation.

The IL-4 treated macrophages acted as a representation of alternatively activated macrophages that are typically anti-inflammatory. The cluster plot for the IL-4 treated conditions shows a similar inversion when the high Fc coated particles were added (Figure 12). The plot also shows the IL-4 treated and untreated macrophages respond in a similar manner with the exception of IL-1α and IL-12α. The addition of 0.5 μm Fc particles results in minimal expression across a majority of the genes while adding 1 μm Fc particles leads to an increased expression of the previously minimally expressed genes. This is reflected in the fold change analysis.

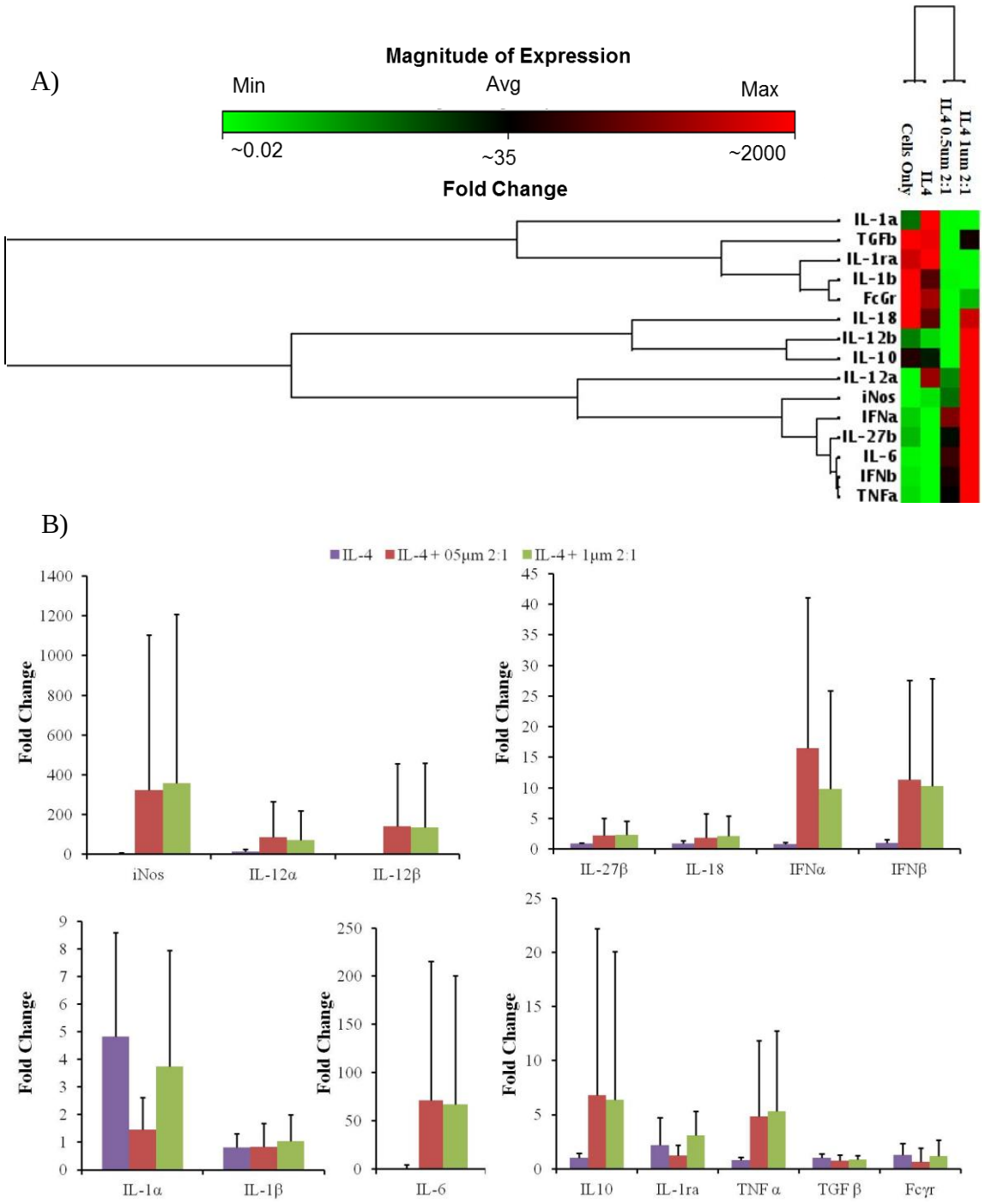

Figure 12: Effects of the addition of high Fc density particles after IL-4 treatment on cytokine and mRNA expression levels.

(A) Cluster plot shows the shift in magnitude of gene expression and (B) Fold change graphs show expression levels compared to untreated macrophages, error bars represent standard deviation.

3.3.6 High Density Fc Particles Result in Significant Increase of TNFα and IL-12

To confirm the mRNA gene expression levels also resulted in secreted protein, an ELISA was performed on frozen aliquots of the conditioned media from experimental conditions. IL-10 and IL-1α were tested, but results were below the detection level of the assay. However successful results were obtained for TNFα and IL-12, with the exception of LPS treated groups which exceeded the limit of the assay. This was seen even after a 1:100 dilution compared to the other treated groups. The amount of TNFα produced by macrophages treated with 0.5 μm with high Fc densities of 2:1 and 1:1 was significantly higher than the untreated macrophages as well as the BSA only coated and low Fc density particle condition of 1:5. In the 1 μm treated conditions, only the 1:1 Fc condition was significantly higher that the untreated condition.

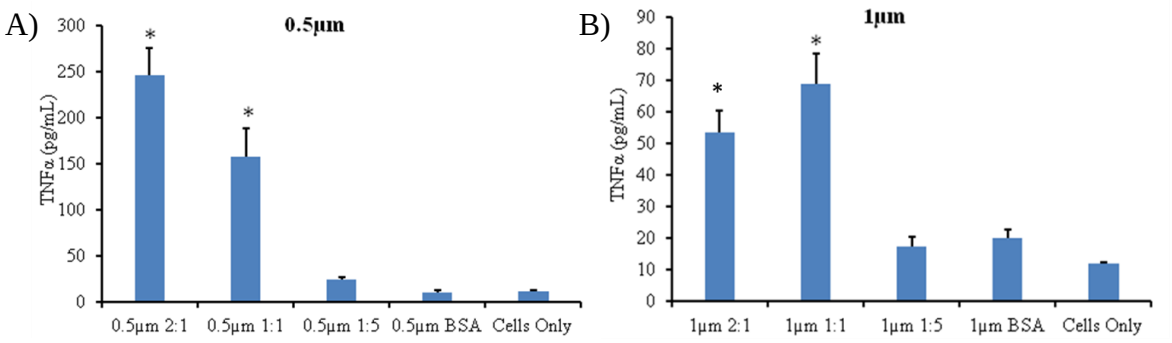

Figure 13: Amount of TNFα is affected by particle size and Fc density.
TNFα is significantly increased for (A) high Fc densities coated 0.5 μm particles but (B) only for the 1:1 Fc density in 1 μm particle treated cells. (N>5, * denotes significance compared to the Cells Only condition with $p<0.05$)

For the IL-4 treated macrophages, the addition of high Fc density particles lead to a significant increase in TNFα production (Figure 14). The addition of 0.5 μm Fc particles to IL-4 treated macrophages resulted in similar levels of TNFα produced in non-IL-4 treated macrophages. However, the addition of 1 μm particles to IL-4 treated macrophages lead to higher levels of TNFα production than seen in non-IL-4 treated macrophages.

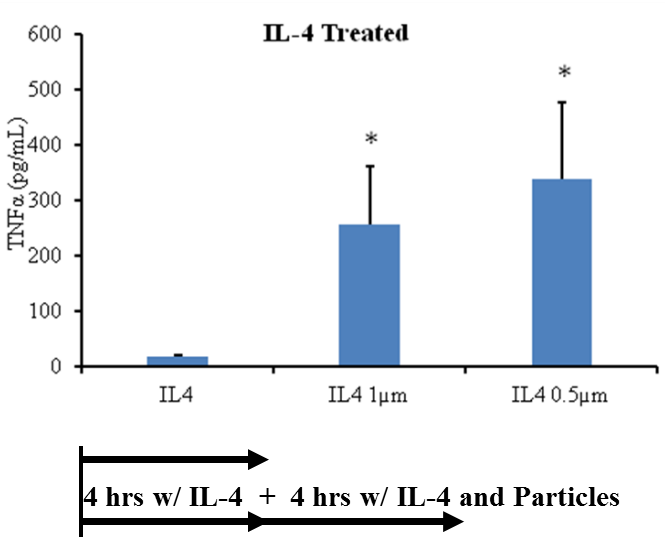

Figure 14: Amount of TNFα increases for IL-4 treated macrophages with the addition of high Fc density particles.
Media from IL-4 only treated macrophages was collected after 4 hours while pretreated macrophages were treated with IL-4 for 4 hours and then particles were added for an additional 4 hours. N>5, * denotes significance compared to the IL-4 only condition with $p<0.05$

The amount of IL-12 secreted by 0.5 µm high Fc density particle treated macrophages was significantly higher than untreated cells (Figure 15A). However, there were not significant changes in IL-12 secretion for any of the 1 µm treated macrophages (Figure 15B). While there were no significant changes, the IL-12 production did increase for high Fc 1 µm treated macrophages. IL-12 production was significantly increased for in IL-4 treated macrophages when 0.5 µm and 1 µm high Fc density particles were added (Figure 16).

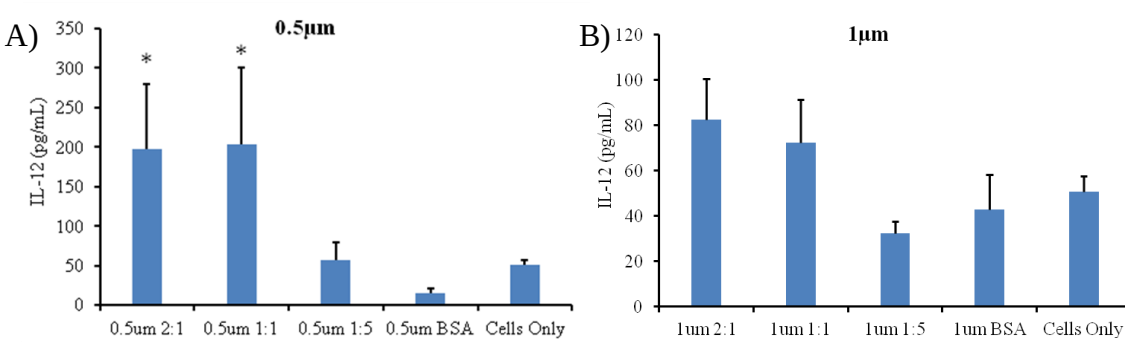

Figure 15: Amount of IL-12 is affected by particle size and Fc density.
IL-12 is significantly increased for (A) high Fc densities coated 0.5 µm particles but (B) there was no significant difference in 1 µm particle treated cells. (N>4, * denotes significance compared to the Cells Only condition with $p<0.05$)

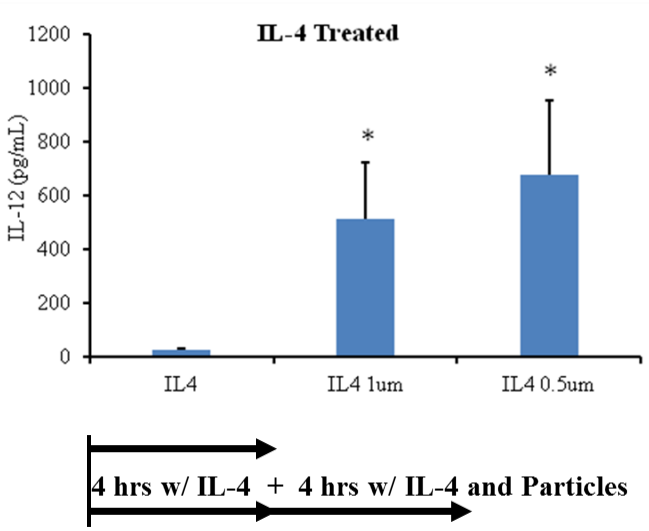

Figure 16: Amount of IL-12 increases for IL-4 treated macrophages with the addition of high Fc density particles.
Media from IL-4 only treated macrophages was collected after 4 hours while pretreated macrophages were treated with IL-4 for 4 hours and then particles were added for an additional 4 hours, N>5, * denotes significance compared to the IL-4 only condition with $p<0.05$

3.4 Discussion

One important mechanism for recognizing threats in the body is opsonization—the coating of invading pathogens with antibodies marks them as a "threat" or a "danger signal". This process can prevent biological activity of pathogenic molecules through steric interference (e.g. interfering with binding to cells or other biological targets), but

also tags the pathogen for recognition by macrophages and other antigen-presenting cells through the external orientation of the constant region of the antibody molecule known as the crystallizable fragment (Fc) [104].

In these studies we quantified the phagocytic activity of macrophages as a function of Fc density and particle size. We successfully varied the Fc density on microparticles for all tested sizes. We then analyzed the effects of Fc density on attachment alone by conducting a low temperature study. We found that while particle size did play a role in attachment, Fc density did not. The results of our particle internalization assays showed a strong dependence between the Fc density and particle size on the average number of microparticles adhered to and internalized by the macrophage population (Figure 17). While size dependence of particles has been shown to affect phagocytosis in previous studies [30, 73, 105], this is the first study to look at the combined effects of Fc density and particle size on phagocytosis, which both play an important role [95]. Smaller particles (0.5 μm and 1 μm) showed a strong correlation between Fc density and the average number of internalized microparticles per cell. However for the larger particles (3 μm and 4.5 μm), an increase in Fc density resulted in no significant change in the average number of microparticles phagocytosed per cell. For the 2 μm BSA-only coated particles, an apparent anomaly from the general trend was seen in the average number of internalized particles per cell. The BSA-only particles were internalized in significantly higher levels compared to the Fc-functionalized particles. Others have shown that BSA-only particles can be internalized by macrophages, most likely through scavenger receptors [106, 107]. However, the 2 μm particle may represent a special case due to the topography of the macrophage membrane. Previous studies have shown that the macrophage membrane ruffles are spatially tuned with an average curvature of approximately 2 μm [30], suggesting a mechanism for physical selection of particles by size.

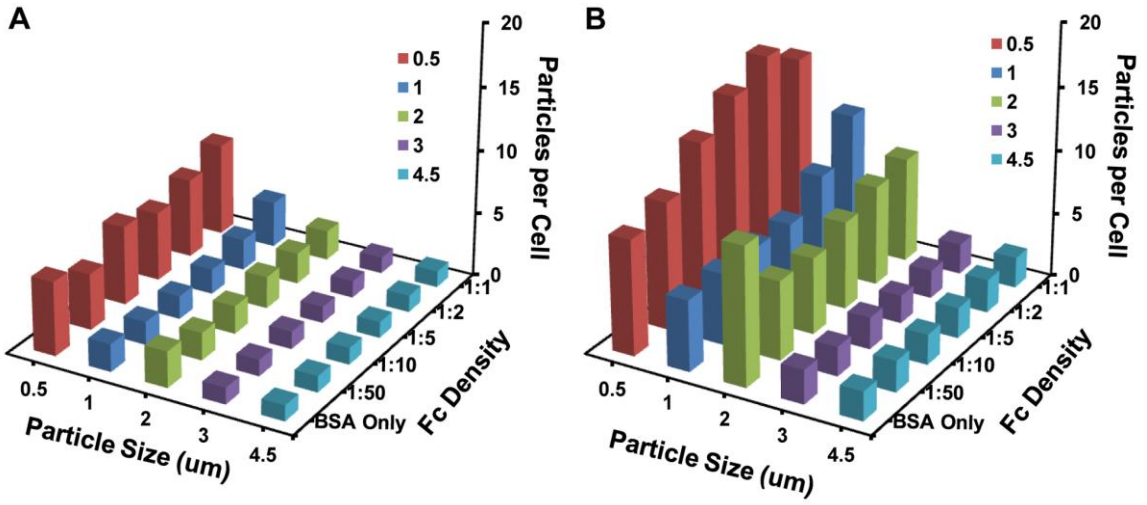

Figure 17: Summary of the average number of attached and internalized microparticles per cell for each particle size and Fc density condition.
(A) The attachment of particles to macrophages does not have a strong dependence on microparticles size and Fc density. (B) The internalization of particles by macrophages is highly dependent on microparticle size and Fc density with an overall trend of the average number of internalized particles decreasing as microparticle size increases and Fc density decreases.

The fluorescent microscopy images of the internalization of small particles (0.5 μm and 1 μm) (Figure 5b, c) showed a great disparity in the phagocytic activity of individual macrophages, which we confirmed through further flow cytometry analysis (Figure 7). High density of Fc resulted in an increase in phagocytosed particles, but also an increase in cells that do not phagocytose any particles (Figure 7b, 0.5 μm and 1 μm). Since our macrophage line is assumed to be relatively homogenous, the enhanced activity seen only when small particles were added, could be due to a positive feedback mechanism that causes cells that initially internalize particles to then more actively search for new particles.

One important goal of our study is to develop a set of design parameters by which we can better deliver particles to macrophages for specific biomedical applications. It may be useful to target the microparticles to a subset of macrophages by defining a set of physical and biochemical signals through a combination of particle size, avidity, and/or

other (as yet untested) receptor ligands for "designer drug" therapies. We found the percentage of phagocytic cells is dependent on both particle size and Fc density. The maximum number of particles per cell were internalized for the smaller 0.5 μm and 1 μm particles functionalized with high Fc densities, despite only approximately 65% of the cells classified as phagocytic. The mid-sized particles of 2 μm are phagocytosed by the highest percentage of macrophages (90%), regardless of Fc density. The larger 3 μm and 4.5 μm particles, while only phagocytosed by a smaller portion of the macrophage sample, nonetheless accounted for the greatest amount of total volume of microparticles phagocytosed.

Our attachment data shows that the initial interaction and attachment of the microparticle with the macrophage was most strongly affected by particle size. However, phagocytic activity and particle internalization was found to be dependent on both particle size and Fc density. The kinetics of internalization may also influence the phagocytic activity of macrophages. A previous study investigated the internalization rates of particles from 3-9 μm and found no significant difference in the phagocytic rate for the sizes tested, even when particles were functionalized with Fc. However, internalization rates of smaller particles and the effect of Fc density were not evaluated [30].

A possible explanation for a significant dependence on size in the initial and ongoing processes of phagocytosis has been posited to result from the dynamics of cell signaling components recruited in the process. A theoretical model suggests that larger particles will require the cell membrane receptors to diffuse over larger distances resulting in the cell membrane taking longer to envelop the particle. Particle size can also lead stalling of the phagocytosis process and lead to the low phagocytosis rates we found for the 3 μm and 4.5 μm particles [99]. Smaller particles require the recruitment of fewer signaling components before their engulfment, providing for less time to be affected by inhibitory signals such as wortmannin, LY294002, or dominant-negative SHIP-1 [108,

109]. Furthermore, it has been suggested that there is a specific size threshold of 0.5-1 μm whereby the macrophage phagocytosis transitions from a coated vesicle-mediated uptake into an actin-mediated uptake. While actin is crucial for the formation of the phagocytic cup, these reports suggest a size threshold of 2 μm before inhibitors that prevent Fc receptor signaling to the actin cytoskeleton are generated [56, 108, 109]. The action of size-dependent inhibitory signals would also account for why there exists a consistently low average number of microparticles per cell for the 3 μm and 4.5 μm particles regardless of Fc density. It will be important to more fully understand these inhibitors if we hope to take advantage of the increased volume of delivery associated with internalization of larger particles. For example, nanoparticles are frequently touted as superior delivery method due to their greater surface area per unit volume compared to microparticles [37]. However, the volume of particles decreases with the third power of diameter, which is a detriment for delivering significant amounts of encapsulated drugs or imaging agents into the cell interior via nanoparticles.

Not only are these results relevant to the direct delivery of microparticles to macrophages, but they are also important to understanding the downstream effects of the internalization of these particles. This approach to immunoengineering will have a broad impact on drug delivery to macrophages as well as altering macrophage phenotype for a desired application. The recognition of immune threats can occur through physical cues or the many different biological receptors on the cell surface. A major distinction between the different receptor pathways is the immune-activation state they induce in the macrophage. Receptors that bind to "self" products intended for waste removal will not trigger immune activation; those cells will simply increase in size (if necessary) and then engulf and degrade the recognized substance in a non-inflammatory process. However, receptors that recognize substances that are potentially dangerous to the body (e.g. through PAMP-receptors or Fc receptors) will trigger activation of the macrophage, leading to secretion of immune mediators and enhanced intracellular degradative capacity

to deal with the active insult represented by the engulfed threat. Opsonization of microparticles tends to favor activation of cells as it is a natural mechanism of targeting foreign substances for recognition and response, but will tend to not lead to full cellular activation in the absence of secondary "danger signals" [32, 56]. In the future we plan to examine how the size and Fc density of particles also affect cytokine production during and after phagocytosis, indicating changes in macrophage phenotype. As we investigate the activation of the immune system with Fc-functionalized particles, the inclusion of bioactive substances such as small-molecule drugs, antibiotics, cytokines or chemokines, or vaccine targets, either on or contained in the microparticles, could lead to a broad-based immune delivery system that is tunable to experimental or clinical needs: one that could be either inflammatory or not; affect a broad or more targeted population of macrophage cells; or deliver small amounts of highly active substances, or larger amounts of less active materials.

The gene expression and secreted protein results from this study show that both particle size and Fc density coating have a strong impact on macrophage response. While the goal was to pinpoint exact shifts in macrophage phenotype as a result of particle size and Fc density coating, this was not easily apparent. This is not surprising as characterizing and classifying macrophage phenotype is a complicated and subjective field. As a whole, the gene expression levels for 0.5 μm particles coated with high levels of Fc showed an increase in M1 associated markers. This profile was not seen as clearly in the 1 μm particles. However, these expression levels were much lower than those in the LPS only group. In fact, Fc particles were able to inhibit pro-inflammatory expressions levels in macrophages there first exposed to LPS. This then suggest a bias towards a M2b phenotype, which is often associated with immune-complexes. The M2b phenotype is often listed as having both pro- and anti-inflammatory effects. Our results suggest the 0.5 μm particles lead to a pro-inflammatory M2b phenotype while the 1 μm lead to an anti-inflammatory M2b phenotype when given alone.

Previous studies have shown delivering particles coated in high levels of Fc resulted in a decrease of IL-12 and IL-10 [32] and macrophages treated with immune complexes are known to display a similar shift [1, 57]. This was not seen in our results as we saw an increase in IL-12 production with the exception of LPS treated groups. When high Fc density particles were added after LPS treatment, decreased levels of gene expression were seen for IL-12α and IL-12β. However decreased expression was also observed for IL-10. Further studies are needed to fully characterize the effects on secreted protein, such as ELISA analysis on conditioned media and evaluation at a longer time point of 24 hours. The lack of a longer time point may also explain the lack of correlation with previously published results as there may not have been enough time for macrophages to secrete protein in response to the stimulus of the particles. Previously published works have also used particles or erythrocytes that are greater than 2 μm in size. As we saw the 0.5 μm particles functionalized with high a Fc density coating elicited the strongest IL-12 secretions, this would suggest that the size of the particle plays a vital role in response. High levels of IL-12 were not seen in the 0.5 μm particles with low levels of Fc coating or the BSA only coated particles. This suggests a combination of high Fc coating and small particle size can reverse the suppression of IL-12 production previously seen in immune-complex studies. The amount of TNFα secreted by the addition of 0.5 μm particles with high Fc density coatings, suggests a strong pro-inflammatory response. As in the case of IL-12, this was dependent on both particle size and Fc density. However further studies incorporating larger particles and longer time points will be needed to confirm these results. These experiments should also be repeated in bone marrow macrophages derived from mice deficient in FcRγ chain or wild type macrophages that first have their FcR blocked to show that these effects are dependent on FcRγ ligation.

If validated, these results would have a broad impact on the fields of biomaterials and immunomodulation with applications in cancer biology, pathogen-associated

infections, and vaccine development. This is due to these particles showing a slight shift to a pro-inflammatory response. However this pro-inflammatory state was never as severe as seen in the LPS treated groups, and in fact reduced the inflammatory state for those LPS treated groups. Fc coated particles could for example then be used to switch tumor associated macrophages into a more inflammatory state that could reverse the immunosuppressive environment around the tumor. [14, 48] The same can be said for intracellular bacterium, such as *Mycobacterium tuberculosis*, *Leishmania major*, and *Listeria monocytogenes*.[110] These smaller, high Fc coated particles could be used in conjunction with current drug regiments to not only delivery the drug, but to also activate the macrophage to fully degrade the bacterium and prevent it from continually spreading within the host.

CHAPTER 4 Fc OPSONIZED PARTICLES FOR CONTROLLED COMPLEMENT ACTIVATION[2]

4.1 Introduction

The body's immune response is comprised of a vital system of cells and macromolecules that help to regulate homeostasis as well as respond to, kill, and clear invading pathogens or waste products [5, 8, 9, 29]. Components of the immune system have also been shown to play a role in a variety of disease processes such as cancer, [7] atherosclerosis, [46, 47] and numerous other autoimmune and immune deficiency diseases [4, 63, 64]. In total, chronic immune-related disease affects ~5% of the United States population each year, [111] highlighting the importance of developing a novel method for modulating the body's immune response in a directed and "tunable" manner. The humoral immune response represents the body's use of specific proteins, including immunoglobulins and complement components, to opsonize and/or inactivate invading pathogens while also initiating cytotoxic processes and recruiting immune cells through chemotaxis [3, 5, 112]. The complement system [13, 80, 113, 114] comprises a group of proteins that become enzymatically activated through one of three pathways: the classical, alternative, and lectin pathways [22, 23, 63, 64]. The classical pathway is activated by the binding of C1 monomers to closely apposed Fc regions of a single IgM or multiple IgG molecules, and formation of the C1 complex [115-117].

---

[2] Adapted and Modified from Pacheco, Patricia M., et al. "Tunable complement activation by particles with variable size and Fc density." *Nano LIFE* 3.02 (2013).

If one of these pathways is initiated by an invading pathogen, the complement proteins are activated in a cascading manner, resulting in the deposition of complement proteins on the surface of the pathogen and the formation of a membrane attack complex, also known as a terminal complement complex (TCC). The TCC forms a nanoscale transmembrane channel leading to loss of integrity of the bilayer membrane and osmotic lysis of the pathogen [22, 23]. Diffusion of the proteolytic fragments of these deposited complement components also interact with other immune cells, such as neutrophils and macrophages, to amplify the phagocytosis signal(s) and aid in the clearance of the targeted pathogen [23, 33, 63, 64]. While the complement system represents only a portion of the humoral response, any knockdown of complement component receptors severely impairs the overall humoral immune response [118]. In addition, the complement system is also involved in the transition to and effectiveness of the adaptive immune response, as successful complement activation has been shown to act as an adjuvant to improve vaccine effectiveness [12, 13].

The interaction of micro- and nanoparticles with humoral immune constituents provides an opportunity to modulate the magnitude and location of the innate immune response. Particle induced immunomodulation can be accomplished through physical signals, such as particle size and shape; chemical signals, such as material composition; and biological signals, such as opsonization; resulting in an opportunity for rational design and control of an immune response suited for specific applications (i.e. a "tunable" immune response) [30, 67, 119-122]. Particles have previously been used in immune related applications as delivery platforms for vaccine development and in the study of phagocytosis [13, 24, 30, 119, 123]. In our phagocytosis studies, particles were coated in immunoglobulin gamma (IgG) antibody so that the crystallizable fragment (Fc) of the antibody is orientated outwards. This Fc portion of the antibody is then able to interact with Fc-receptors on the surface of immune cells to trigger receptor-mediated phagocytosis. Consistent with previous work, these studies demonstrate that the size of

the particle and the density of Fc can affect the efficiency of phagocytosis and cytokine production by macrophages [30, 31, 124]. However, in contrast to previous work, these studies established a minimum Fc coverage and a maximum size threshold for biological and physical stimulation of the complement cascade.

While the destruction of pathogens through lysis that results from the insertion of the membrane attack complex is typically seen as the traditional role of the complement system, recent studies have shown that it also plays a key role in the body's response to tumors [23, 65, 66] and the effectiveness of vaccines [12, 13]. This only further highlights the need for a tunable design platform for location-specific complement system modulation. Despite the large role of Fc functionalized particles in the study and manipulation of macrophages, only a few studies have investigated Fc functionalized particles to understand their role in activating the complement system [13, 80, 113, 114]. Previous studies have found that particle size can affect complement system activation, possibly due to the physical effect of the curvature of small particles on complement constituent assembly [125-127]. The C1 complex assembles in direct contact with apposed Fc molecules, and is only stabilized and retained when the C1q head is bound multivalently to Fc molecules [128, 129]. Therefore, the density of Fc molecules on a particle, as well as their orientation, may also affect complement activation. While efficient activation of complement is an important defense against pathogens, uncontrolled activation may lead to "self" tissue damage [130]. Rationally designed modulation of the complement response will allow development of a wide range of therapeutic agents for many different immunopathologies.

We hypothesize that micro- and nanoparticles functionalized with IgG molecules orientated with the Fc regions outwards are capable of stimulating the complement system in a manner that depends upon the particle size and density of the opsonizing IgG antibody. Therefore by controlling these variables, we can modulate the complement system in a tunable manner. The design of micro- and nanoparticles for nanoscale control

of Fc stimulants may be useful as a clinical therapeutic agent to augment and modulate the immune response through the complement system.

4.2 Materials and Methods

4.2.1 Microparticle Opsonization

Carboxylated polystyrene particles of 0.5 μm, 1 μm, 2 μm, and 4 μm diameters were purchased from Polysciences (Warrington, PA) and Bangs Laboratories (Fishers, IN). An illustration representing the particle functionalization process is shown in Figure 18. The particles were first incubated in a 2 mg/mL bovine serum albumin (BSA) (Sigma Aldrich, St. Louis, MO) solution to adsorb a saturating layer of BSA onto the surface of the particles. The amount of BSA added was increased with the total amount of particle surface area to keep the BSA coating on the particles uniform, in accordance with manufacturer's recommendations. To confirm that the amount of BSA added was in fact saturating, we used fluorescently labeled BSA in increasing and decreasing concentrations. The fluorescence was then measured using a flow cytometer. This BSA coating serves to orient the Fc portion of the bound anti-BSA IgG molecules to the exterior. To vary the amount of exposed Fc domains on the particles, sheep polyclonal anti-BSA IgG antibody (Abcam, Cambridge, MA) was then added in various molar ratios. We began with a minimum molar ratio of 1:50 representing a single IgG molecule to every 50 BSA molecules that were originally added, creating a dilute surface density of Fc molecules on the particles. The ratio was then increased to a maximum of 2:1. To ensure a high density Fc coverage on the 4 μm particles, we also created two additional sets of particles coated with molar ratios of 5:1 and 10:1. For each functionalization step, we allowed the particles to incubate with the proteins for at least 2 hours at room temperature in phosphate buffered saline (PBS) at a pH ~7.2 (Invitrogen, Carlsbad, CA). After the incubation period, the particles were washed 3 times through centrifugation and PBS exchange. We also reserved a set of particles that were coated in only BSA. To

demonstrate that Fc density was varied successfully, we examined a sample of each particle condition through incubation with a fluorescently labeled rabbit anti-sheep IgG secondary antibody (Abcam, Cambridge, MA). The particles were then analyzed using a flow cytometer. The flow cytometer recorded the fluorescent intensity per particle and 50,000 events were recorded for each condition, the mean fluorescent intensity represents the arithmetic mean for those events. The measured fluorescent intensity corresponds to Fc density on the particles.

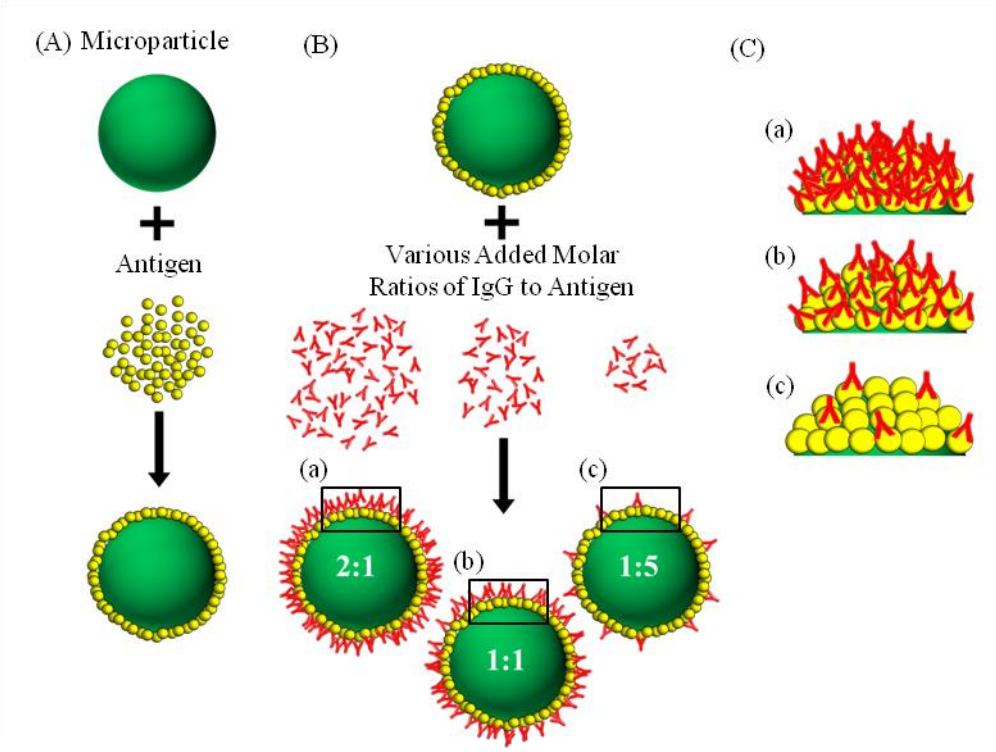

Figure 18: Microparticle functionalization process.
(A) Antigen is adsorbed onto the particle surface at a saturating density and then (B) IgG is added in increasing molar ratios and (C) to create particles with variable Fc density.

4.2.2 Flow Cytometry

Measurement of Fc density on all particle samples was analyzed using a flow cytometer (BD Accuri C6, Franklin Lakes, NJ) after incubation with the fluorescently labeled secondary antibody. Fluorescence was measured with a 630 ± 30 nm bandpass

filter capable of detecting the fluorescent marker. The resulting mean fluorescent intensity (MFI) of the particle sample for each Fc density condition was calculated using the CFlowPlus software (BD, Franklin Lakes, NJ) and FlowJo (Tree Star, Inc., Ashland, OR). We also recorded the number of microparticles per mL to establish the particle concentration of each sample.

4.2.3 Serum Collection

Whole blood was first collected from 2 healthy, consenting human donors with approval from the GIT IRB #H10011. Approximately 10 mL of whole blood was collected from each donor and was allowed to clot at 4°C. The samples were then centrifuged at 2,000 G for 10 minutes. The resulting serum from each sample was decanted and transferred to a sterile centrifuge tube. Centrifugation was repeated to remove any residual red blood cells, which resulted in approximately 5 mL of serum collected from each donor. For complement mediated cytotoxicity studies normal human serum was purchased (Quidel). This same normal human serum, as well C1 deficient, C4 deficient and Factor B deficient serum purchased from Quidel were also used to characterize the complement pathways activated by our Fc particles.

4.2.4 Complement Activation Assay

The MicroVue CH50 Enzyme Immunoassay (EIA) (Quidel) was used to evaluate the magnitude of complement activation as a result of the addition of Fc functionalized particles to human serum (Figure 19). This kit is used clinically to determine complement system deficiencies by measuring the amount of generated terminal complement complexes [131, 132]. Included in the kit is heat aggregated gamma globulin (HAGG) activator, which we use as a positive control. The kit was used according to the manufacturer's instructions. Approximately 10-30 million particles were added to serum samples from both donors for each Fc density and particle size condition. The CH50 EIA measures the amount of TCC generated through the use of TCC specific antibodies. The

amount of antibody binding is directly correlated to the amount of fully formed TCC that results in 50% hemolytic lysis in accordance with the kit standards and quality control. Results are shown in CH50 unit equivalents per milliliter (CH50 U Eq/mL).

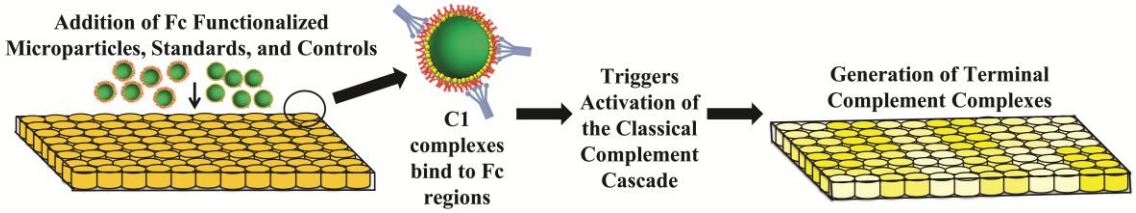

Figure 19: Overview of CH50 EIA
Microparticles, standards and controls are added to wells containing human serum. During incubation, C1 complex components present in the serum begin to bind to Fc regions and the resulting complex triggers the complement system cascade; this results in the generation of the terminal complement complexes (TCC).

4.2.5 Monte Carlo Simulation of Complement Activation

To better examine the effect of Fc density on complement activation by Fc-coated particles, we modeled the surface assembly of the C1 complex via multiple immobilized Fc molecules, a critical step of complement activation. A Monte Carlo simulation [133] of antibodies randomly distributed on a gridded antigen-coated surface was modeled in MATLAB (MathWorks, Natick, MA). An $N \times N$ grid was created to represent a portion of the surface area of the particles. Each element of the grid represents a region of a single densely packed Fc molecule, formed by attachment of IgG antibody to surface-immobilized antigens. We estimate each element to therefore correspond to a 18 nm × 18 nm square of the particle surface. A random number generator determined whether each element was occupied by a Fc molecule by assigning a value of "0" or "1" to each element on the grid. The probability of occupation was varied to simulate an increase in the amount of Fc on the surface. A total of 100 simulated surfaces were created to represent a range of Fc occupancy. Since the C1 complex binds multivalently to several

Fc molecules, we search for dense Fc regions by using a window of elements with a size equivalent to the fully-assembled C1 complex. We choose a window size of 3 × 3 elements. The window was raster scanned over the entire grid to evaluate the number of regions which contain a threshold number Fc molecules or greater. We used a threshold value of 4 Fc molecules in the results. Since these regions will more potently initiate the assembly and stabilization of the C1 complex [130] and trigger enzymatic activation of subsequent complement signaling molecules, a complement activation metric was developed to quantify the number of dense Fc regions. The metric uses an algorithm to first identify regions that are Fc-dense, then counts the total number of those regions within the $N \times N$ grid. A variety of threshold numbers of Fc molecules were used to identify regions of sufficient density to contribute towards the complement activation metric. The algorithm prohibited double counting of high-density Fc regions by removing previously identified elements that contributed to the complement activation metric. After all elements in the grid were evaluated, we calculated the total complement activation by summing the number of Fc-dense regions. The simulation for each antibody occupancy percentage was repeated ten times and the results were averaged. A grid size of 15 × 15 elements or greater all produced results that converged to a consistent complement activation metric when normalized to the fully occupied value.

4.2.6 Complement Deposition Analysis

The amount of complement components deposited on the surface of high Fc density condition of 2:1 and BSA only coated particles, was determined in a similar manner as previously done by others [134]. Microparticles and serum, both normal human serum and C4 deficient serum, were incubated in the same concentrations used for the CH50 EIA. After the 1 hour incubation period, the particles and serum were collected and centrifuged at 1500 G for 10 minutes. The supernatant was decanted and replaced by a 5% sterile filtered milk solution. Particles were resuspended and allowed to incubate at

room temperature for 30 minutes to prevent any future non-specific binding. After the incubation period, the particles were centrifuged at 1500 G for 10 minutes and the milk solution decanted. The microparticles for each condition were split into 4 microcentrifuge tubes. Mouse anti-human antibodies for C1q, C3b, C4b, and Sc5b9 were added to each respective tube at a 1:25 dilution in accordance with manufacturer's instructions. The particles and primary antibody were incubated at room temperature for 30 minutes. After incubation the particles were centrifuged as before and replaced with a AlexaFluor 488 labeled donkey anti-mouse secondary antibody at a 1:2000 dilution in accordance with manufacturer's instructions. The particles and secondary antibody were incuabated for 30 minutes at room temperature protected from light. After the incubation period the particles were centrifuged again and replaced with a 1% PFA solution. Particles incubated in no serum and only incubated with the secondary antibody served as controls for non-specific binding of the primary and secondary antibody respectively.

4.2.7 Complement Mediated Cytotoxicity Assay

A DH5α strain of *Escherichia coli* was used to evaluate if complement system activation from our particles could be applied towards directed complement mediated cytotoxicity. The strain was a gift of the lab of Dr. Craig Forest, by way of the lab of Dr. Brian Hammer. *E. coli* was plated on LB agar plates overnight. The following day individual colonies were collected and inoculated in 15 mL conical tubes containing LB broth. All bacteria were grown in a humidified incubator at 37ºC. The concentration of bacteria was calculated by taking the absorbance measurement at OD600 with a value of 0.1 corresponding to 1E8 CFU/mL. Approximately 5E5 CFU were added per well of a 96-well plate for all experiment conditions. For wells treated with particles, approximately 5E6 particles were add per well. Conditions with serum were treated with 14 μL of human serum. HAGG was added at 86 μL per as previously done. Isopropyl alcohol was added at a total concentration of 10% as a positive control for *E. coli* death.

The total volume of each well was adjusted to 125 uL with LB broth. The *E. coli* was allowed to incubate with each condition for 4 hours at 37ºC. After the incubation period, the contents of each well were stained with the Live/Dead BacLight Bacterial Viability kit (LifeTechnologies) in accordance with manufacturer's instructions. The contents were then analyzed using flow cytometry.

4.2.8 Statistical Analysis

Statistical analysis was conducted by using analysis of variance to determine significance of variables. Tukey- Kramer honestly significant difference (HSD) was used for post-hoc analysis to determine significance between each group.

4.3 Results

4.3.1 Increased Molar Ratio of Antibody Results in Increased Density of Fc

We evaluated the average Fc density per particle by measuring the mean fluorescent intensity (MFI) with flow cytometry (Figure 20 and Figure 21). Fluorescently tagged secondary antibody was used to quantify the relative Fc density per particle. For the particle sizes of 0.5 μm, 1 μm, 2 μm, and 4 μm, we measured the MFI for each of the Fc conditions, defined as the molar ratio of Fc to BSA antigen, for the values of: 2:1, 1:1, 1:5, 1:10, and 1:50. We also evaluated the highly-saturated molar ratios of 5:1 and 10:1 for the 4 μm particle. As the Fc density was increased, the measured MFI of the particles also increased. We also evaluated the MFI of BSA-only particles and saw minimal fluorescence at each particle size.

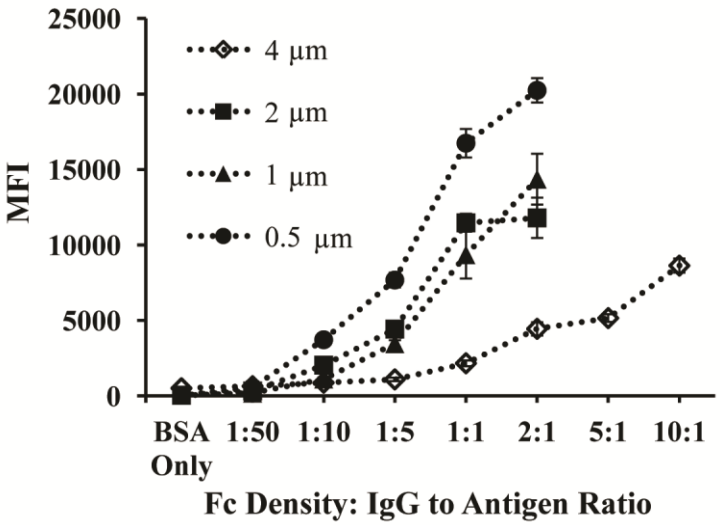

Figure 20: MFI for each Fc density condition across the different particle sizes used for this study.

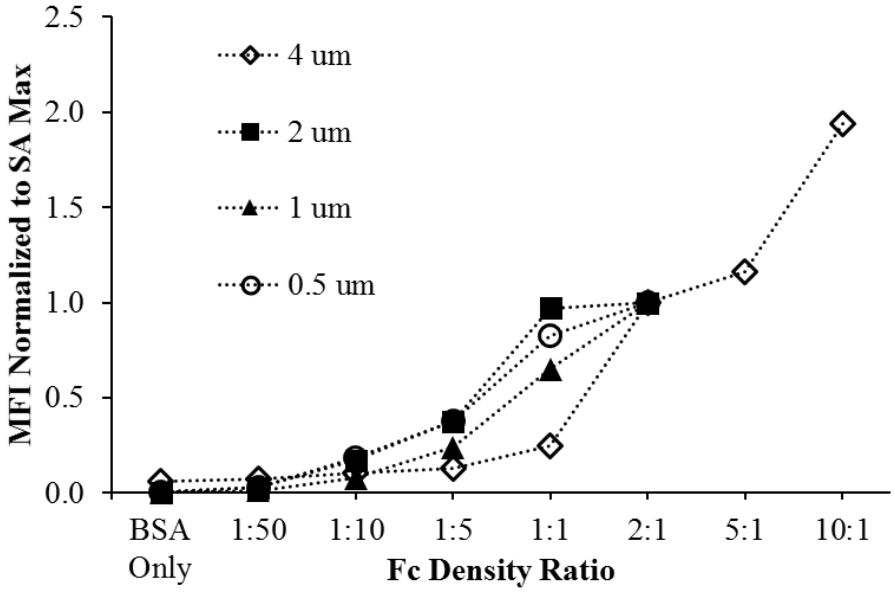

Figure 21: Normalized MFI to particle surface area and the maximum Fc condition of 2:1.

Confirms that as the Fc density increases, the normalized MFI increases as well. The MFI for each Fc condition and particle size was first normalized by the particle surface area and then normalize to the value for the Fc density of 2:1.

4.3.2 Effects of Particle Size on Complement Activation

The effect of particle size on complement system activation was determined by evaluating the amount of CH50 equivalents produced as a result of particles coated at the 2:1 Fc density condition (Figure 22). The complement system was successfully activated using Fc-functionalized particles of size 0.5 μm, 1 μm, 2 μm, and 4 μm. For all but the 4 μm particle sizes, CH50 equivalents were generated at comparable levels to the HAGG activator. We found that equivalent numbers of 4 μm particles generated significantly decreased levels of complement activation than the smaller sized particles ($p<0.01$).

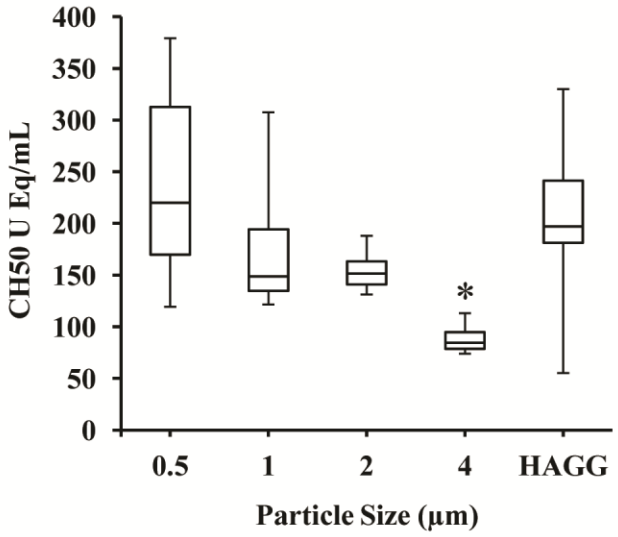

Figure 22: Effect of particle size on complement system activation.
*, significantly different from HAGG control ($p<0.01$); N=4.

4.3.3 Complement System Activation Depends on Fc Density

To better understand our results concerning the effects of particle size (Figure 22), the various sized particles were used to evaluate the effects of Fc density on complement system activation. We tested three Fc density conditions, corresponding to a molar ratio of Fc:BSA of 2:1, 1:1, and 1:5 for all particle sizes, as well as particles coated in BSA-only. In addition, to ensure maximal Fc coverage of the 4 μm particles, 5:1 and 10:1 ratios were also tested. HAGG activator was our positive control. Our results showed a remarkable dependence of complement activation on Fc density for all particle sizes

(Figure 23 and Figure 24). For the 0.5 μm, 1 μm, and 2 μm particle sizes, the 2:1 condition, representing a high Fc density, successfully activated the complement system and produced levels of CH50 equivalent to or surpassing the positive HAGG control. In all cases, the 1:1 condition shows a level of complement activation significantly above background ($p<0.05$), but below the 2:1 complement activation levels. The 1:5 and BSA-only particles did not activate the complement system efficiently, as the amount of CH50 equivalents generated was significantly lower than the positive control ($p<0.005$) as well as the high Fc density conditions of 1:1 ($p<0.05$) and 2:1 ($p<0.001$). Therefore, Fc density is a significant dependent variable in complement system activation.

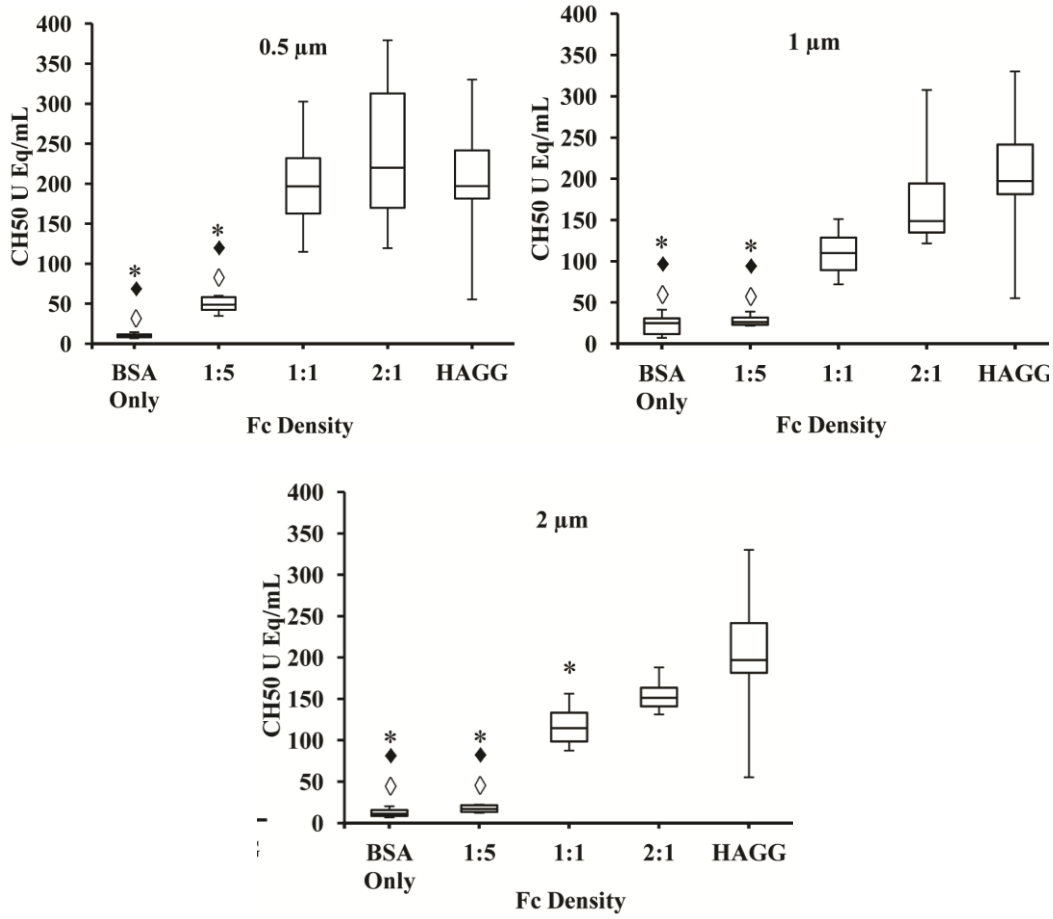

Figure 23: Effect of Fc density and particle size on complement system activation.
*, significantly different (SD) from HAGG ($p<0.005$); ♦, SD from 2:1 Condition ($p<0.001$); ◊, SD from 1:1 Condition ($p<0.05$); N=8 replicates (N=16 replicates for HAGG)

We observed that for the 4 μm particles, the 2:1 Fc condition did not fully activate the complement system to the level seen in other functionalized particles or in the positive control. To test whether this lack of efficient complement system activation was due to insufficient antibody binding to the particle surface, we also evaluated the effect of higher amounts of added IgG [5:1 and 10:1 ratios (Figure 24)]. Despite the increased amount of Fc used to functionalize the particles, we did not observe increased levels of CH50 equivalent activation. This result indicates that 4 μm particles activate complement at lower levels than other particle sizes not because a lack of saturating Fc, but for a reason related to particle size.

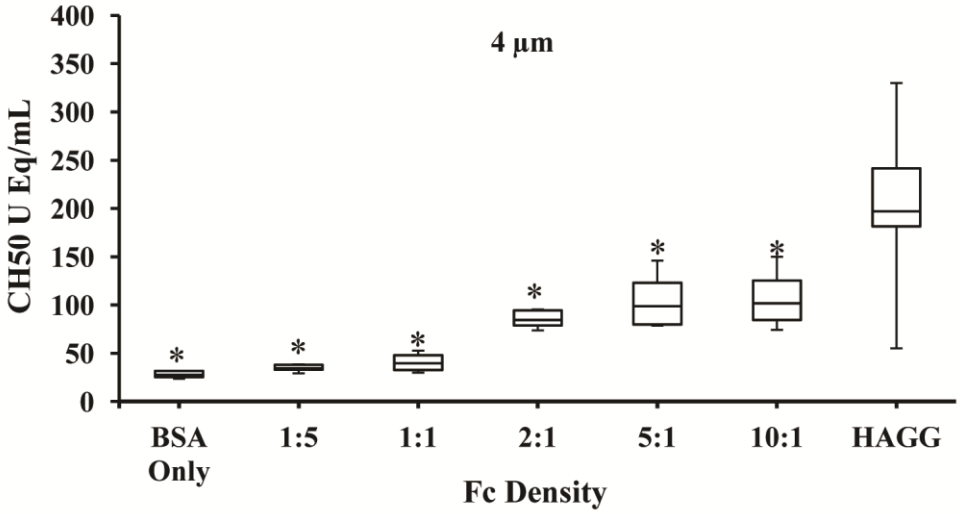

Figure 24: Fc density on larger particles does not affect complement system activation.
*, significantly different from HAGG ($p<0.001$); N=8 replicates (N=16 replicates for HAGG)

4.3.4 High Fc Density Particles Activate the Classical and Alternative Complement Pathways

To determine through which complement pathway activation was proceeding, we tested two different complement deficient sera. C1 deficient serum allowed us to evaluate alternative pathway activation and Factor B deficient allowed us to evaluate classical pathway activation. Our results show that the HAGG activator resulted in comparable

amounts of complement activation in the Factor B deficient serum as was seen in normal human serum. However HAGG activation levels were greatly diminished in the C1 deficient serum, indicating the importance of the classical pathway. A similar pattern was observed in the 0.5 µm and 1 µm high Fc density particles, however, in the C1 deficient serum, the high Fc density particles are capable of activating significantly greater levels of complement compared to the HAGG control, indicating a partial utilization of the alternative pathway (Figure 25). This is not strictly an effect of the material properties of the particles, as there was only minimal expression of complement in the BSA only coated particles in the Factor B and C1 deficient serum (Figure 26).

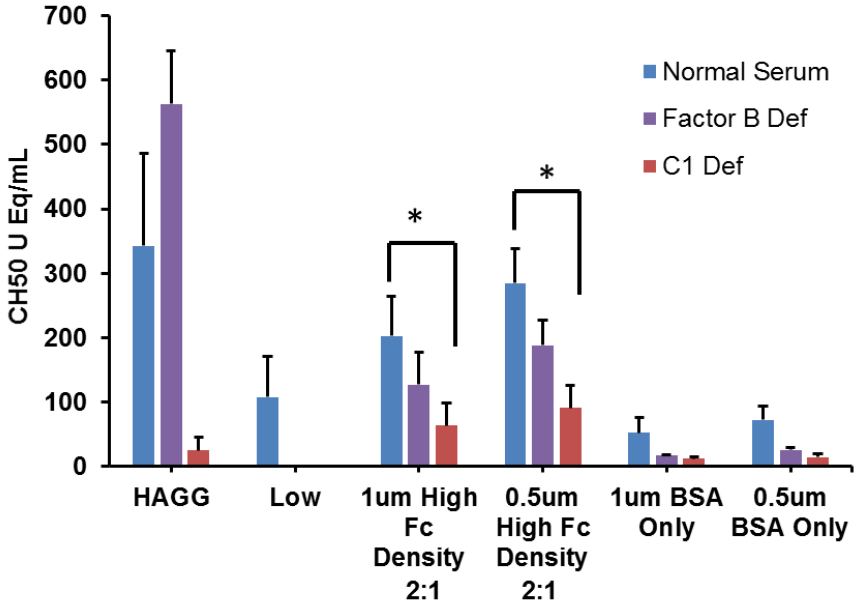

Figure 25: Complement system activation in normal, Factor B deficient, and C1 deficient human serum.
*, $p<0.05$

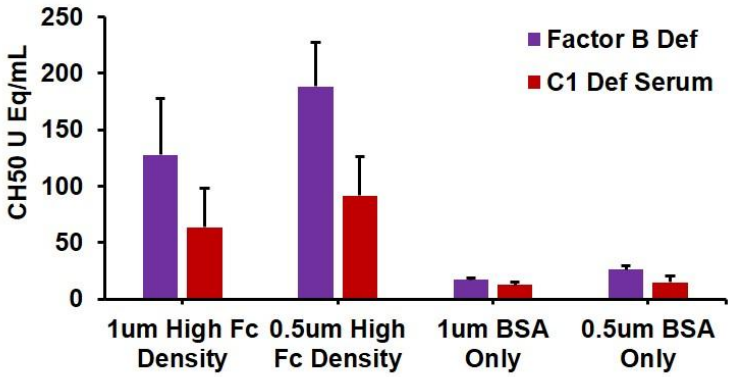

Figure 26: High Fc density microparticles successfully activate complement system in Factor B and C1 deficient serum.

4.3.5 Complement Deposition on Particle Surfaces

We have shown that high Fc density coated particles are capable of activating the complement system. To further understand Fc particle-mediated activation of complement, we measured the deposition of activated complement components on the particle surface. Using flow cytometry analysis, we first set our positive gate based on the "no serum" treated conditions as a control for non-specific binding. We then calculated the average percentage of events that were positive for each complement component (Figure 27). We found that 40-50% of the particles were positive for C3b, a component that is needed for activation in all pathways. This was the most common complement component found on the particles. SC5b9, an analog to TCC, was the next most common component found on the particles with approximately 30% of the particles averaging as positive. There were minimal levels of C1q and C4b components found on the particles.

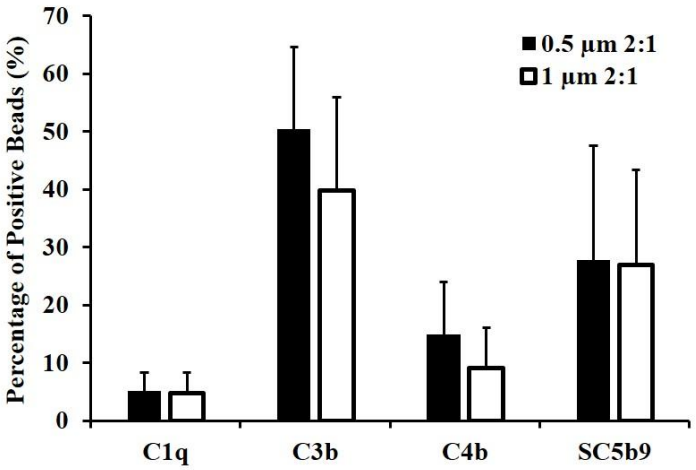

Figure 27: Complement deposition on high Fc coated particles.

As it was expected for C1q to be highly present on the particles due to the classical complement system activation, the complement deposition protocol was repeated with C4 deficient serum. This would prevent any deposited C1q from being further catalyzed and possibly removed from the particle surface. We found that the percentage of particles positive for C1q approximately tripled when incubated in C4 deficient serum (Figure 28).

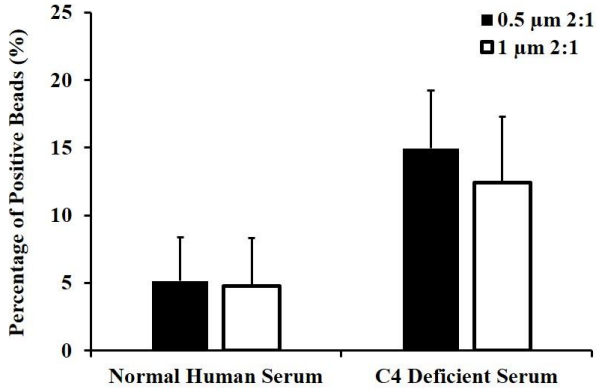

Figure 28: Increased C1q deposition in high Fc coated particles treated with C4 deficient serum.

4.3.6 Monte Carlo Simulation of Complement Activation

To estimate the appropriate window size for determining a threshold Fc density, we compared the size of closely packed antibody-antigen complex, represented by each element in the grid, to the C1 complex size. While individual BSA molecules occupy a linear distance of 7 nm [135], electron microscopy analysis of BSA-antibody complexes determined an average root mean square end-to-end distance of 18 nm [136, 137]. We acknowledge that these measures are only to illustrate an estimate for the dimension of the grid, as antibody antigen binding regions are flexible [138]. The linear dimension of the binding region of the C1 complex is determined by the reach of two flexible C1q arms of 18.5 nm length each and a fibril-like stalk of width 4.5 nm [115]. The total diameter is approximately 41 nm, though the specific geometry may vary due to the orientation of the globular c-terminal regions [139]. Microscopic analysis of antibody complexes and assembled C1q structures on opsonized lipid vesicles show C1 complex size ranging between 50 nm to 100 nm [140, 141]. Comparing the element size of 18 nm to the size of a C1 complex, which ranges from 41 nm to over 50 nm, we determine that a window of 3×3 elements most closely approximates the spatial reach of the C1 complex.

To determine the threshold number of Fc molecules necessary to assemble a C1 complex, we note that the affinity for the assembled C1 complex to Fc molecules increases dramatically in the case of multimers of Fc molecules [129]. Clq monomers show only weak binding, in the range of micromolar affinity, to the Fc regions of isolated IgG. However multiple, closely-spaced Fc molecules, such as those in immune complexes to repetitive molecular motifs, increase the binding of multivalent Clq a thousand-fold and enhance affinity to the few nanomolar [115, 128, 129, 142]. In our model of complement activation, we varied the number of Fc molecules within the 3×3 window in order to contribute to the complement activation metric.

Based upon our experimental data, the activation of the complement system by Fc-functionalized micro and nanoparticles did not increase in a manner proportional to Fc

density, but instead showed a minimum threshold of density. To develop a model of complement activation by micro/nanoparticles, we performed a Monte Carlo simulation of the complement system activation process that captures the need for a local high density of Fc molecules to initiate C1 complex formation and the subsequent classical complement cascade products. This model assumed an array of antibody binding sites and included a probability of antibody binding at any given site, as shown in a schematic in Figure 29A. A grid of elements was generated, in which each element corresponds to a site of possible antigen-antibody complex formation and therefore presentation of Fc. A random number generator determined the binding of the antibody to the antigen. An example of a result of the antibody binding and Fc display over a grid is shown in Fig. Figure 29B. In this example, the grid contains 15 × 15 elements and the probability of each element containing a Fc molecule is 20%, which is represented as a "1" in each grid element. A 20% occupancy percentage nominally corresponds to the condition of 1:5 molar ratio of antibody to BSA. The probability of antibody bound at each element corresponds to the amount of surface area covered by antibodies for a sufficiently large grid. In this example we identified by red boxes dense Fc clusters as 4 or more molecules inside the 3 X 3 window, and therefore likely sites of complement activation through C1 complex formation. An activation metric was calculated for the grid at each occupancy percentage and plotted in Figure 29C. The results of the activation metric revealed a very low activation value for an occupancy of 0-20%, with a dramatic increase for higher occupancy values, consistent with requirement of C1 multivalency. As we expected, a high probability of antibody binding corresponded to a saturated complement activation value. Other threshold values of Fc within the window of elements were also tested. Values of 3 or greater most accurately fit the experimental data.

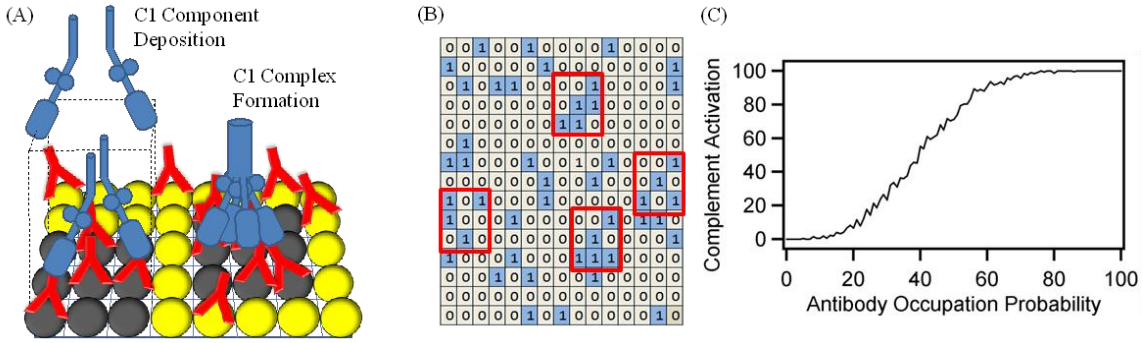

Figure 29: Monte Carlo simulation of complement system of activation.
(A) A schematic of packed antigens (spheres) and partial surface coverage of antibodies (Y's) displaying Fc binding sites. A C1 complex assembles on regions of high Fc density, identified by dark filled spheres, contributing to complement activation. (B) Monte Carlo grid of 15 x 15 elements, where the probability of antibody binding at each element is 20% and displayed as a "1" in each grid element. An algorithm has identified 4 regions of dense Fc clusters outlined in red, which contribute to the complement system activation metric. (C) A complement activation metric calculates the number of regions of high Fc density. Very low activation is seen below 20% occupancy with a dramatic increase at high occupancy values.

4.3.7 Complement Mediated Cytotoxicity

Bactericidal activity is a primary function of complement *in vivo*, therefore we studied the effect of our Fc coated particles towards complement mediated cell cytotoxicity. Flow cytometry was used to analyze the percentage of dead *E. coli* for each condition in accordance with manufacturer's recommendations. As preliminary experiments showed that the fluorescence used to stain live cells also absorbed onto the surface the particles, we used yellow-green fluorescent carboxylated particles. The fluorescence from these particles is so strong, that a side scatter gate in conjunction with the green fluorescence filter was used to gate out the particles. We were then able to gate around the live and dead stained *E. coli*. Our results show that complement components present within the normal human serum result in approximately 30% *E. coli* death and percentage of dead bacterium was reduced in heat inactivated serum. This result indicates that serum is inherently bactericidal through complement pathways. [143] The HAGG positive control used in complement system activation assays resulted in less *E. coli*

death than the serum only control. As expected, the addition of IPA resulted in very high levels of *E. coli* death. (Figure 30)

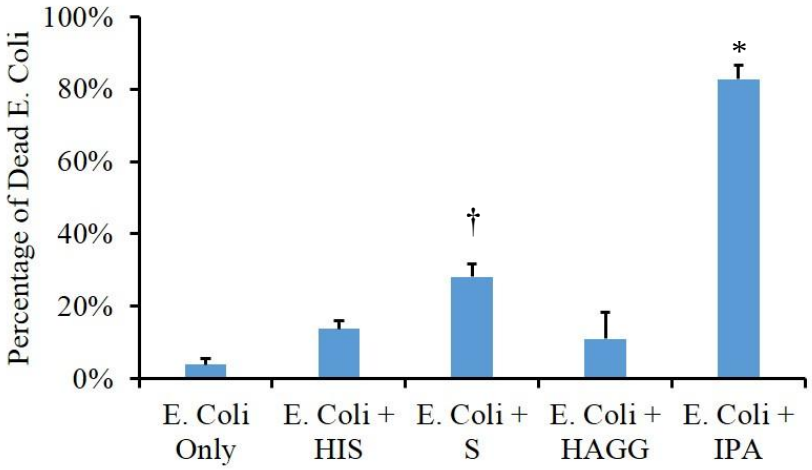

Figure 30: Percentage of *E. coli* death as a result of control conditions.
With heat inactivated serum (HIS), normal human serum (S), heat aggragated gamma globulin (HAGG), isopropyl alcohol (IPA). *, significantly different from all conditions, $p<0.05$; †, significantly different from *E. coli* only and *E. coli* + HAGG, $p<0.05$ using ANOVA and Tukey HSD (N=5)

The addition high Fc density particles alone resulted in low levels of *E. coli* death, suggesting that the particles alone are not cytotoxic. Adding normal human serum to *E. coli* and Fc particle treated conditions lead to increased amounts bacterium death. There were no significant increases in *E. coli* death with the addition of the Fc coated particles.

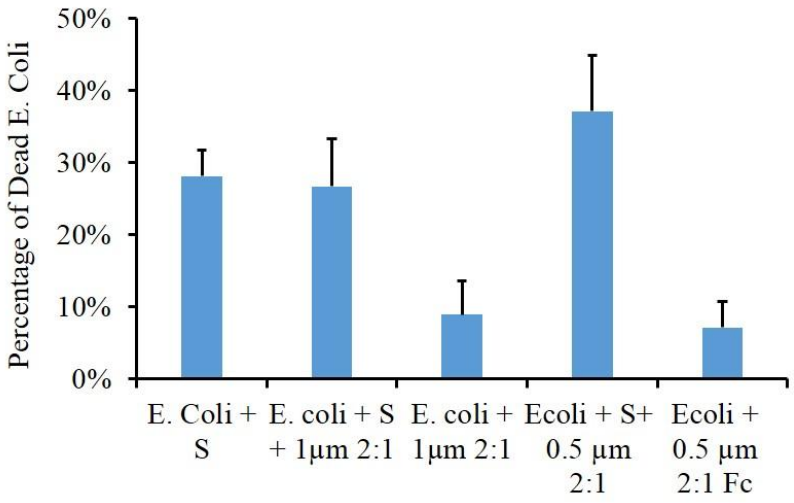

Figure 31: Percentage of E. coli death as a result of high Fc coated particles.
With normal human serum (S), (N=5)

4.4 Discussion

The immune system is a vital and intricate system necessary for the clearance and defense against invading pathogens, as well as to maintain systemic homeostasis [5, 8, 9, 29]. Therefore, the ability to initiate, direct, and/or modulate the immune system could prove to be an important means to treat and prevent multiple immune-related disorders [4, 7, 46, 47, 63, 64, 111]. The complement system has been shown to play a role not only in immune-specific diseases [63, 64], but in vaccine efficacy [13] and inhibition of tumor growth [65, 66]. By using micro- and nanoparticles, we have adapted a well-established method previously used to study other immune components [13, 24, 26, 30, 94] to the activation and modulation of the complement system.

We successfully varied the density of Fc presentation on the particles by varying the molar ratio of IgG added to particles coated with BSA. Our results showed that Fc density has a significant impact on the magnitude of complement activation. While several studies have shown that multiple IgG molecules are needed to efficiently activate the classical complement pathway, none have examined the effect of Fc density when displayed on micro- and nanoparticles. Our results from the complement component

deficient sera and complement deposition study further characterize the complement system activation resulting from high Fc density coated particles.

It is surprising that an Fc density of 1:5 did not successfully activate the complement system for any of the particle sizes. A 1:5 antibody:antigen ratio nominally represents 20% surface coverage, although the measured coverage varies from 15% to 35% as determined from flow cytometry (Figure 20). For uniformly distributed antibody of 20% surface coverage, a Monte Carlo simulation calculated average spacing between Fc molecules as approximately 2.1 element spaces, corresponding to a separation of 38 nm if we assume an antibody-antigen complex size of 18 nm. However, due to stochastic variation in the antibody binding, each particle will on average contain a significant amount of surface area that locally displays a sufficiently high density of Fc to activate complement. Our model has determined that the proportion of the particle surface with a high local density of Fc increases nonlinearly with the surface coverage, as seen in Fig. 7C. This result suggests a possible explanation for the observed nonlinearity of complement activation with Fc density. We hypothesize therefore that an essential trigger for complement activation by Fc-coated particles is the assembly of the C1 complex on the surface of the particles via binding to multiple, closely apposed Fc molecules. Our model is meant to only illustrate the importance of Fc density in nonlinearly activating complement, as it neither accounts for possible confounding effects such as antibody aggregation on the particle surface, Fc orientation due to particle surface curvature, nor other factors that may trigger or inhibit complement activation.

While high Fc density conditions activated the complement system for all the tested particle sizes, the size of the particle played a significant role in determining the magnitude of the activation. For the 0.5 μm and 1 μm particles, there is no complement response for low density of Fc, but immune stimulation increases dramatically to a plateau at higher Fc density values. The 2 μm particle supports a more tunable platform for complement activation. For the 2 μm particles, only the highest Fc density condition

of 2:1 activated the complement system at comparable levels to the HAGG activator. The next highest Fc density condition of 1:1 activated the complement system in significantly lower levels than the HAGG activator ($p<0.005$), but it was still higher than the 1:5 and BSA-only condition ($p<0.05$). This apparent switch from a binary-like response in smaller particles to a tunable response in mid-range sized particles further highlights the importance of particle size to complement system response. Larger 4 μm particles showed an even less efficient complement activation response. Even at the highest antibody levels tested (10:1), complement activation plateaued at less than half of the positive HAGG control.

This result is all the more surprising considering the number of particles was held constant for each of the experimental conditions during the activation study. Remarkably, when we consider the amount of complement system activation by Fc-functionalized particles per unit surface area, the dependence on particle size is even more clearly demonstrated. It might be expected that complement system activation would be proportional to the surface area of beads and the absolute degree of Fc presentation. Instead, we found that the complement activation per unit area was over 4 orders of magnitude larger for the 0.5 μm beads compared to the 4 μm beads. In addition, a power law function describes the relationship between complement activation per unit area of each particle and particle size, with an exponential dependence of −2.5 (Figure 8). This effect results from the combination of lower maximum complement activation for larger particles, as well as an increased surface area of the larger beads. Previous work has shown that an increase in polymer surface area results in an increase in complement system activation [80, 126]. Our work thus suggests that functionalization of particles with IgG can reverse the effects of decreased total surface area.

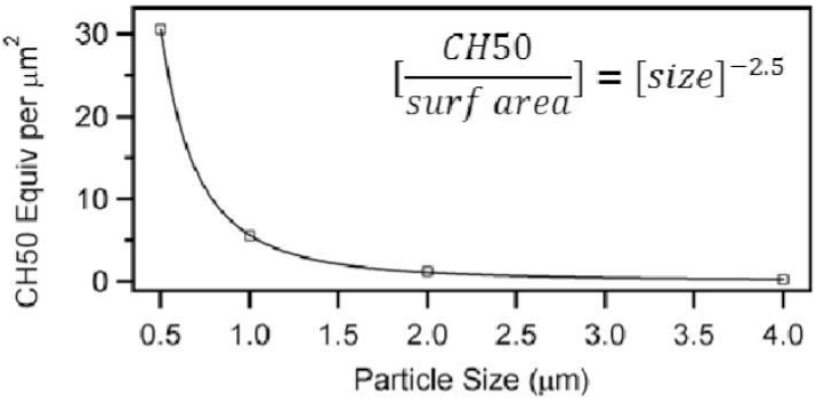

Figure 32: Maximum measured complement activation per μm^2 of particles versus particle size.

This study represents the first time that polymeric particles artificially coated in Fc were used to activate the complement system. While previous studies had suggested that crosslinking of multiple Fc molecules was the only requirement for initial activation by the classical pathway, our results suggest that the presence of multiple Fc regions is not sufficient to fully activate complement. In our studies, we observed that the complement system response decreases with increasing particle size, for a given Fc density condition. The sensitive dependence of the complement response on Fc density indicates the importance of nanoscale effects in efficiently modulating the response and that particle size can be an independent means to adjust the level of complement response once a threshold of Fc density is attained. While we cannot rule out a possible confounding effect in which particles prepared with similar treatments produce unequal Fc densities, the effect of particle size on complement activation may also be due to inherent biological properties of the complement system.

The topographic curvature of IgM-functionalized particles and peptidoglycan layers has been shown to influence the strength of complement activation, potentially through changes of the orientation of the Fc molecules. This same group found that complement system activation was maximized for 250 nm particles with decreased activation for both larger and smaller particle sizes. However, as they used IgM

antibodies to dextran already present in human serum samples and did not prefunctionalize their particles, these results could not be used to determine the impact of particle size on complement and the preference of IgM binding to particles of different size. As IgM are sufficient to activate complement, this method also does not allow the tuning of complement activation, either through variation in Fc density or through particle size, especially in the micron scale. [126] We cannot currently say whether the observed effect is due to the influence of surface curvature, the decrease of diffusive motion leading to increased depletion of reactants, or to some other effect. However, regardless of the reason, the observed inefficiency of complement activation with 4 μm beads could lead to the development of complement-modulation therapeutic agents, while nanoscale particles are likely more suited to more fully activating complement.

The results of our complement mediated cytoxicity assays are a proof of concept for future studies for directing complement system activation. Future experiments are needed to determine if there is a saturation level for particle mediated complement system activation and if this will correlate with cell death. These results could then be applied to biomedical needs in which controlled cell death is required such as for drug-resistant infections and cancer. However, these efforts will need to be balanced against the possible effect of increased inflammation as cleaved complement components act as powerful chemokines.

Better understanding the variables involved in successful complement system activation will improve our ability to take advantage of nanotechnology in basic or applied immunology. Due to the powerful nature of successful complement system activation, as well as the multiple naturally-occurring safeguards in place to prevent an autoimmune response, the observed dependence on particle size and Fc density affirms our hypothesis of the importance of nanoscale effects on complement control. As the complement system response is essential for clearance of pathogens and vaccine efficacy, the ability to modify and/or fine-tune the magnitude of complement system activation

with nanotechnology holds significant promise in these broad reaching fields. However, further study is needed to adequately delineate and fully understand the effects of particle size and Fc density, as well as to further identify the specific range of Fc presentation needed to successfully activate the complement cascade.

CHAPTER 5 INTERACTIONS OF Fc OPSONIZED MICROPARTICLES AND BCG WITH MACROPHAGES

5.1 Introduction

Bacillus Calmette-Guerin (BCG) is the sole FDA approved vaccine for the prevention of active tuberculosis due to *Mycobacterium tuberculosis* infection. The BCG vaccine was considered very effective upon its release in 1920s, but overtime various studies have shown a wide range in efficacy from 0-80%. While there seems to be a considerable protective effect on young infants and studies in mice, this protection can wane dramatically in cases of adult pulmonary infection. The high rates of initial infection, as well as the increasing number of multi-drug resistant tuberculosis infections, highlight the need for an improved tuberculosis vaccine. [19, 21, 49] There are many suggested reasons behind this wide range in efficacy. One is the loss of immunogenic or virulent factors of the vaccine, which is a live strain of *Mycobacterium bovis,* as it was passaged over time. Another includes the exhaustion of the local immune response due to the lack of clearance of the vaccine due to T cell depletion over time. This would suggest that increased uptake of the vaccine after initial delivery and increasing the local immune response may increase vaccine efficacy. Others have shown that the vaccine does not interact with local macrophages upon injection. [82]

There are currently a multitude of different approaches to solve these shortcomings of the vaccine such as developing a variety of subunit vaccines, addition of adjuvants, or using a particle based delivery platform. [144-148] With the goal of targeting intracellular pathogens, which typically evade the lysosome, to the macrophage lysosome to ensure full degradation, one group primed macrophages with Fc coated particles. The Fc particles crosslinked the Fc receptors on the macrophage surface and triggered downstream internal cell signaling that led to the recruitment of LAMP1. This

causes the lysosome to mature and results in pathogen degradation. [62] However, the need to deliver the particles an hour before the vaccine would be difficult to implement clinically. Therefore, we set out to show that delivering Fc particles and BCG together, would lead to increased internalization of BCG and targeting of BCG to the mature lysosome. We chose two particle sizes, 0.5 μm and 1 μm, based on our successful results from previously published studies that showed increased levels of phagocytosis and complement system activation for these sizes. [149, 150] While this would have a significant application in vaccine efficacy, there are also applications for treatment of tuberculosis and other intracellular pathogens that evade lysosome maturation.

5.2 Materials and Methods

5.2.1 Cell Culture

Mycobacterium bovis, Bacillus Calmette-Guerin (BCG) Pasteur strain, was originally purchased from ATCC. Cultures were initially plated on 7H10 agar plates. These agar plates were composed of Middlebrook 7H10 agar with a 10% oleic acid, albumin, dextrose, and beef catalase (OADC) supplement. After approximately 4 weeks, colonies were collected and inoculated into Middlebrook 7H9 broth supplemented with sodium pyruvate and a 10% albumin, dextrose, and beef catalase (ADC). More information on the specific reagent formulations can be found in Appendix A.2.1. Cultures were grown for an additional 4 weeks before use in phagocytosis experiments. All cultures were grown in a humidified incubator at 37ºC.

Prior to use in experiments, a sample of the liquid culture was centrifuged for 10 minutes at 3000 G. The broth was then decanted and replaced with PBS. The mixture was then briefly vortexed and then sonicated. After sonication, the mixture was then passed through a 22 gauge syringe, in order to ensure single cell suspension. The concentration of liquid cultures was determined in accordance with previously published methods. A spectrophotometer was used to measure the OD580 with an absorbance reading of 0.1

corresponding to 6.7E7 colony forming units (CFU) per mL. RAW 264.7 murine macrophages were cultured as outlined in Section 3.2.2. BCG was stained with TxRd on a shaker table for 45 minutes. The TxRd BCG was then washed twice through centrifugation and PBS to remove any unbound stain.

5.2.2 Microparticle Opsonization

Both yellow-green fluorescent and non-fluorescent polystyrene microparticles were used and were opsonized as outlined in Sections 3.2.1 and 4.2.1.

5.2.3 Phagocytosis

Phagocytosis assays were conducted using a similar protocol as outlined in Section 3.2.3. Approximately 500,000 RAW 264.7 macrophages were plated per well in a 6-well plate in complete, serum supplemented DMEM media and allowed to incubate overnight. Autoclaved coverslips were added to each well prior to cell plating if microscopy was to be done. Prior to phagocytosis experiments, the wells were washed with phosphate buffered saline solution and then refilled with 0.5 mL of DMEM alone. For the BCG alone and BCG with microparticles conditions, approximately 10 CFUs of BCG per macrophage were added per well. For microparticle only conditions, approximately 20 particles were added per macrophage while only 10 particles per macrophage were added for BCG with microparticles conditions. The following microparticle sizes were tested using both a high Fc density ratio of 2:1 (antibody to antigen) and BSA only conditions: 0.5 μm, 1 μm, and 4 μm. The phagocytosis incubation ranged from 2 hours, for microscopy analysis, and 4 hours, for flow cytometry analysis, at 37ºC in a humidified incubator with 5% CO2. Following the incubation period, the content of each well was decanted. The well was then washed with PBS twice to remove any unattached microparticles or bacteria.

5.2.4 Microscopy

To characterize the effects of test conditions on lysosome maturation, we used two different fluorescent schemes. We first attempted a commercially available fluorescent stain called Lysosenor (Life Technologies). Lysosensor has been used in previous studies to stain only the lysosome and the fluorescence of the stain increases as the lysosome becomes more acidic. This stain was added immediately after the cells were washed as this is a live cell stain. Multiple concentrations were tested to determine the optimal amount for image analysis. The wells were then imaged directly using a Nikon Epi-Fluorescence inverted microscope.

Our second method involved immunofluorescence using a primary antibody for the lysosome maturation marker LAMP-1 followed by an AlexaFluor488 conjugated secondary antibody (Abcam). DAPI was used to stain the nucleus as outlined in Section 3.2.5. To fix the cells, a 4% paraformaldehyde (PFA) solution was added to each well for 10 minutes. The wells were then washed twice with PBS. A permeabilazation solution, comprised of 0.1% TritonX and PBS, was added for 30 minutes at room temperature. The solution was then decanted and a 5% BSA blocking solution was then added for another 30 minutes at room temperature. After washing the wells twice, the primary antibody solution was added and allowed to incubate overnight at 4°C. The wells were then washed 3 times, before adding the secondary antibody solution. After 30 minutes at room temperature and protected from light, the wells were washed 3 times and then the DAPI solution was added for 5 minutes. The coverslips were then transferred to glass slides treated with an anti-fade solution, outlined in Section 3.2.5, and sealed with nail polish. The slides were then imaged using a Zeiss 710 Confocal microscope.

5.2.5 Flow Cytometry

Following the phagocytosis incubation period and washing steps, 0.5 mL of PBS was added to each well. The cells were then detached from the plate surface by scraping

and transferred to a microcentrifuge tube. Flow cytometry was then conducted as outlined in Section 3.2.4.

5.2.6 Nitric Oxide Assay

To determine the amount nitric oxide produced by the macrophages as a result of the microparticles and/or BCG, we used a commercially available Griess assay (Promega). For this, we tested the decanted media from the phagocytosis experiments at 4 hours or 24 hours. The assay was performed in accordance with manufacturer's instructions and the resulting absorbance was measured at 535 nm using pathlength correction.

5.3 Results

5.3.1 Microparticles Lead to Increased Levels of BCG Phagocytosis

Flow cytometry was used calculate the percentage of macrophages positive for BCG as well as the relative amount of BCG associated with each macrophage. The macrophage population was initially gated from non-internalized BCG and/or particles and other cellular debris. This macrophage population was then plotted along the forward scatter and the TxRd fluorescent channel. The untreated macrophages, or cells only, condition was used to gate cells that were negative for BCG by setting a threshold on the TxRd fluorescent channel. Examples of the gating used are shown below (Figure 33). The mean fluorescent intensity of the TxRd labeled BCG was also recorded of the entire macrophage population and for the BCG positive gated population.

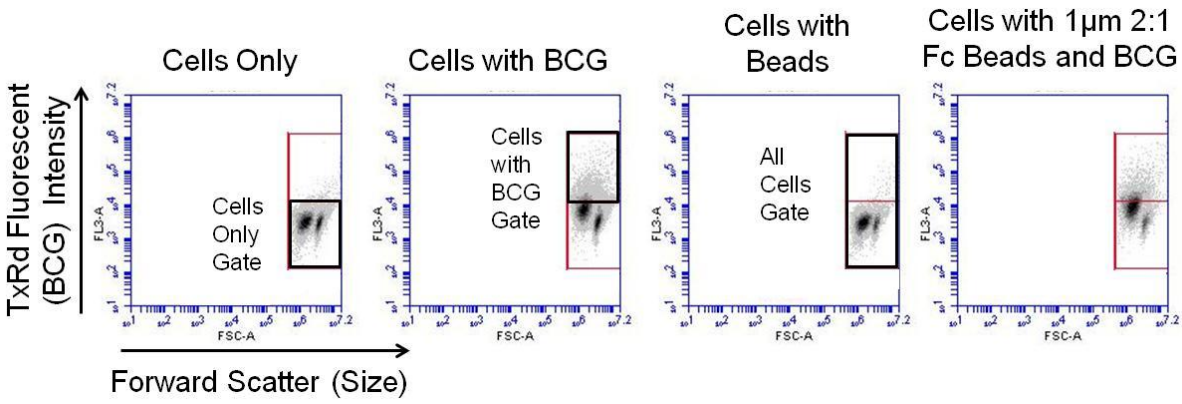

Figure 33: Example of flow cytometry gating scheme used to determine BCG positive macrophages.

Our flow cytometry results show an increase in the percentage of macrophages that were positive for BCG when microparticles were added during incubation and this was further confirmed using fluorescence microscopy (Figure 34). The median percentage of macrophages associated with BCG, when BCG was delivered alone, was approximately 15%. When high density Fc coated particles were added, for both 0.5 µm and 1 µm, that number more than double to 42% and 43%, respectively. However, BSA only coated particles also resulted in similar levels of BCG positive macrophages. There was no significant difference in the percentage of BCG positive cells between the Fc coated particles and BSA only coated particle treated conditions. While these particle treated conditions did result in an increase of overall percentage of macrophages positive for BCG, there was large variation between replicates. Therefore there was no significant difference between particle and BCG treated macrophages and only BCG treated macrophages.

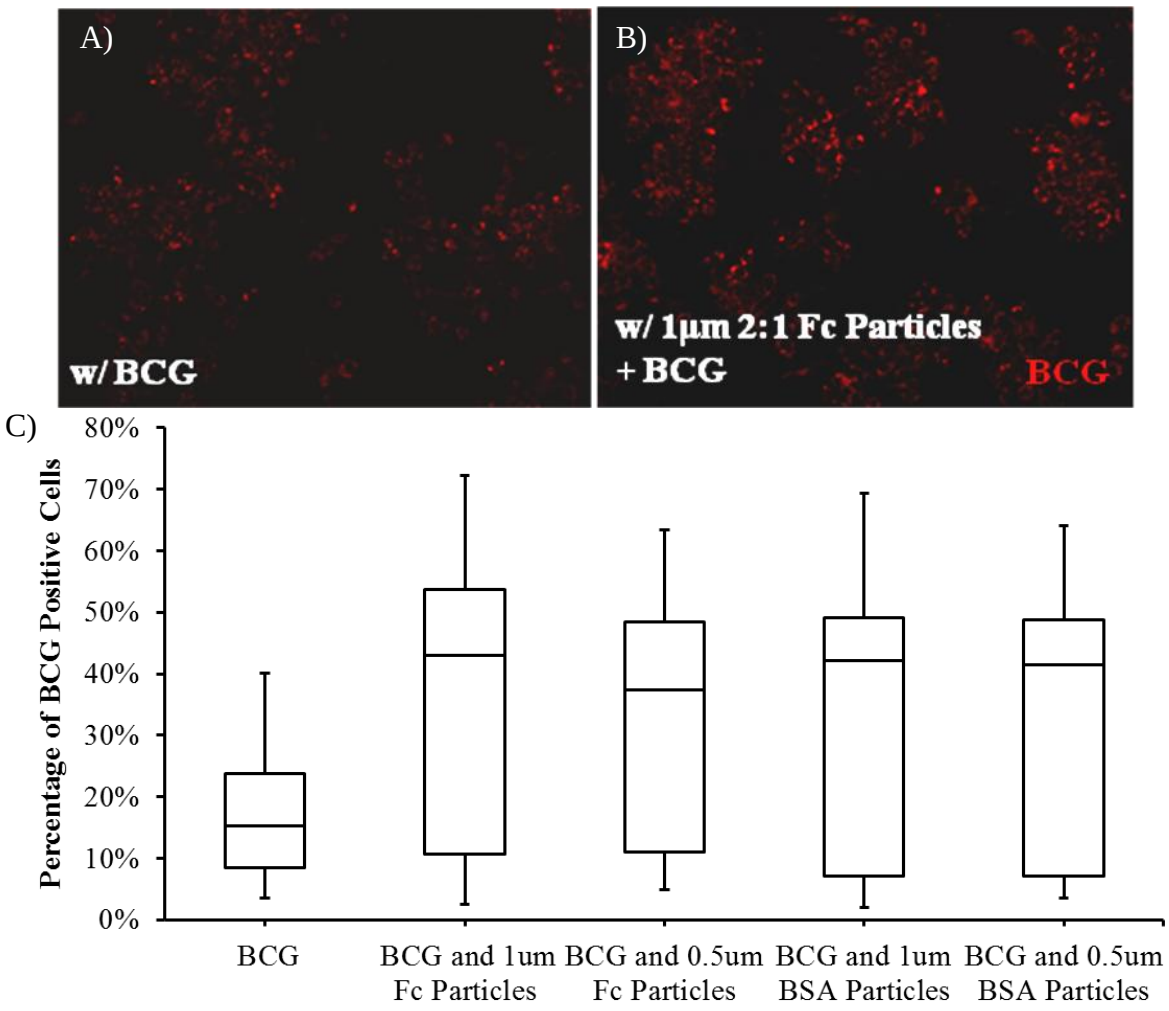

Figure 34: Microparticles added with BCG lead to increased levels of BCG internalization.
Fluorescent microscopy shows (A) the amount of BCG associated with macrophages when delivered alone compared to (B) when delivered with 1 µm 2:1 high Fc density coated particles. (C) Shows that adding microparticles, Fc coated or BSA only, leads to increases in the percentage of macrophages positive for BCG. (N>6)

We then measured the mean TxRd fluorescent intensity for the BCG positive macrophages to determine if fewer macrophages were internalizing greater levels of BCG (Figure 35). There was no significant difference in mean fluorescent intensity across any of the particle and BCG treated macrophages or the BCG only treated macrophages. To determine if there were small amounts of BCG below our gating threshold we also calculated the mean fluorescent intensity of the entire macrophage population (Figure

36). We found that the median value of the MFI for the BCG only group was slightly lower than the particle and BCG treated groups. None of these results were significantly different from each other.

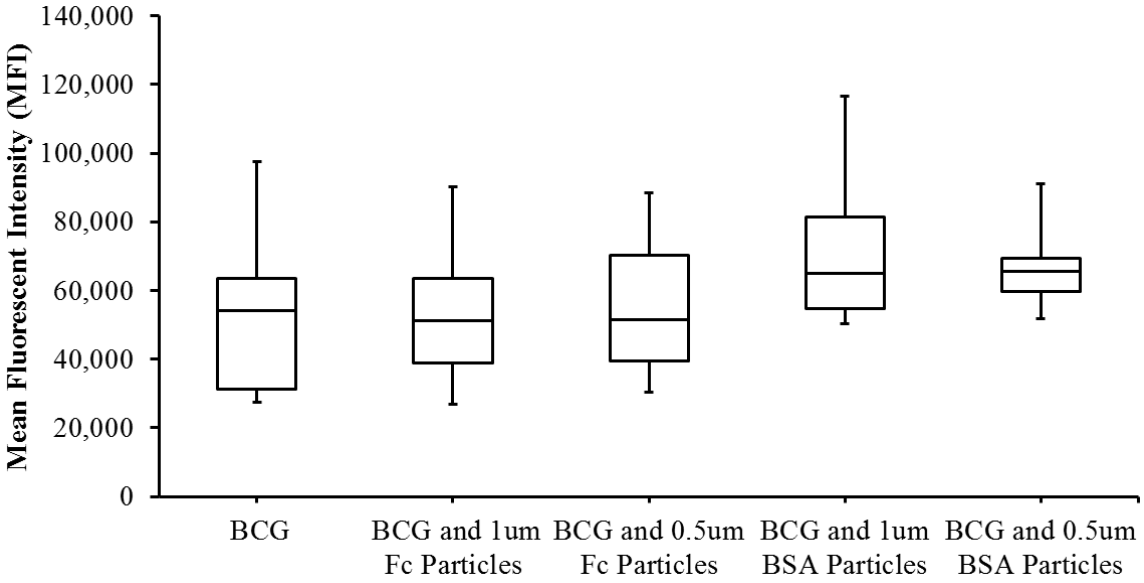

Figure 35: Mean TxRd fluorescent intensity of BCG positive macrophages.

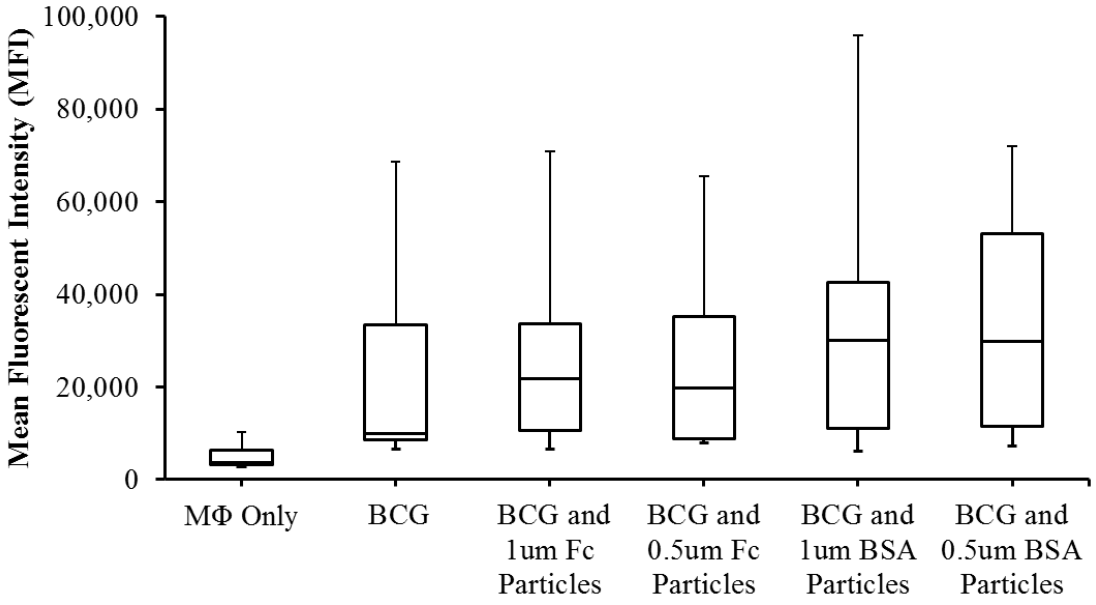

Figure 36: Mean TxRd fluorescent intensity of entire macrophage population.

As we saw that Fc coating on the particles did not impact the amount of BCG internalized, we repeated our experiments with a larger 4 µm particle that was coated only in BSA. We have previously shown that macrophages do phagocytose 3 µm and 4.5 µm in great numbers. Therefore this allowed us to evaluate if the increase in BCG positive cells was a result of smaller, more easily phagocytosable particles or an additional foreign presence. Our results show that the 4 µm BSA only coated particles with BCG and the 0.5 µm 2:1 high Fc density coated particles with BCG treated macrophages had similar levels of BCG positive macrophages (Figure 37). Repeating our analysis on the mean TxRd fluorescent intensity showed no significant changes across the different treatment groups (Figure 38).

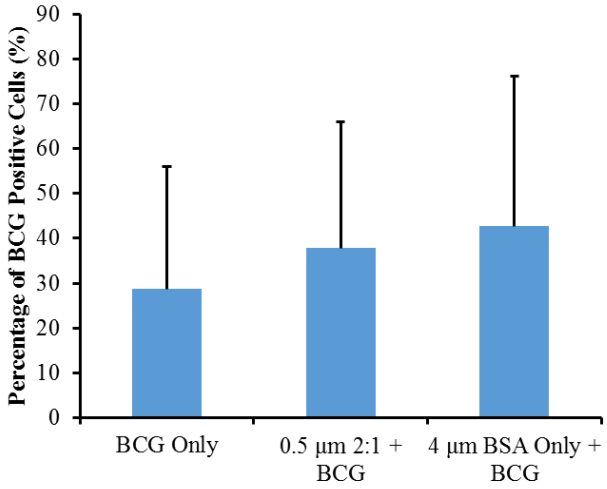

Figure 37: Percentage of BCG positive macrophages when treated with 4 µm BSA coated particles and BCG.

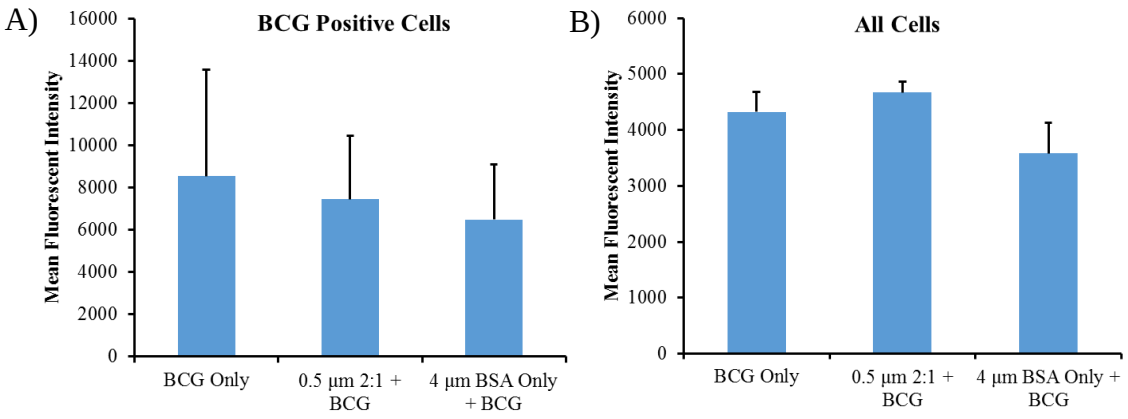

Figure 38: Mean fluorescent intensity of 4 µm BSA coated and BCG treated macrophages.
MFI of (A) BCG positive macrophages and (B) all treated macrophages.

We also determined whether macrophages needed to be primed with Fc coated particles before adding BCG. The macrophages were pretreated with either BCG or 0.5 µm 2:1 Fc coated particles for one hour, before the 0.5 µm 2:1 Fc coated particles or BCG, respectively, were added to the wells. The total amount of time the BCG was allowed to incubate with the macrophages was kept constant at 4 hours. BCG only and 0.5 µm 2:1 Fc coated particles with BCG were used as comparisons. We found there was no significant difference between the percentage of BCG positive macrophages for any of the tested populations (Figure 39).

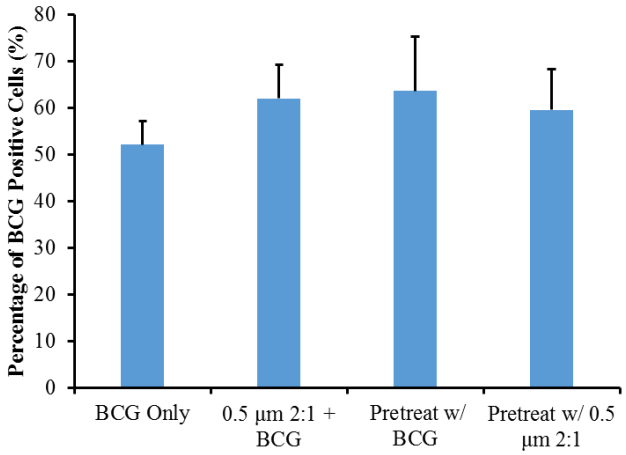

Figure 39: Percentage of BCG positive cells when macrophages are pretreated with BCG or Fc coated particles.
It should be noted that these results are preliminary with N=2

5.3.2 Fc Microparticles with BCG Result in Increased Nitric Oxide Production

Nitric oxide production was measured after 4 hours and 24 hours. After 4 hours, there was a slight increase in nitric oxide production in macrophages treated with BCG compared to the macrophage only group. Adding 1 μm 2:1 Fc coated particles led to a greater increase in nitric oxide and this increase was maintained in the presence of BCG (Figure 40A). For the 24 hour treated groups, an LPS treated group was added as a positive control while a 1 μm BSA coated particle was added as a negative control. After 24 hours, the differences between the particle and BCG treated groups were minimal (Figure 40B). There were significantly low levels of nitric oxide in the untreated macrophage only group. The concentration of nitric oxide was slightly lower in the BCG only and 1 μm BSA with BCG treated macrophages, but they were not significantly different.

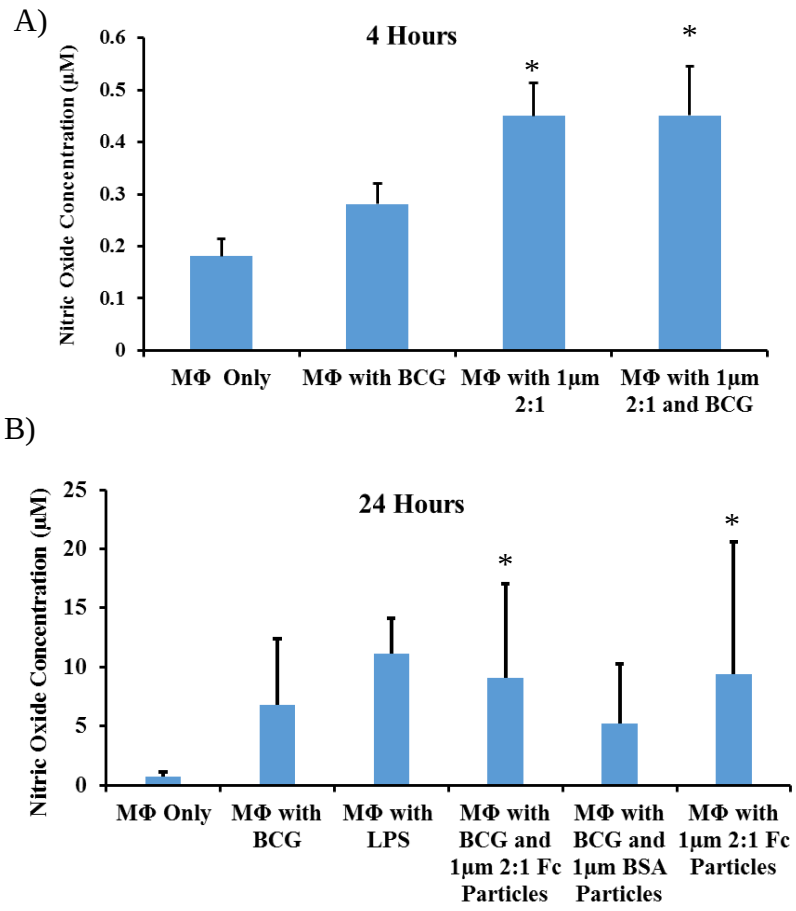

Figure 40: Nitric oxide production macrophages treated by BCG and 1 µm Fc coated particles.
Concentration of nitric oxide after (A) 4 hours (N=3) and (B) 24 hours (N=4). *, significantly different from MΦ only, $p<0.05$, using ANOVA with Tukey HSD.

5.3.3 No Correlation with the Addition of Fc Microparticles with BCG and Lysosome Maturation

Confocal microscopy was used to image the distribution of the LAMP-1 through BCG and BCG with particle treated cells (Figure 41). These images show that LAMP-1 is more distributed in treated macrophages compared to untreated macrophage controls. However, there was a not a strong correlation between LAMP-1 colocalization with BCG in macrophages treated with BCG alone or with BCG and 1 µm or 0.5 µm 2:1 Fc coated particles. There was also no correlation between LAMP-1 intensity for any of the treated macrophage groups.

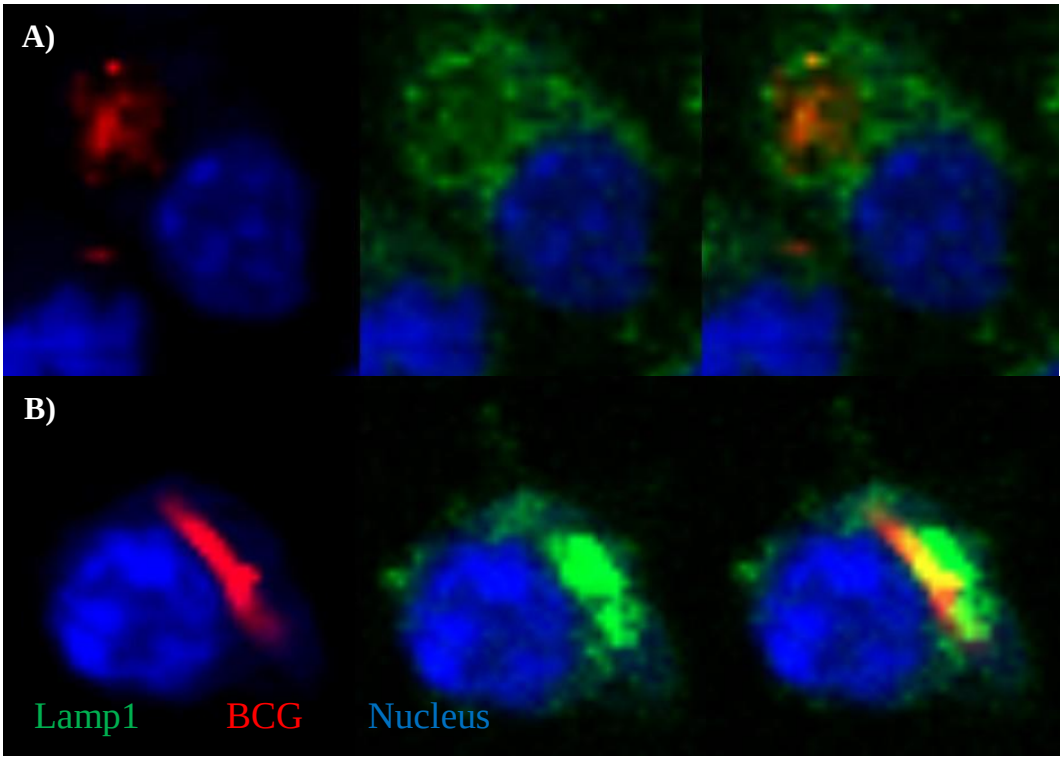

Figure 41: Representative confocal images of BCG and lysosome staining. This shows BCG stained in red and LAMP-1 stained in green with blue representing the nucleus of (A) macrophages treated with 0.5 µm 2:1 Fc coated particles with BCG and (B) BCG only.

5.3.4 Microparticles and BCG Are Less Likely to be Phagocytosed Together

As there was no correlation with lysosome maturation, we then analyzed our images to determine the amount of treated macrophages that were positive for both particles and BCG. Clusters of particles as well as BCG could be detected using brightfield microscopy. BCG could also be detected with the 534 nm laser. LAMP-1 expression was imaged using a 488 nm laser. We found that the majority of macrophages positive for particles, were not positive for BCG (Figure 42). The percentage of macrophages that were positive for particles, BCG, or both was quantified by counting the cells from confocal microscopy images. Images from macrophages that were treated with 1 µm 2:1 Fc particles and BCG at the same time or were treated with 0.5 µm 2:1 Fc particles for one hour and then BCG was added. The results show that the percentage of macrophages positive for BCG stayed constant at approximately 30%. When

macrophages were primed with Fc particles first, the percentage of macrophages positive for both BCG and beads increased from 10% to 20%. The amount of LAMP-1 expressed did not seem to vary, whether the cell phagocytosed BCG and/or particles or did not. Macrophages that phagocytosed large number of particles appeared to form a large vacuole around the particles that was lined with LAMP-1 expression.

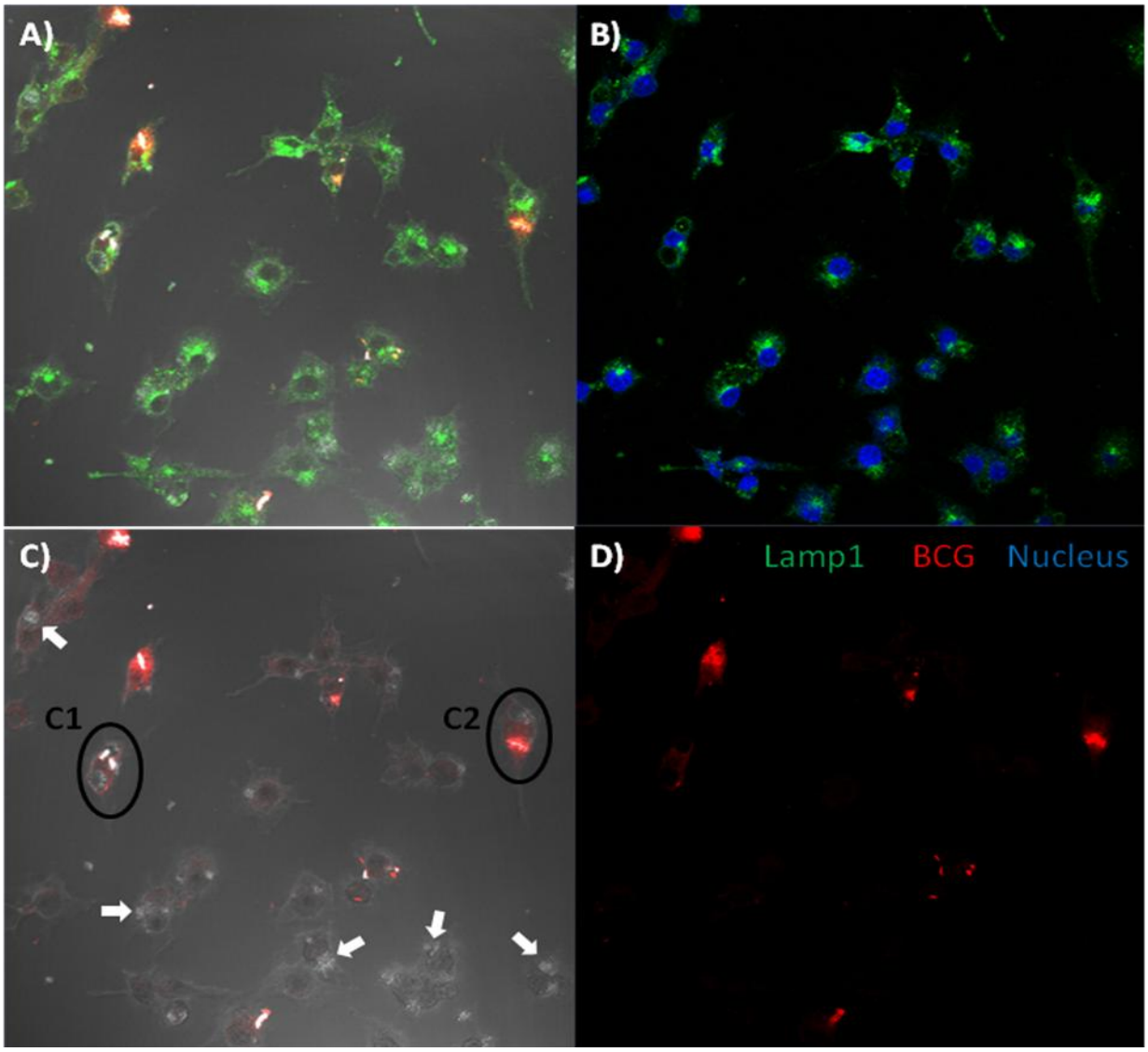

Figure 42: Confocal microscopy shows macrophages are not likely to be positive for both particles and BCG.
(A) Overlap of brightfield, green fluorescence, and red fluorescence filters (B) Overlap of green fluorescence and blue fluorescence (C) Overlap of brightfield and red fluorescence with white arrows pointing to clusters of internalized particles. Shows macrophages that phagocytosis large numbers of particles do not phagocytosis large amounts of BCG.

Exceptions are noted by the two cells circled in black. Arrows point at cells with large numbers of particles (D) Red fluorescent filter showing amount of BCG phagocytosed

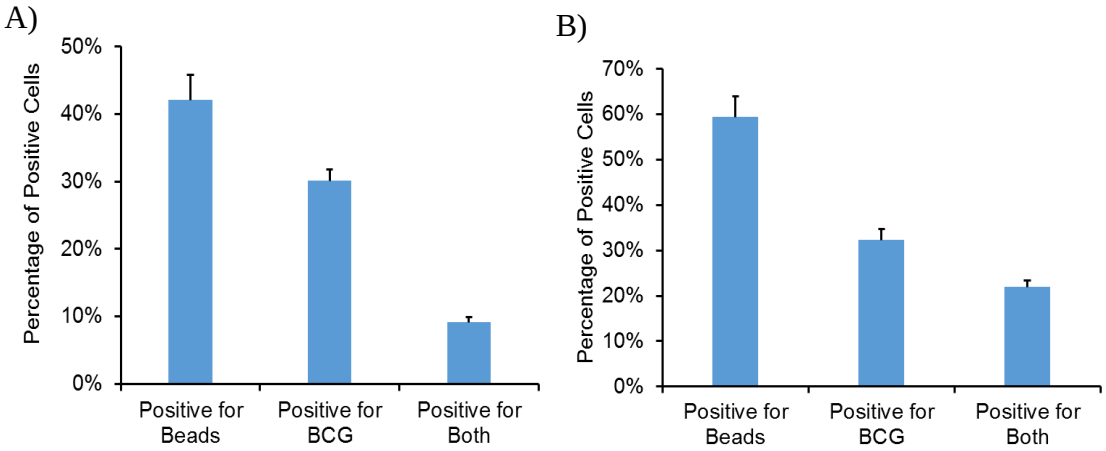

Figure 43: Percentage of macrophages positive for beads, BCG, or both.
A) Macrophages were treated with 1 µm 2:1 Fc beads and BCG or B) macrophages were treated with 0.5 µm 2:1 Fc beads first for one hour before BCG was added.

5.4 Discussion

While these results were not expected and seem to reject the hypothesis, we have made observations that pose a multitude of additional questions for future studies. It was thought that the addition of Fc coated microparticles to BCG would result in increased phagocytosis and lysosome maturation as shown in previous studies [62]. However, our results suggest that it is the addition of the just the microparticle alone, whether functionalized with Fc or coated in BSA only, that leads to greater levels of phagocytosis. That this result was seen in 0.5 µm, 1 µm, and 4 µm particles, suggest microparticle size was not a significant variable. While the Fc coating, or lack thereof, did not significantly affect the percentage of macrophages positive for BCG, this does not mean biochemical signals were not a factor. We have previously shown that the addition of microparticles, both Fc and BSA coated, affects cytokine expression and secretion (Sections 4.3.5 and 3.3.6). Therefore we can assume the complicated feedback loop of cytokine signaling between macrophages that have phagocytosed particles and/or BCG plays a significant role in BCG phagocytosis. One method to test for this in future experiments would be to

use conditioned media from macrophages treated with Fc coated particles. We can also repeat gene expression analysis on Fc coated particle and/or BCG treated macrophages.

Our results also showed that there was no change in mean fluorescent intensity of BCG positive macrophages. This suggests that the macrophages internalizing BCG in the presence of particles are doing so at the same level of BCG only treated macrophages. Overall more BCG is thus internalized by the macrophages in the particle treated conditions. This increase in the amount of BCG internalized would correspond to increased clearance of the vaccine and interaction of BCG with macrophages as an antigen presenting cell. If the macrophages do fully process the BCG for antigen presentation then the bacterium is also destroyed. This would also show that our particles may be used as an antibiotic to enhance macrophage destruction of tuberculosis and resist residency of the bacteria intracellularly. Our particles could then be used as a supplement to current treatments and use patient's own immune system to clear the infection.

To prevent unnecessary repeated experiments on multiple variables, there is a need for better understanding of how these particle based immune complexes interact with macrophages in the presence of BCG. Previous studies have shown that mice deficient in the Fcγ chains increased the susceptibleness of the animal to infection and increased an immunosuppressive response [151]. The previous work with Fc coated particles and BCG with the resulting increase in lysosome maturation had two different conditions that my work. One, they used 2 μm particles, and two, they first primed the macrophages with the Fc coated particles before adding BCG. [62] Our results show no difference between groups that were first primed with Fc coated particles or BCG. If the increase in lysosome maturation was in part due to the particle size, this would suggest the macrophage may be more receptive to particles that are approximately on the same size scale as BCG. The 4 μm that we tested may fall just beyond the upper boundary for size mediated enhanced BCG uptake. Therefore we can repeat our experiment using 2 μm particles or rod shaped particles in order to better mimic BCG. We can also compare

these results to BCG opsonized with IgG and Fc coated particles that are first bound to BCG.

We also attempted to answer how the addition of Fc coated particles might reverse many of the immunosuppressive characteristics of tuberculosis [152] and its analogous form in BCG. Induction of nitric oxide has been shown to lead to increased BCG death [153] which is why we wanted to quantify the amount our particles induced. We found that initially there was approximately a 30% increase as a result of our particles, but this difference diminished overtime. Further evaluation will be needed to determine if a small increase in nitric oxide production after initial treatment is enough for full vaccine clearance. However these results may be promising *in vivo* as the initial nitric oxide production may affect the response of macrophages recruited to the site of tuberculosis infection and prevent the infection from spreading within these newly arrive hosts. This also goes back to activating macrophages so they are better capable of fully processing the bacterium, whether it is the vaccine grade or an actual infection. Previous studies have shown the addition of LPS to macrophages before adding BCG lead to increased clearance of the bacterium. [154] While this supports the argument that priming macrophages into a pro-inflammatory state will result in better clearance of the bacterium, this is not an ideal candidate for vaccine implementation. The strong response LPS provides will likely lead to cytotoxic effects and a severe reaction in patients. If our Fc coated particles prove to provide an attenuated inflammatory response, either through macrophage or complement system activation, the may still prove to be a viable option.

CHAPTER 6 CONCLUSIONS AND FUTURE DIRECTIONS

The field of immunology has always been a broad and impactful. The more recent field of immunoengineering allows us to not only modify the immune response, but to purposefully engineer a response for a desired application. The humoral immune response is not only a front line defender against invading pathogens, but also strongly impacts the adaptive immune response. The Fc region is a powerful immunomodulator within the humoral response and using this fragment in various surface densities allows us to attempt to control the immune response. Microparticles are an ideal platform as a number of variables can be controlled and tested. Certain properties, such as the material of the particle, can then be changed in the future depending on the application while keeping other variables, such as size and coating, the same. This work has shown that microparticles coated with various Fc densities can have a strong impact on macrophage and complement system response.

6.1 Fc Density and Microparticle Size Effect Macrohpage Phagocytosis and Phenotype

Our results in CHAPTER 3 show that both Fc density and microparticle size have a strong affect on macrophage response. Smaller microparticles (0.5 μm and 1 μm) coated in high densities of Fc led to the greatest number of particles internalized per cell. The larger particles (3 μm and 4.5 μm) resulted in significantly lower levels of internalized particles, but the greatest amount of volume of internalized particle per cell. These results suggest particle size and Fc density can be varied for different goals of drug delivery applications. If the goal of the delivery is to deliver the greatest number of particles or provide a stronger initial input to macrophages, then smaller particles would be ideal. However if the goal is to deliver the greatest amount of payload, then larger particles are preferred. There are limitations to this study, as the Fc pathway was never

blocked or inhibited to ensure that phagocytosis was FcR mediated. Future studies should be done to confirm FcR mediated phagocytosis, as well as a better understanding of the kinetics of internalization. Time-lapse microscopy can be used to determine how particles are internalized and if certain macrophages become more activated than others.

The results from the gene expression and cytokine secretion analysis shows that the size and Fc density of the particle affects macrophage response. This was true even when the particle sizes were what we previously considered small at 0.5 μm and 1 μm. The most powerful results were seen in the macrophages that were first treated with IL-4 and LPS as the response was inverted when Fc coated particles were added. This reverse of macrophage response was seen even though the original stimulus of IL-4 and LPS was not removed from the media. The reverse in response for both alternative and classically activated macrophages suggest that Fc coated particles induce a phenotype that lies between these two states. Further work is needed to confirm this through expanded cytokine secretion analysis and expanding the incubation period. The increased levels of TNFα and IL-12 with the addition of high Fc density particles suggests a more pro-inflammatory response. While TNFα production has been associated with increased FcR crosslinking, previous work has shown that levels of IL-12 production typically decreases. This could be an effect of particle size and most studies used larger particles or immune complexes alone. However, the amount of IL-12 produced may still be lower than IL-10 which would be in accordance with previous work. Repeating ELISA analysis with a proper dilution would provide further context. For future biomaterials applications, it would be important to understand if the gene expression and cytokine secretion levels are a result of the act of internalization or FcR crosslinking or combination of the two. This could be decoupled by coating a substrate with Fc ligands so the macrophages could bind but not phagocytose the complex. These results would be important for *in vivo* testing as a particle or substrate based platform, such as a hydrogel, could be delivered.

These results could then be applied to *in vivo* models where a shift in macrophage is desired such as chronic inflammation or sepsis.

6.2 Fc Coated Microparticles Successfully Activate the Complement System

Chapter 4 showed the complement system could be activated by Fc coated particles and the level of activation could be controlled by changing the particle size and Fc density. This represents the first instance to our knowledge in which complement system activation has been achieved through Fc coated particles. While the majority of the resulting complement activation was through the classical pathway, a significant portion was also through the alternative pathway. This suggests the high Fc coated particles will be able to activate the complement system *in vivo* even in cases where a person is deficient in C1. However, there were significant lower levels of complement activation for larger particles. While curvature has been suggested to play a role in complement activation for unopsonized materials, it is not well understood why the larger particles failed to activate complement. Further studies are needed to understand why this occurred. One possibility would be that the 4 μm particles provide more surface area for initial complement components to deposit. The disperse spread of the initial components may prevent the cascade from completing. This could be tested by diluting the amount of 4 μm particles so that the total surface area of is equivalent to that of the 0.5 μm and 1 μm used previously. It also important to understand the minimal amount of particles needed for complement system activation to prevent toxic autoimmune effects.

However, our proof of principle for inducing cytotoxic effect on *E. coli* showed only a modest increase in bacterial death compared to the inherent bactericidal properties of serum. While our complement deposition results showed that some of the activated complement components deposited on the cell surface, a portion likely remained in solution. As our EIA kit did not separate the particles from serum when determining the amount TCC formed, we cannot confirm the exact proportion deposited on particles

versus solution. By repeating the complement EIA on serum that has particles removed first, we could determine the amount of TCC free to deposit on potential *in vivo* surfaces. In the case of *E. coli* cytotoxicity, complement activation was not sufficient to result in bacterial death in significantly greater amounts than serum only conditions. The 10:1 bead to bacterium was used as a proof of principle and is unlikely to be feasible clinically with the current particle sizes used. However the beads would show greater promise in the case of serum-resistant bacteria or in the case of complement deficient patients. [143]Further study is needed to determine if particle concentration, as well as decreased particle size, affects complement system activation and complement mediated cytotoxicity. In addition, we hypothesize that a Janus particle capable of directly binding a bacterium while activating the complement may lead to enhanced and selective cytotoxicity. Beyond cytotoxicity, complement system activation can be used to harness the powerful chemotactic effects of cleaved complement components C3a and C5a. Transwell migration assays can be performed to determine if Fc particle mediated complement activation leads to increased recruitment of various immune cells. We can also begin applying our Fc coated particles to known vaccine *in vivo* models to determine if an adjuvant effect is present.

6.3 Microparticles Affect BCG and Macrophage Response

In Chapter 5 we attempted to show that Fc coated particles would lead to increase phagocytic activity of macrophages as well as increased lysosome maturation. However, the addition of a microparticles, no matter their protein coating, led to increased levels of phagocytosis. It is unlikely that it is the size of the particle, as there was also no difference when larger 4 μm particles were added. This suggests the addition of particles alone triggers macrophages to become more phagocytic of BCG. However as previous research has shown particles treated with 2 μm particles resulted in increased phagocytosis of BCG as well as increased lysosome mature, a repeated study with 2 μm

may be warranted. Previous work by others and work demonstrated in Chapter 2 showed that shows 2 μm particles may be ideal for triggering phagocytosis, particularly due to topographical characteristics of macrophages.

The amount of nitric oxide produced and LAMP-1 expression was also not significantly different between BCG and Fc particle treated conditions. While this was discouraging, a critical observation was made relating to colocalization of BCG and Fc coated microparticles. Macrophages that internalize high numbers of Fc coated microparticles did not internalized BCG and vice versa. This should be further examined and confirmed using flow cytometry. In this case, it should be noted that microparticles that are previously labeled with fluorescence will overpower any signal from TxRd labeled BCG. The use of conditioned media from macrophages treated with Fc coated particles can be used to determine if the increased phagocytosis of BCG is due to cytokine signaling. Microfluidic technology can then be used to carry out qRT-PCR on invidual macrophages. This could show the differences in macrophage response between macrophage that internalize BCG versus Fc coated particles. To ensure these responses are mediated through Fc pathways, macrophages deficient in FcR should be used as a negative control.

Repeated phagocytosis experiments will be carried out that label earlier components of the lysosome maturation pathway, such as β-actin, Rab5, Rab7, and PI3P. This would show when the lysosome maturation process stalls during internalization of BCG and how the delivery of Fc coated particles affects each maturation step. Another method for determining lysosome maturation is by determining the amount of BCG degraded within the lysosome. Treated macrophages will be lysed with the lysate plated on agar plates to determine the viable CFUs. This would have broad implications on vaccine development as well a method for clearance of infection.

6.4 Perspective

This thesis showed the humoral immune response can be tuned using microparticles of various size and Fc coating density (Table 3). The phagocytosis results not only provide a greater understanding of how the combined effect of Fc density and particle size have on particle internalization, but we have also generated a particle internalization “toolbox” through which future researchers can tune particle variables to achieve desired applications. Quantifying macrophage phenotype is a complicated field, but the completed gene expression results provide a guide that will allow researchers to focus on genes that significantly modulate. This also suggests that macrophage plasticity can be altered upon delivery of a particle based system. The ability to alter macrophage response after initial priming will benefit a variety of pathologies including atherosclerosis, sepsis, allergy, and wound healing. Controlled complement system activation is significant to the immunology field, as this is the first time complement activation occurred through Fc coated particles. The complement system cannot be overlooked within the biomaterials field as complement system activation may be affecting the host response in a manner that is unexpected, such as increased cell death. These results also show the complement system can be activated through multiple pathways by Fc coated particles which is important to consider for patients who may be deficient in a single pathway components. The results from incubation of Fc coated particles and BCG with macrophages show that direct interaction of particles with macrophages is not needed for uptake in BCG. This highlights the importance of paracrine signaling that can be harnessed for altering macrophage response.

Table 3: Summary of effects of Fc density and particle size on macrophage and complement system response.

Immune Component	Fc Density	Particle Size	Effect
Macrophage	↑	↓	↑ Phagocytosis ↑ TNFα and IL-12
Macrophage	-	↑	↓ Phagocytosis
Complement System	↑	↓	↑ Complement Activation

Macrophages represent a powerful but complicated system which can be altered via particles after initial activation. Controlled complement system activation can be achieved and exploited in a variety of applications including vaccine development and chemotaxis. The results from this work can be applied to the greater fields of biomaterials and immunoengineering in hopes of better understanding important physical and biochemical design variables for the desired response.

APPENDIX

A.1. Supplemental Information for Microparticle Internalization

A.1.1. Protein Levels Used for Particle Coating

Particle Size (um)	Mass of Particles Functionalized (ug)	Antigen Added (ug)	IgG Added (ug)					
			1:1	1:2	1:5	1:10	1:50	BSA Only
4.5	1000	38.1	38.1	19.1	7.62	3.81	0.76	0.00
3	1000	57.1	57.1	28.6	11.4	5.71	1.14	0.00
2	1000	85.7	85.7	42.9	17.1	8.57	1.71	0.00
1	500	85.7	85.7	42.9	17.1	8.57	1.71	0.00
0.5	500	171.4	171.4	85.7	34.3	17.1	3.43	0.00

Figure A 1: Amounts of antigen and IgG added for each particle size and ratio condition.

A.1.2. Verification of Fc Coating on Particles

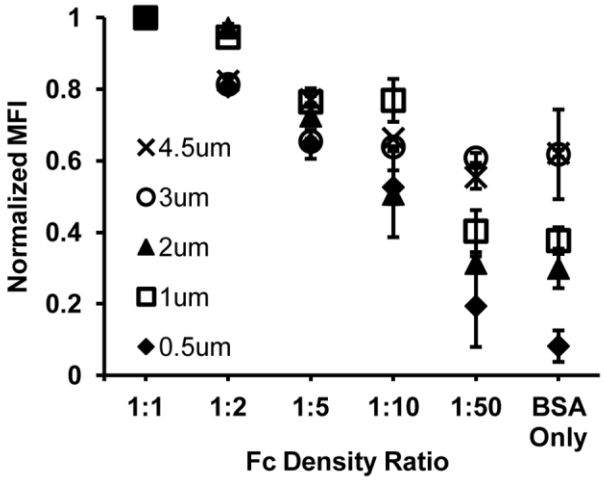

Figure A 2: Normalized mean fluorescence intensity of yellow-green fluorescent microparticles labeled with TexasRed fluorescently conjugated secondary antibodies.

Decreasing normalized MFI corresponds to decreased Fc density for fluorescent particles, however there is evidence of possible non-specific absorption of the secondary antibody and difficulty in fully compensating for the high background fluorescence of the microparticle core.

A.1.3. Examples of Flow Cytometry Gating

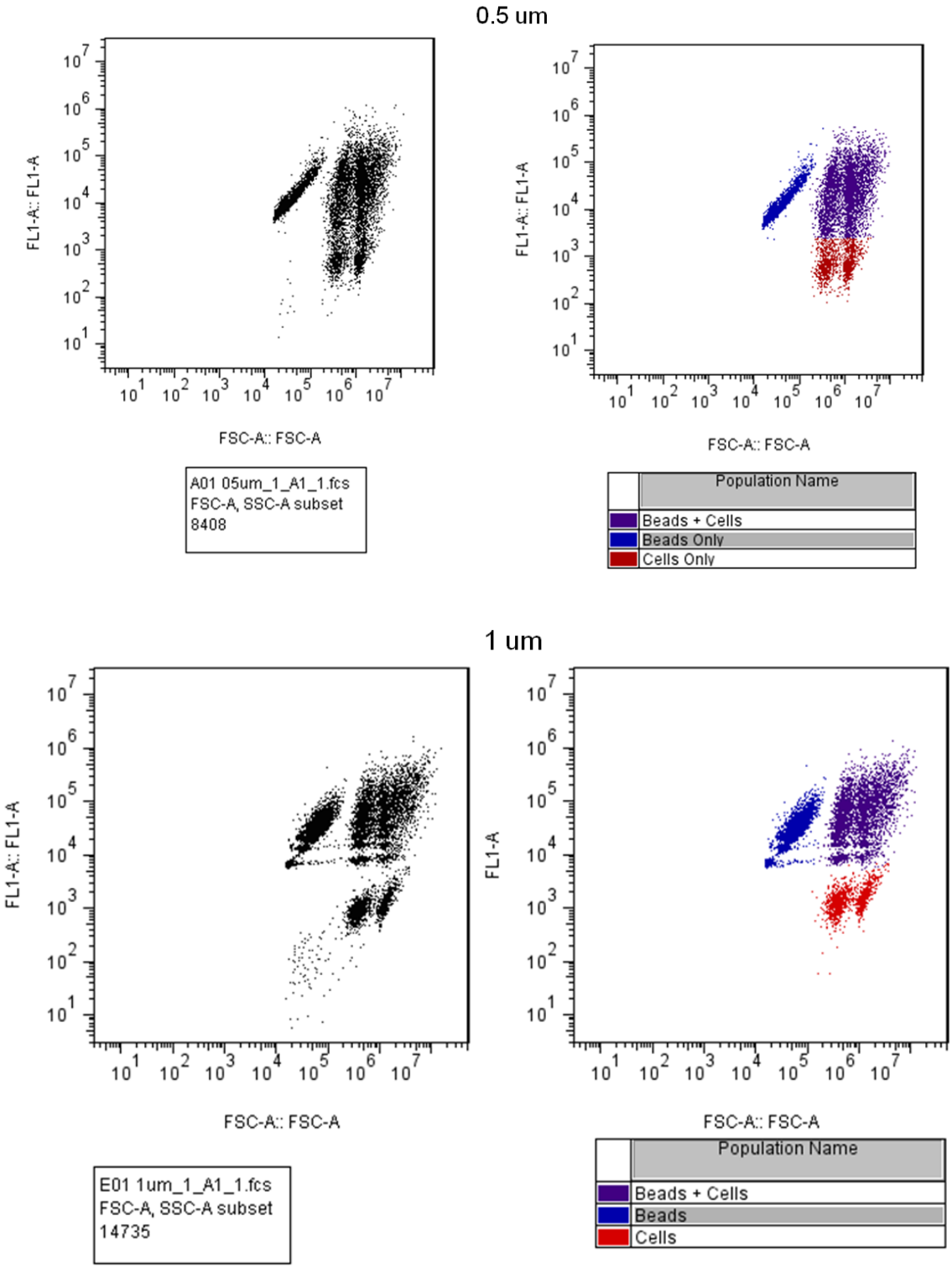

2 um

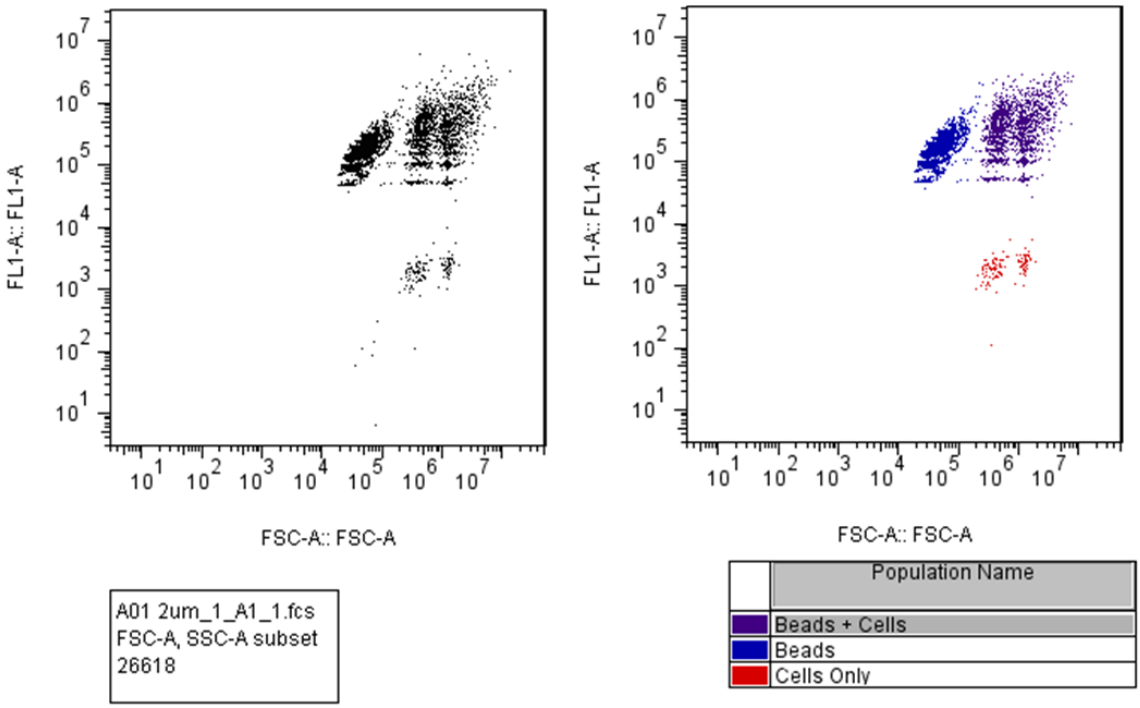
FL1-A:: FL1-A
FSC-A:: FSC-A
A01 2um_1_A1_1.fcs
FSC-A, SSC-A subset
26618
Population Name
Beads + Cells
Beads
Cells Only

3 um

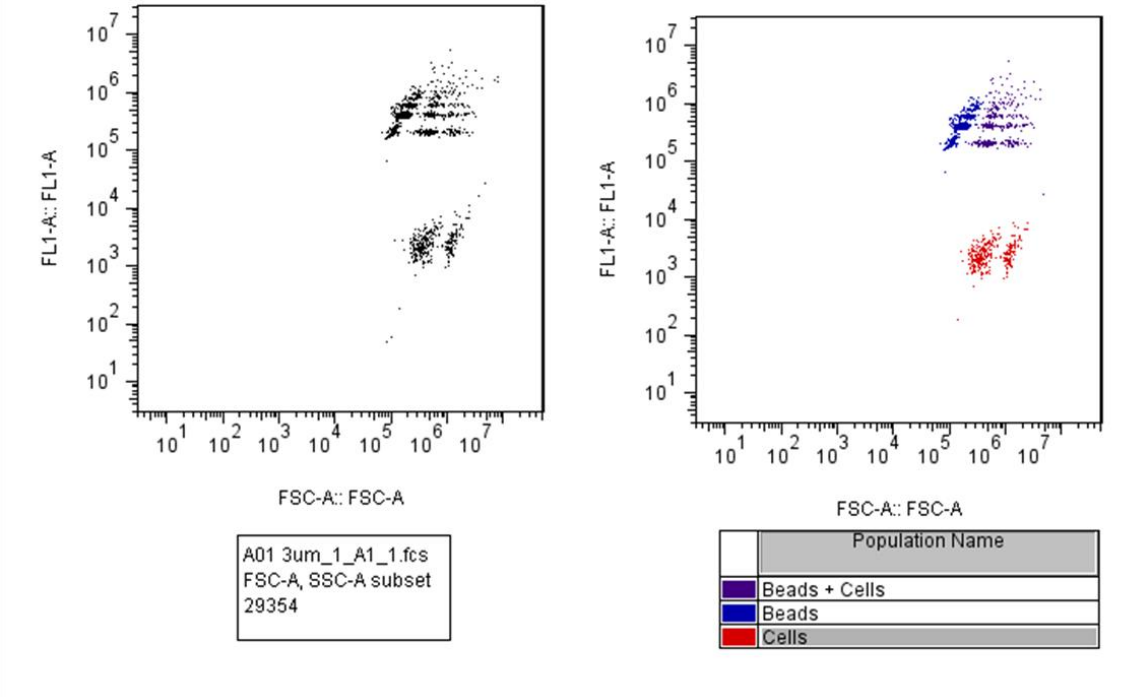
FL1-A:: FL1-A
FSC-A:: FSC-A
A01 3um_1_A1_1.fcs
FSC-A, SSC-A subset
29354
Population Name
Beads + Cells
Beads
Cells

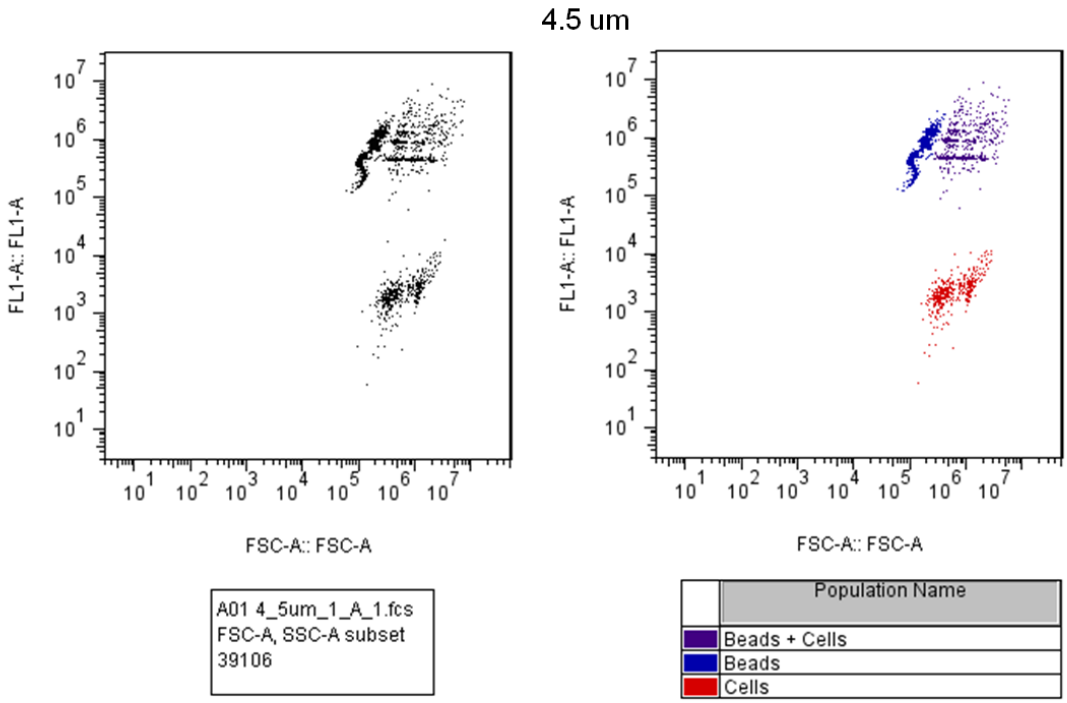

Figure A 3: Examples of Gating Methodology

A.1.4. Additional Quantification of Internalized Particles

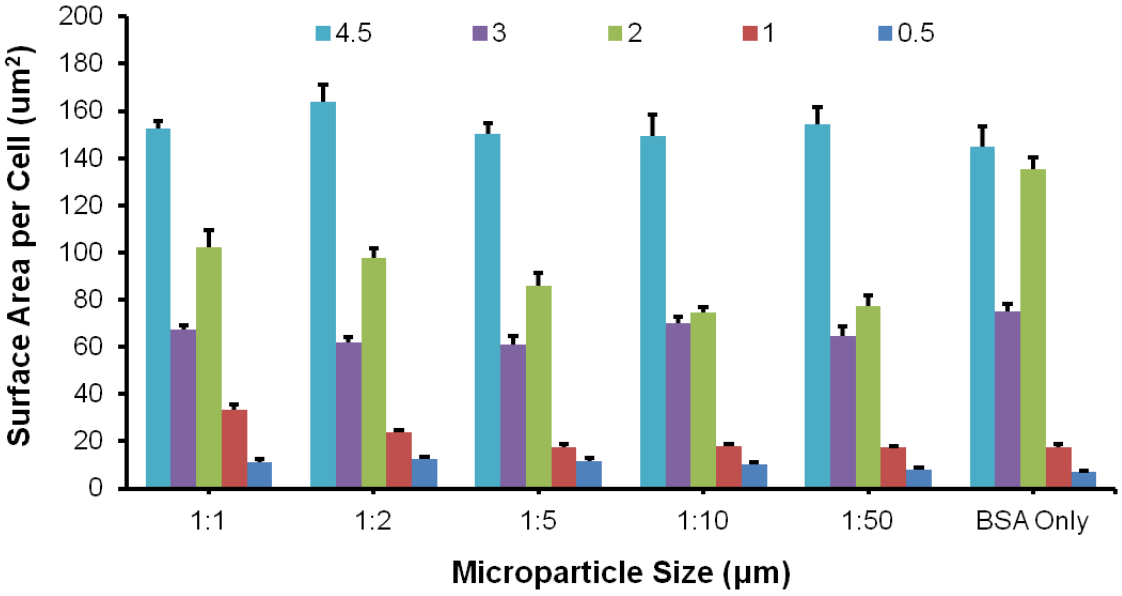

Figure A 4: Surface area of particles internalized per cell for different functionalizations.
The total surface area of internalized particles by macrophages for different particle sizes and Fc densities. BSA-only particles are shown for comparison.

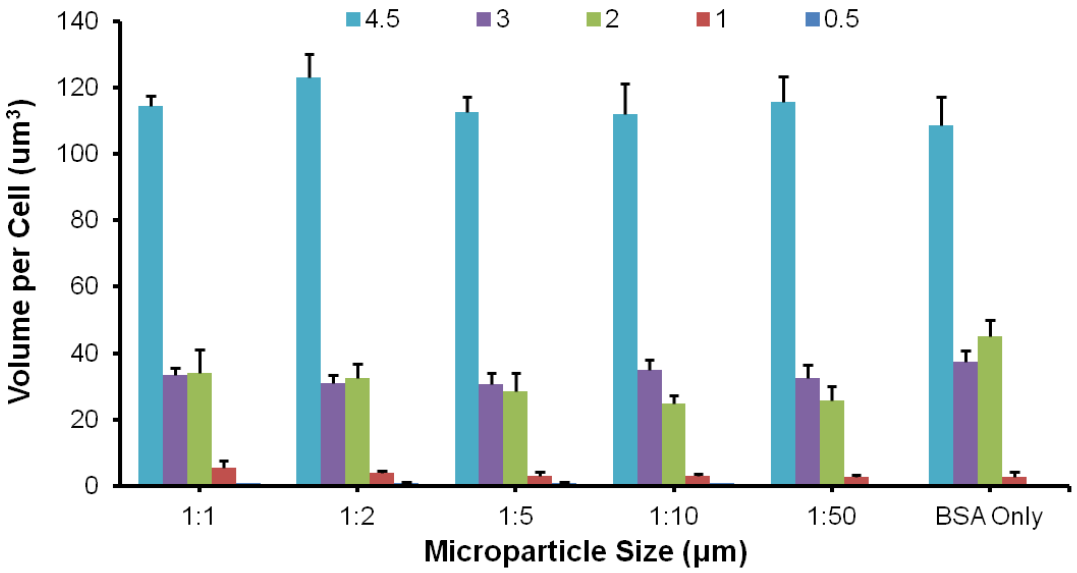

Figure A 5: Volume of particles internalized per cell for different functionalizations. The total volume of internalized particles by macrophages for different particle sizes and Fc densities. BSA-only particles are shown for comparison.

A.2. Supplemental Information for Mycobaterium bovis Interactions

A.2.1. Mycobacterium bovis culture

To create the Middlebrook 7H10 agar plates, 19 g of Middlebrook 7H10 agar was added to a flask containing 900 mL of deionized water and 5 mL of glycerol. This mixture was then stirred over a hotplate until the agar dissolved. The flask and contents were autoclaved and then cooled to approximately 55ºC. The OADC supplement was composed of 0.05 g of oleic acid, 5 g of bovine albumin, 2 g dextrose, and 0.004 g of beef catalase. This supplement was then added to 100 mL of deionized water and 0.85 g of sodium chloride. After the supplement fully dissolved, the solution was sterile filtered before adding it to the agar mixture. The supplement agar was then poured into 100 cm sterile petri dishes.

To create the Middlebrook 7H9 broth, 4.7 g of Middlebrook 7H10 agar and 4.4 g of sodium pyruvate was added to a flask containing 900 mL of deionized water and 2 mL

of glycerol. This mixture was then stirred over a hotplate until the broth dissolved. The flask and contents were autoclaved and then cooled to approximately 55ºC. The ADC supplement was composed of 5 g of bovine albumin, 2 g dextrose, and 3 mg of beef catalase. This supplement was then added to 100 mL of deionized water. After the supplement fully dissolved, the solution was sterile filtered before adding it to the broth mixture.

REFERENCES

1. Mosser, D.M. and J.P. Edwards, *Exploring the full spectrum of macrophage activation.* Nature Reviews Immunology, 2008. **8**(12): p. 958-969.
2. Anderson, J.M., A. Rodriguez, and D.T. Chang, *Foreign body reaction to biomaterials.* Seminars in Immunology, 2008. **20**(2): p. 86-100.
3. Tan, T.T. and L.M. Coussens, *Humoral immunity, inflammation and cancer.* Current Opinion in Immunology, 2007. **19**(2): p. 209-216.
4. Smith, D.A. and D.R. Germolec, *Introduction to immunology and autoimmunity.* Environmental health perspectives, 1999. **107 Suppl 5**: p. 661-5.
5. Parkin, J. and B. Cohen, *An overview of the immune system.* Lancet, 2001. **357**(9270): p. 1777-89.
6. Parkin, J. and B. Cohen, *An overview of the immune system.* Lancet, 2001. **357**(9270): p. 1777-1789.
7. Finn, O.J., *Cancer immunology.* The New England journal of medicine, 2008. **358**(25): p. 2704-15.
8. Delves, P.J. and I.M. Roitt, *The immune system. Second of two parts.* The New England journal of medicine, 2000. **343**(2): p. 108-17.
9. Delves, P.J. and I.M. Roitt, *The immune system. First of two parts.* The New England journal of medicine, 2000. **343**(1): p. 37-49.
10. Girard-Pierce, K.R., et al., *A novel role for C3 in antibody-induced red blood cell clearance and antigen modulation.* Blood, 2013. **122**(10): p. 1793-801.
11. Suresh, M., et al., *Complement component 3 is required for optimal expansion of CD8 T cells during a systemic viral infection.* Journal of Immunology, 2003. **170**(2): p. 788-794.
12. Stager, S., et al., *Natural antibodies and complement are endogenous adjuvants for vaccine-induced CD8+ T-cell responses.* Nature medicine, 2003. **9**(10): p. 1287-92.
13. Reddy, S.T., et al., *Exploiting lymphatic transport and complement activation in nanoparticle vaccines.* Nature biotechnology, 2007. **25**(10): p. 1159-1164.
14. Sica, A., et al., *Macrophage polarization in tumour progression.* Seminars in Cancer Biology, 2008. **18**(5): p. 349-355.
15. Mosser, D.M., *The many faces of macrophage activation.* Journal of Leukocyte Biology, 2003. **73**(2): p. 209-212.
16. Martinez, F.O., L. Helming, and S. Gordon, *Alternative Activation of Macrophages: An Immunologic Functional Perspective.* Annual Review of Immunology, 2009. **27**: p. 451-483.
17. Gordon, S., *Alternative activation of macrophages.* Nature Reviews Immunology, 2003. **3**(1): p. 23-35.
18. Kigerl, K.A., et al., *Identification of two distinct macrophage subsets with divergent effects causing either neurotoxicity or regeneration in the injured mouse spinal cord.* The Journal of neuroscience : the official journal of the Society for Neuroscience, 2009. **29**(43): p. 13435-44.
19. Flynn, J.L., *Immunology of tuberculosis and implications in vaccine development.* Tuberculosis, 2004. **84**(1-2): p. 93-101.

20. Flynn, J.L., J. Chan, and P.L. Lin, *Macrophages and control of granulomatous inflammation in tuberculosis.* Mucosal Immunology, 2011. **4**(3): p. 271-278.
21. Skeiky, Y.A.W. and J.C. Sadoff, *Advances in tuberculosis vaccine strategies.* Nature Reviews Microbiology, 2006. **4**(6): p. 469-476.
22. Sim, R.B. and S.A. Tsiftsoglou, *Proteases of the complement system.* Biochemical Society transactions, 2004. **32**(Pt 1): p. 21-7.
23. Ricklin, D., et al., *Complement: a key system for immune surveillance and homeostasis.* Nature immunology, 2010. **11**(9): p. 785-97.
24. Reddy, S.T., M.A. Swartz, and J.A. Hubbell, *Targeting dendritic cells with biomaterials: developing the next generation of vaccines.* Trends in Immunology, 2006. **27**(12): p. 573-579.
25. Peppas, N.A. and R. Langer, *New challenges in biomaterials.* Science, 1994. **263**(5154): p. 1715-20.
26. Mitragotri, S. and J. Lahann, *Physical approaches to biomaterial design.* Nature Materials, 2009. **8**(1): p. 15-23.
27. Kou, P.M. and J.E. Babensee, *Macrophage and dendritic cell phenotypic diversity in the context of biomaterials.* Journal of Biomedical Materials Research Part A, 2011. **96A**(1): p. 239-260.
28. David, S. and A. Kroner, *Repertoire of microglial and macrophage responses after spinal cord injury.* Nature Reviews Neuroscience, 2011. **12**(7): p. 388-399.
29. Gordon, S. and P.R. Taylor, *Monocyte and macrophage heterogeneity.* Nature reviews. Immunology, 2005. **5**(12): p. 953-64.
30. Champion, J.A., A. Walker, and S. Mitragotri, *Role of particle size in phagocytosis of polymeric microspheres.* Pharmaceutical research, 2008. **25**(8): p. 1815-1821.
31. Gallo, P., R. Goncalves, and D.M. Mosser, *The influence of IgG density and macrophage Fc (gamma) receptor cross-linking on phagocytosis and IL-10 production.* Immunology Letters, 2010. **133**(2): p. 70-77.
32. Mosser, D.M., P. Gallo, and R. Goncalves, *The influence of IgG density and macrophage Fc (gamma) receptor cross-linking on phagocytosis and IL-10 production.* Immunology Letters, 2010. **133**(2): p. 70-77.
33. Carroll, M.C., *The complement system in regulation of adaptive immunity.* Nature immunology, 2004. **5**(10): p. 981-6.
34. Yoon, J., K.J. Lee, and J. Lahann, *Multifunctional polymer particles with distinct compartments.* Journal of Materials Chemistry, 2011. **21**(24): p. 8502-8510.
35. Standley, S.M., et al., *Acid-degradable particles for protein-based vaccines: Enhanced survival rate for tumor-challenged mice using ovalbumin model.* Bioconjugate Chemistry, 2004. **15**(6): p. 1281-1288.
36. Loomis, K., K. McNeeley, and R.V. Bellamkonda, *Nanoparticles with targeting, triggered release, and imaging functionality for cancer applications.* Soft Matter, 2011. **7**(3): p. 839-856.
37. Kohane, D.S., *Microparticles and nanoparticles for drug delivery.* Biotechnology and bioengineering, 2007. **96**(2): p. 203-9.
38. Aderem, A. and D.M. Underhill, *Mechanisms of phagocytosis in macrophages.* Annu Rev Immunol, 1999. **17**: p. 593-623.

39. Underhill, D.M. and A. Ozinsky, *Phagocytosis of microbes: complexity in action.* Annu Rev Immunol, 2002. **20**: p. 825-52.
40. Stout, R.D. and J. Suttles, *Functional plasticity of macrophages: reversible adaptation to changing microenvironments.* Journal of Leukocyte Biology, 2004. **76**(3): p. 509-513.
41. Laskin, D.L., B. Weinberger, and J.D. Laskin, *Functional heterogeneity in liver and lung macrophages.* J Leukoc Biol, 2001. **70**(2): p. 163-70.
42. Hoeffel, G., et al., *Adult Langerhans cells derive predominantly from embryonic fetal liver monocytes with a minor contribution of yolk sac-derived macrophages.* J Exp Med, 2012. **209**(6): p. 1167-81.
43. Schulz, C., et al., *A lineage of myeloid cells independent of Myb and hematopoietic stem cells.* Science, 2012. **336**(6077): p. 86-90.
44. Medzhitov, R. and C.A. Janeway, *Innate immunity: Impact on the adaptive immune response.* Current Opinion in Immunology, 1997. **9**(1): p. 4-9.
45. Fearon, D.T. and R.M. Locksley, *The instructive role of innate immunity in the acquired immune response.* Science, 1996. **272**(5258): p. 50-3.
46. Hansson, G.K. and P. Libby, *The immune response in atherosclerosis: a double-edged sword.* Nature reviews. Immunology, 2006. **6**(7): p. 508-19.
47. Ross, R., *Atherosclerosis--an inflammatory disease.* The New England journal of medicine, 1999. **340**(2): p. 115-26.
48. Sica, A. and V. Bronte, *Altered macrophage differentiation and immune dysfunction in tumor development.* Journal of Clinical Investigation, 2007. **117**(5): p. 1155-1166.
49. Andersen, P. and T.M. Doherty, *The success and failure of BCG - implications for a novel tuberculosis vaccine.* Nature Reviews Microbiology, 2005. **3**(8): p. 656-662.
50. Armstrong, J.A. and P.D. Hart, *Response of Cultured Macrophages to Mycobacterium-Tuberculosis, with Observations on Fusion of Lysosomes with Phagosomes.* Journal of Experimental Medicine, 1971. **134**(3): p. 713-&.
51. Bhatt, K. and P. Salgame, *Host innate immune response to Mycobacterium tuberculosis.* J Clin Immunol, 2007. **27**(4): p. 347-62.
52. Mantovani, A., et al., *The chemokine system in diverse forms of macrophage activation and polarization.* Trends in Immunology, 2004. **25**(12): p. 677-686.
53. Dandrea, A., et al., *Stimulatory and Inhibitory Effects of Interleukin (Il)-4 and Il-13 on the Production of Cytokines by Human Peripheral-Blood Mononuclear-Cells - Priming for Il-12 and Tumor-Necrosis-Factor-Alpha Production.* Journal of Experimental Medicine, 1995. **181**(2): p. 537-546.
54. Heyman, B., *Regulation of antibody responses via antibodies, complement, and Fc receptors.* Annual review of immunology, 2000. **18**: p. 709-37.
55. Ravetch, J.V. and S. Bolland, *IgG Fc receptors.* Annual Review of Immunology, 2001. **19**: p. 275-290.
56. Swanson, J.A. and A.D. Hoppe, *The coordination of signaling during Fc receptor-mediated phagocytosis.* Journal of leukocyte biology, 2004. **76**(6): p. 1093-1103.

57. Sutterwala, F.S., et al., *Selective suppression of interleukin-12 induction after macrophage receptor ligation.* The Journal of experimental medicine, 1997. **185**(11): p. 1977-85.
58. Anderson, C.F. and D.M. Mosser, *Cutting edge: biasing immune responses by directing antigen to macrophage Fc gamma receptors.* Journal of immunology, 2002. **168**(8): p. 3697-701.
59. Mosmann, T.R. and R.L. Coffman, *TH1 and TH2 cells: different patterns of lymphokine secretion lead to different functional properties.* Annual review of immunology, 1989. **7**: p. 145-73.
60. Abbas, A.K., K.M. Murphy, and A. Sher, *Functional diversity of helper T lymphocytes.* Nature, 1996. **383**(6603): p. 787-93.
61. Aderem, A. and D.M. Underhill, *Mechanisms of phagocytosis in macrophages.* Annual Review of Immunology, 1999. **17**: p. 593-623.
62. Joller, N., et al., *Antibodies protect against intracellular bacteria by Fc receptor-mediated lysosomal targeting.* Proceedings of the National Academy of Sciences of the United States of America, 2010. **107**(47): p. 20441-20446.
63. Walport, M.J., *Complement. Second of two parts.* The New England journal of medicine, 2001. **344**(15): p. 1140-4.
64. Walport, M.J., *Complement. First of two parts.* The New England journal of medicine, 2001. **344**(14): p. 1058-66.
65. Markiewski, M.M. and J.D. Lambris, *Is complement good or bad for cancer patients? A new perspective on an old dilemma.* Trends in Immunology, 2009. **30**(6): p. 286-292.
66. Markiewski, M., et al., *Modulation of the anti-tumour immune response by complement.* Molecular immunology, 2008. **45**(16): p. 4151-4151.
67. Kumar, M.N.V.R., *Nano and microparticles as controlled drug delivery devices.* Journal of Pharmacy and Pharmaceutical Sciences, 2000. **3**(2): p. 234-258.
68. Champion, J.A. and S. Mitragotri, *Role of target geometry in phagocytosis.* Proceedings of the National Academy of Sciences of the United States of America, 2006. **103**(13): p. 4930-4.
69. Swartz, M.A., S.T. Reddy, and J.A. Hubbell, *Targeting dendritic cells with biomaterials: developing the next generation of vaccines.* Trends in Immunology, 2006. **27**(12): p. 573-579.
70. Hubbell, J.A., S.N. Thomas, and M.A. Swartz, *Materials engineering for immunomodulation.* Nature, 2009. **462**(7272): p. 449-460.
71. Kwon, Y.J., et al., *In vivo targeting of dendritic cells for activation of cellular immunity using vaccine carriers based on pH-responsive microparticles.* Proceedings of the National Academy of Sciences of the United States of America, 2005. **102**(51): p. 18264-18268.
72. Dinauer, N., et al., *Selective targeting of antibody-conjugated nanoparticles to leukemic cells and primary T-lymphocytes.* Biomaterials, 2005. **26**(29): p. 5898-5906.
73. Zauner, W., N.A. Farrow, and A.M. Haines, *In vitro uptake of polystyrene microspheres: effect of particle size, cell line and cell density.* J Control Release, 2001. **71**(1): p. 39-51.

74. Tollis, S., et al., *The zipper mechanism in phagocytosis: energetic requirements and variability in phagocytic cup shape.* Bmc Systems Biology, 2010. **4**.
75. Badylak, S.F., et al., *Macrophage Phenotype as a Determinant of Biologic Scaffold Remodeling.* Tissue Engineering Part A, 2008. **14**(11): p. 1835-1842.
76. Yoshida, M. and J.E. Babensee, *Poly(lactic-co-glycolic acid) enhances maturation of human monocyte-derived dendritic cells.* Journal of Biomedical Materials Research Part A, 2004. **71A**(1): p. 45-54.
77. Bartneck, M., et al., *Induction of specific macrophage subtypes by defined micro-patterned structures.* Acta Biomaterialia, 2010. **6**(10): p. 3864-3872.
78. Chonn, A., P.R. Cullis, and D.V. Devine, *The Role of Surface-Charge in the Activation of the Classical and Alternative Pathways of Complement by Liposomes.* Journal of Immunology, 1991. **146**(12): p. 4234-4241.
79. Montdargent, B., D. Labarre, and M. Jozefowicz, *Interactions of functionalized polystyrene derivatives with the complement system in human serum.* Journal of biomaterials science. Polymer edition, 1991. **2**(1): p. 25-35.
80. Montdargent, B., et al., *Complement Activation and Adsorption of Protein-Fragments by Functionalized Polymer Surfaces in Human Serum.* Biomaterials, 1992. **13**(9): p. 571-576.
81. Andersson, J., et al., *Binding of C3 fragments on top of adsorbed plasma proteins during complement activation on a model biomaterial surface.* Biomaterials, 2005. **26**(13): p. 1477-1485.
82. Abadie, V., et al., *Neutrophils rapidly migrate via lymphatics after Mycobacterium bovis BCG intradermal vaccination and shuttle live bacilli to the draining lymph nodes.* Blood, 2005. **106**(5): p. 1843-1850.
83. Harding, C.V. and W.H. Boom, *Regulation of antigen presentation by Mycobacterium tuberculosis: a role for Toll-like receptors.* Nature Reviews Microbiology, 2010. **8**(4): p. 296-307.
84. Gordon, S. and P.R. Taylor, *Monocyte and macrophage heterogeneity.* Nature Reviews Immunology, 2005. **5**(12): p. 953-964.
85. Hodge, S., et al., *Azithromycin increases phagocytosis of apoptotic bronchial epithelial cells by alveolar macrophages.* Eur Respir J, 2006. **28**(3): p. 486-95.
86. Harris, M., *Monoclonal antibodies as therapeutic agents for cancer.* Lancet Oncology, 2004. **5**(5): p. 292-302.
87. Akewanlop, C., et al., *Phagocytosis of breast cancer cells mediated by anti-MUC-1 monoclonal antibody, DF3, and its bispecific antibody.* Cancer Research, 2001. **61**(10): p. 4061-4065.
88. Gallucci, S. and P. Matzinger, *Danger signals: SOS to the immune system.* Curr Opin Immunol, 2001. **13**(1): p. 114-9.
89. Trinchieri, G., *Interleukin-12: a proinflammatory cytokine with immunoregulatory functions that bridge innate resistance and antigen-specific adaptive immunity.* Annual review of immunology, 1995. **13**: p. 251-76.
90. Mitragotri, S. and J. Lahann, *Physical approaches to biomaterial design.* Nat Mater, 2009. **8**(1): p. 15-23.
91. Fahmy, T.M., et al., *Inflammasome-activating nanoparticles as modular systems for optimizing vaccine efficacy.* Vaccine, 2009. **27**(23): p. 3013-3021.

92. Ahsan, F., et al., *Targeting to macrophages: role of physicochemical properties of particulate carriers--liposomes and microspheres--on the phagocytosis by macrophages.* J Control Release, 2002. **79**(1-3): p. 29-40.
93. Zhang, Y., A.D. Hoppe, and J.A. Swanson, *Coordination of Fc receptor signaling regulates cellular commitment to phagocytosis.* Proceedings of the National Academy of Sciences of the United States of America, 2010. **107**(45): p. 19332-7.
94. Blanchette, C.D., et al., *Decoupling internalization, acidification and phagosomal-endosomal/lysosomal fusion during phagocytosis of InlA coated beads in epithelial cells.* PloS one, 2009. **4**(6): p. e6056.
95. Decuzzi, P. and M. Ferrari, *The role of specific and non-specific interactions in receptor-mediated endocytosis of nanoparticles.* Biomaterials, 2007. **28**(18): p. 2915-2922.
96. Zhang, S.L., et al., *Size-Dependent Endocytosis of Nanoparticles.* Advanced Materials, 2009. **21**(4): p. 419-+.
97. Yue, T.T. and X.R. Zhang, *Molecular understanding of receptor-mediated membrane responses to ligand-coated nanoparticles.* Soft Matter, 2011. **7**(19): p. 9104-9112.
98. Herant, M., et al., *Protrusive Push versus Enveloping Embrace: Computational Model of Phagocytosis Predicts Key Regulatory Role of Cytoskeletal Membrane Anchors.* Plos Computational Biology, 2011. **7**(1).
99. Gao, H.J., W.D. Shi, and L.B. Freund, *Mechanics of receptor-mediated endocytosis.* Proceedings of the National Academy of Sciences of the United States of America, 2005. **102**(27): p. 9469-9474.
100. Herant, M., V. Heinrich, and M. Dembo, *Mechanics of neutrophil phagocytosis: experiments and quantitative models.* Journal of Cell Science, 2006. **119**(9): p. 1903-1913.
101. Zhang, X., R. Goncalves, and D.M. Mosser, *The isolation and characterization of murine macrophages.* Current protocols in immunology / edited by John E. Coligan ... [et al.], 2008. **Chapter 14**: p. Unit 14 1.
102. Weischenfeldt, J. and B. Porse, *Bone Marrow-Derived Macrophages (BMM): Isolation and Applications.* CSH protocols, 2008. **2008**: p. pdb prot5080.
103. Steinkamp, J.A., et al., *Phagocytosis: flow cytometric quantitation with fluorescent microspheres.* Science, 1982. **215**(4528): p. 64-6.
104. Mammen, M., S.K. Choi, and G.M. Whitesides, *Polyvalent interactions in biological systems: Implications for design and use of multivalent ligands and inhibitors.* Angewandte Chemie-International Edition, 1998. **37**(20): p. 2755-2794.
105. Tabata, Y. and Y. Ikada, *Effect of the Size and Surface-Charge of Polymer Microspheres on Their Phagocytosis by Macrophage.* Biomaterials, 1988. **9**(4): p. 356-362.
106. Kobzik, L., *Lung Macrophage Uptake of Unopsonized Environmental Particulates - Role of Scavenger-Type Receptors.* Journal of Immunology, 1995. **155**(1): p. 367-376.
107. Palecanda, A., et al., *Role of the scavenger receptor MARCO in alveolar macrophage binding of unopsonized environmental particles.* Journal of Experimental Medicine, 1999. **189**(9): p. 1497-1506.

108. Cox, D., et al., *A requirement for phosphatidylinositol 3-kinase in pseudopod extension.* The Journal of biological chemistry, 1999. **274**(3): p. 1240-7.
109. Cox, D., et al., *A regulatory role for Src homology 2 domain-containing inositol 5'-phosphatase (SHIP) in phagocytosis mediated by Fc gamma receptors and complement receptor 3 (alpha(M)beta(2); CD11b/CD18).* The Journal of experimental medicine, 2001. **193**(1): p. 61-71.
110. Dietrich, G., et al., *Delivery of antigen-encoding plasmid DNA into the cytosol of macrophages by attenuated suicide Listeria monocytogenes.* Nature biotechnology, 1998. **16**(2): p. 181-185.
111. Whitacre, C.C., *Sex differences in autoimmune disease.* Nature immunology, 2001. **2**(9): p. 777-80.
112. Heinrich, V. and C.Y. Lee, *Blurred line between chemotactic chase and phagocytic consumption: an immunophysical single-cell perspective.* Journal of Cell Science, 2011. **124**(18): p. 3041-3051.
113. Moghimi, S.M., et al., *Material properties in complement activation.* Advanced drug delivery reviews, 2011. **63**(12): p. 1000-7.
114. Szebeni, J., et al., *Activation of complement by therapeutic liposomes and other lipid excipient-based therapeutic products: prediction and prevention.* Advanced drug delivery reviews, 2011. **63**(12): p. 1020-30.
115. Porter, R.R. and K.B. Reid, *Activation of the complement system by antibody-antigen complexes: the classical pathway.* Advances in protein chemistry, 1979. **33**: p. 1-71.
116. Schumaker, V.N., P. Zavodszky, and P.H. Poon, *Activation of the first component of complement.* Annual Review of Immunology, 1987. **5**: p. 21-42.
117. Duncan, A.R. and G. Winter, *The Binding-Site for Clq on Igg.* Nature, 1988. **332**(6166): p. 738-740.
118. Molina, H., et al., *Markedly impaired humoral immune response in mice deficient in complement receptors 1 and 2.* Proceedings of the National Academy of Sciences of the United States of America, 1996. **93**(8): p. 3357-3361.
119. Demento, S.L., et al., *Inflammasome-activating nanoparticles as modular systems for optimizing vaccine efficacy.* Vaccine, 2009. **27**(23): p. 3013-3021.
120. Al-Hanbali, O., et al., *Concentration dependent structural ordering of poloxamine 908 on polystyrene nanoparticles and their modulatory role on complement consumption.* J Nanosci Nanotechnol, 2006. **6**(9-10): p. 3126-33.
121. Moghimi, S.M., et al., *Causative factors behind poloxamer 188 (Pluronic F68, Flocor)-induced complement activation in human sera. A protective role against poloxamer-mediated complement activation by elevated serum lipoprotein levels.* Biochimica et biophysica acta, 2004. **1689**(2): p. 103-13.
122. Vonarbourg, A., et al., *Parameters influencing the stealthiness of colloidal drug delivery systems.* Biomaterials, 2006. **27**(24): p. 4356-73.
123. Ahsan, F.L., et al., *Targeting to macrophages: role of physicochemical properties of particulate carriers-liposomes and microspheres-on the phagocytosis by macrophages.* Journal of Controlled Release, 2002. **79**(1-3): p. 29-40.
124. Vorup-Jensen, T., *On the roles of polyvalent binding in immune recognition: Perspectives in the nanoscience of immunology and the immune response to nanomedicines.* Advanced drug delivery reviews, 2012. **64**(15): p. 1759-81.

125. Devine, D.V., et al., *Liposome-Complement Interactions in Rat Serum - Implications for Liposome Survival Studies.* Biochimica Et Biophysica Acta-Biomembranes, 1994. **1191**(1): p. 43-51.
126. Pedersen, M.B., et al., *Curvature of synthetic and natural surfaces is an important target feature in classical pathway complement activation.* Journal of Immunology, 2010. **184**(4): p. 1931-45.
127. Harashima, H., et al., *Synergistic effect between size and cholesterol content in the enhanced hepatic uptake clearance of liposomes through complement activation in rats.* Pharmaceutical research, 1996. **13**(11): p. 1704-1709.
128. Burton, D.R., *Immunoglobulin G: functional sites.* Molecular immunology, 1985. **22**(3): p. 161-206.
129. Wright, J.K., et al., *Dimeric, trimeric and tetrameric complexes of immunoglobulin G fix complement.* The Biochemical journal, 1980. **187**(3): p. 775-80.
130. Lambris, J.D., K.B. Reid, and J.E. Volanakis, *The evolution, structure, biology and pathophysiology of complement.* Immunology today, 1999. **20**(5): p. 207-11.
131. Flierl, M.A., et al., *Complement C3 serum levels in anorexia nervosa: a potential biomarker for the severity of disease?* Annals of general psychiatry, 2011. **10**: p. 16.
132. Seregin, S.S., et al., *Novel Adenovirus Vectors 'Capsid-Displaying' a Human Complement Inhibitor.* Journal of Innate Immunity, 2010. **2**(4): p. 353-359.
133. Busch, N.A., M.S. Wertheim, and M.L. Yarmush, *Monte Carlo simulation of n-member associating fluids: Application to antigen-antibody systems.* Journal of Chemical Physics, 1996. **104**(11): p. 3962-3975.
134. Gemmell, C.H., *A flow cytometric immunoassay to quantify adsorption of complement activation products (iC3b, C3d, SC5b-9) on artificial surfaces.* J Biomed Mater Res, 1997. **37**(4): p. 474-80.
135. Armstrong, J.K., et al., *The hydrodynamic radii of macromolecules and their effect on red blood cell aggregation.* Biophysical journal, 2004. **87**(6): p. 4259-4270.
136. Murphy, R.M., et al., *Size and Structure of Antigen-Antibody Complexes - Electron-Microscopy and Light-Scattering Studies.* Biophysical journal, 1988. **54**(1): p. 45-56.
137. Ban, N., et al., *Crystal-Structure of an Idiotype Antiidiotype Fab Complex.* Proceedings of the National Academy of Sciences of the United States of America, 1994. **91**(5): p. 1604-1608.
138. Werner, T.C., J.R. Bunting, and R.E. Cathou, *The shape of immunoglobulin G molecules in solution.* Proceedings of the National Academy of Sciences of the United States of America, 1972. **69**(4): p. 795-9.
139. Schneider, S. and M. Zacharias, *Atomic resolution model of the antibody Fc interaction with the complement C1q component.* Molecular immunology, 2012. **51**(1): p. 66-72.
140. Henry, N., J.W. Parce, and H.M. McConnell, *Visualization of specific antibody and C1q binding to hapten-sensitized lipid vesicles.* Proceedings of the National Academy of Sciences of the United States of America, 1978. **75**(8): p. 3933-7.

141. Parce, J.W., N. Henry, and H.M. McConnell, *Specific antibody-dependent binding of complement component C1q to hapten-sensitized lipid vesicles.* Proceedings of the National Academy of Sciences of the United States of America, 1978. **75**(3): p. 1515-8.
142. Hughesjones, N.C. and B. Gardner, *Reaction between the Isolation Globular Subunits of the Complement Component Clq and Igg-Complexes.* Molecular immunology, 1979. **16**(9): p. 697-701.
143. Taylor, P.W., *Bactericidal and Bacteriolytic Activity of Serum against Gram-Negative Bacteria.* Microbiological Reviews, 1983. **47**(1): p. 46-83.
144. Aldwell, F.E., et al., *Oral vaccination of mice with lipid-encapsulated Mycobacterium bovis BCG: Anatomical sites of bacterial replication and immune activity.* Immunology and Cell Biology, 2005. **83**(5): p. 549-553.
145. Aldwell, F.E., et al., *Oral delivery of lipid-encapsulated Mycobacterium bovis BCG extends survival of the bacillus in vivo and induces a long-term protective immune response against tuberculosis.* Vaccine, 2006. **24**(12): p. 2071-2078.
146. Giri, P.K., et al., *Comparative evaluation of intranasal and subcutaneous route of immunization for development of mucosal vaccine against experimental tuberculosis.* Fems Immunology and Medical Microbiology, 2005. **45**(1): p. 87-93.
147. Griffiths, G., et al., *Nanobead-based interventions for the treatment and prevention of tuberculosis.* Nature Reviews Microbiology, 2010. **8**(11): p. 827-834.
148. Hiraishi, Y., et al., *Bacillus Calmette-Guerin vaccination using a microneedle patch.* Vaccine, 2011. **29**(14): p. 2626-2636.
149. Pacheco, P., D. White, and T. Sulchek, *Effects of microparticle size and Fc density on macrophage phagocytosis.* PLoS One, 2013. **8**(4): p. e60989.
150. Pacheco, P.M., et al., *TUNABLE COMPLEMENT ACTIVATION BY PARTICLES WITH VARIABLE SIZE AND Fc DENSITY.* Nano Life, 2013. **3**(2): p. 1341001.
151. Maglione, P.J., et al., *Fc gamma receptors regulate immune activation and susceptibility during Mycobacterium tuberculosis infection.* J Immunol, 2008. **180**(5): p. 3329-38.
152. Clemens, D.L. and M.A. Horwitz, *Characterization of the Mycobacterium tuberculosis phagosome and evidence that phagosomal maturation is inhibited.* J Exp Med, 1995. **181**(1): p. 257-70.
153. Nozaki, Y., et al., *Mechanism of nitric oxide-dependent killing of Mycobacterium bovis BCG in human alveolar macrophages.* Infect Immun, 1997. **65**(9): p. 3644-7.
154. Schaible, U.E., et al., *Cytokine activation leads to acidification and increases maturation of Mycobacterium avium-containing phagosomes in murine macrophages.* J Immunol, 1998. **160**(3): p. 1290-6.